THE STUDY OF LOW-MASS STARS AND BROWN DWARFS

A thesis submitted
for the degree of
Doctor of Philosophy

by

Martin R. Cossburn

Astronomy Group
Department of Physics and Astronomy
University of Leicester

February 1999

ProQuest LLC
789 East Eisenhower Parkway
P.O. Box 1346
Ann Arbor, MI 48106-1346

Abstract

Martin R. Cossburn

The Study of Low Mass Stars and Brown Dwarfs

This thesis describes the search for brown dwarfs in open clusters using optical and infrared photometry, optical spectroscopy and surveys using the Hubble Space Telescope (HST). It also includes an observational study of very low-mass stars (VLMS) using a filter combination (I and Z), unused previously in this field enabling the calibration of the colour (I–Z), for future survey work.

Following a short introduction explaining the reasons for studying brown dwarfs this thesis reviews the theory of their formation and evolution and describes recent searches for brown dwarfs and their results. Modern CCD technology has led to larger and larger area cluster surveys and so chapter 3 reviews this technology and the data reduction software and techniques necessary for analysis.

Chapters 4, 5, 6 and 7 present the observational results. Chapter 4 presents an essentially null result of a deep HST survey in the Pleiades. Chapter 5 presents the data used to calibrate the I–Z colour and chapter 6 describes the discovery of PIZ 1, a brown dwarf in the Pleiades of mass $0.048M_{\odot}$ and effective temperature $\sim$2200K. Chapter 7 presents the infrared follow-up results of a number of recent large area optical surveys.

Chapters 8 and 9 use the results from the latest surveys to determine the mass and luminosity functions of both Praesepe and the Pleiades. In Praesepe the mass function is calculated down to the brown dwarf limit in the cluster and shows no sign of turning down. In the Pleiades the mass function appears to be flattening across the stellar sub-stellar boundary.

Finally in Chapter 10 I summarise the important conclusions from each chapter and identify areas of future work.

Acknowledgments

First I would like to acknowledge the guidance that I have received from my supervisor Richard Jameson over the past 3 years. His help and explanations have resulted in the completion of this thesis within 3 years for which I am extremely grateful. Outside the realms of research his experience and knowledge of some excellent restaurants and drinking establishments around the globe have resulted in a number of highly successful conferences and observing trips. I would also like to thank Simon Hodgkin for introducing me to the wonderful world of data analysis software (IRAF rules!) and "How not to break the telescope" on observing runs.

At Leicester I have had the pleasure of working with some of the greatest minds(!) of modern astronomy. Not least David Pinfield whose support on the roof of the Isaac Newton Telescope in La Palma will never be forgotten. Thanks also to Graham, Chris, Adam, Gordon, Anastasia, Becky, Gareth, Paul, Ray, Norma and Fraser for his musical interludes.

Outside Leicester, thanks to Jon, Liz, Chris, Lou, medium Stu, Rich, Caroline, Dan, Deb, Gordon and Gail. Thanks to Mum and Dad for their constant support and to Pants and Tom for their constructive and informative emails. Thanks also to Maruschka for her support, help and love over the last year through good times and bad.

Finally, thanks to Manchester United for winning 2 out of 3 championships while I have lived here in Leicester.

Publications

1. Discovery of the Lowest Mass Brown Dwarf in the Pleiades.
   M.R. Cossburn, S.T. Hodgkin, R.F. Jameson and D.J. Pinfield, 1997, in ASP Conf. Proc., Brown Dwarfs and Extrasolar Planets, ed. R. Rebolo, E.L. Martin, M.R. Zapatero-Osorio, (San Francisco ASP). in press.

2. Brown Dwarfs in the Pleiades and the Initial Mass Function across the stellar/substellar boundary.
   N.C. Hambly, S.T. Hodgkin, M.R. Cossburn, R.F. Jameson, MNRAS, in press, 1998.

3. Brown Dwarf Candidates in Praesepe.
   D.J. Pinfield, S.T. Hodgkin, R.F. Jameson, M.R. Cossburn, and T.von Hippel, MNRAS 287, 180-188, 1997.

4. Discovery of the Lowest Mass Brown Dwarf in the Pleiades.
   M.R. Cossburn, S.T. Hodgkin, R.F. Jameson and D.J. Pinfield, 1997, MNRAS, 288, L23-L27

5. RIZ Photometry of Low Mass Stars.
   M.R. Cossburn, S.T. Hodgkin, and R.F. Jameson, MNRAS, in press, 1998.

6. New Brown Dwarfs in the Pleiades Cluster.
   M.R. Zapatero-Osorio, R. Rebolo, E.L. Martin, G. Basri, A. Magazzu, S.T. Hodgkin, R.F. Jameson, M.R. Cossburn, 1997, ApJ, 491L, 81

Contents

List of Figures

List of Tables

Chapter 1

Introduction

I will begin this thesis by making one or two definitions that are important in understanding the work that follows. A brown dwarf is an object that forms in the same way as a star but does not have sufficient mass to trigger the nuclear reactions that convert hydrogen to helium in its core. From theory, the mass below which this occurs is approximately $0.08M_{\odot}$. Brown dwarfs therefore differ from planets and giant planets in that these objects are believed to form from the accretion of material from a disk around a young star. The name, brown dwarf, is commonly attributed to Tarter (1975), but the existence of these sub-stellar objects was first postulated by Kumar (1963). Recent reviews on the subject can be found within Liebert & Probst (1987) and Stevenson (1991). An interesting review of the latest understanding of the interiors and low-temperature atmospheres of brown dwarfs can be found within Allard *et al.* (1997).

1.1 Why study brown dwarfs?

By identifying brown dwarfs in open clusters or in the field, one can begin to provide important constraints on the theories of star formation. Some theories predict a minimum formation mass which would be challenged if large numbers of brown dwarfs were discovered.

From studies of the rotational velocities of gas in our own Galaxy and other spiral galaxies, it is known that there exists a significant amount of unseen matter. It is possible that brown dwarfs may contribute to this dark matter if it is of a baryonic nature.

The interior of a brown dwarf, according to theoretical modelling, is degenerate. Their low-temperature atmospheres are difficult to model as a direct consequence of

the presence molecular opacities. Studying the spectra of such objects would help in the understanding of the complexities of energy transport in low-temperature atmospheres. Ultimately, particularly when some brown dwarf masses have been directly measured in binary systems, we may gain a deeper understanding of the physics of very high density degenerate matter.

Finally, the fact that brown dwarfs are so intrinsically faint, they reside at the observational limit, and so it is natural to work at this limit.

1.2 Aims of this Thesis

The work in this thesis aims to continue the search and study of brown dwarfs in open clusters using optical and near infrared filter passbands combined with modern charged coupled device (CCD) technology. The optical survey work revolves around the use of the I and Z filter combination to detect objects below the sub-stellar limit. As with any new colour or observing technique, serious consideration must be given to the calibration of any subsequent photometry. The work in this thesis includes a project that undertakes such a calibration technique. Any brown dwarf candidates discovered in an optical survey need to be followed up with infrared photometry and so this too was carried out in both the Pleiades and Praesepe. Once identified, the results of the various optical and infrared surveys are combined in an attempt to understand the luminosity and mass functions of open clusters and to discover if they are similar (or not as the case may be) to the field distributions of VLMS and brown dwarfs.

1.3 Thesis Structure

In chapter 2 I review the theory of brown dwarfs which includes their formation, evolution and a description of their low temperature atmospheres. I also present a comprehensive review of the various successful and unsuccessful surveys that have been carried out to detect these rather elusive sub-stellar objects. In chapter 3 I describe the CCD and infrared array technology that I have used over the past 3 years. Included in this chapter are descriptions of the necessary photometric and spectroscopic data reduction steps. In chapter 4 I present the results of my first project as a postgraduate student which involved the reduction of images taken using the Hubble Space Telescope (HST). Although the analysis yielded essentially a null result, it was an important introduction to image reduction techniques. Chapter

5 describes the results from an observing run at the Jacobus Kapteyn Telescope (JKT). This observational project was carried out in order to calibrate the I–Z colour. Without this it would be difficult to calibrate the photometry from large area, open cluster surveys at I and Z as a direct result of the lack of standards at Z. The discovery of a brown dwarf in The Pleiades open cluster using the I–Z colour is presented in chapter 6 and resulted from the first observing trip of my research career. In this chapter I describe the observations at the Isaac Newton Telescope (INT), the subsequent image reduction, and the follow-up observations (photometric and spectroscopic) that were needed to help confirm the identity of PIZ 1 as a cluster member. Proper motion measurements and detection of lithium are still required before any membership can be completely assigned. Chapter 7 presents the infrared photometry taken at the United Kingdom Infrared Telescope (UKIRT) in November 1997. 5 individual surveys were followed up (some more completely than others), and cluster membership assigned on the basis of a candidate's position on an I versus I–K colour-magnitude diagram. Chapters 8 and 9 present the mass and luminosity functions for both Praesepe and the Pleiades based on the follow-up infrared photometry in chapter 7. Chapter 10 summarises the conclusions from each chapter and suggests areas of follow-up work to this thesis.

Chapter 2

Review

2.1 Introduction

This chapter summarises the theory, history and methods behind the search for sub-stellar objects. For some time, the Leicester Group has been actively searching for brown dwarfs, and the influence the group has had in this area is described in detail. Many different techniques have been used over the years and the most common are described here. They include searches within young open clusters; as companions to nearby stars and the detection, very recently, of free-floating sub-stellar objects. At the beginning of my PhD, there were a handful of brown dwarf candidates in the published literature. Three years later and there has not only been an explosion in the number of good candidates, but final proof that brown dwarfs really do exist. Confirmation of brown dwarf status is not straight forward, and requires different tests for the different search criteria. This chapter aims to present an account of the success and failures of the many surveys that have taken place, but first takes a brief look at the theory behind these objects.

2.2 The Theory of Brown Dwarfs

A brown dwarf has a mass below $\sim 0.08\ M_{\odot}$, which is slightly dependent on metallicity. Recent models, (see Chabrier & Baraffe (1997)), show that as the fraction of heavier elements decreases, the model isochrones move to hotter effective temperatures and brighter luminosities. As the metallicity decreases the brown dwarf mass limit increases slightly as a result. An object with a mass below $0.3\ M_{\odot}$ is, according to stellar interior calculations, fully convective, represented by an n=3/2 polytrope. A polytrope relates the interior pressure and density having the general

form of $P \propto \rho^{\frac{n+1}{n}}$. $\frac{n+1}{n}$ is equal to γ, the ratio of the specific heats at constant pressure and volume. Calculations by Kumar (1963) showed that with the onset of degeneracy, an object with a mass between 0.07 and 0.09 $M_{\odot}$ would not ignite its hydrogen. During collapse the density of the core rises and the electron fermi energy exceeds the average thermal energy. This produces a degenerate electron gas which supplies the internal pressure necessary to prevent further gravitational collapse. To completely model the interior structure, and subsequent evolution of these objects requires the following input physics :

- the standard equations of stellar structure
- a detailed knowledge of the equation of state
- an understanding of the energy transport mechanisms (in the case of a brown dwarf or VLMS, this would be convection)
- a knowledge of the surface boundary condition (the atmosphere)
- and an understanding of the energy generation mechanisms where appropriate i.e. deuterium and lithium burning.

2.2.1 Evolution of Brown Dwarf ($M < 0.08M_{\odot}$)

At ages before 10^6 years, a brown dwarf will contract under gravity at constant effective temperature (T_e) with decreasing radius and luminosity as they follow the Hayashi track towards the main sequence. They will never reach this destination but will, for a short time period, ignite their small reservoir of deuterium, keeping constant radius, T_e and luminosity, as they sit on the 'deuterium main sequence' for about 3 million years. Once the small fraction of deuterium has been consumed hydrostatic equilibrium breaks down and the brown dwarf will start to contract again. This further contraction leads to the onset of electron degeneracy. The central temperatures never reach the $3x10^6$K required to ignite hydrogen, but the contraction eventually stops, limiting the radius, and allowing the brown dwarf to cool and fade. Figure 2.1 shows how the luminosity, T_e, central temperature T_c and radius evolve with time, using the models of Nelson, Rappaport & Joss (1986).

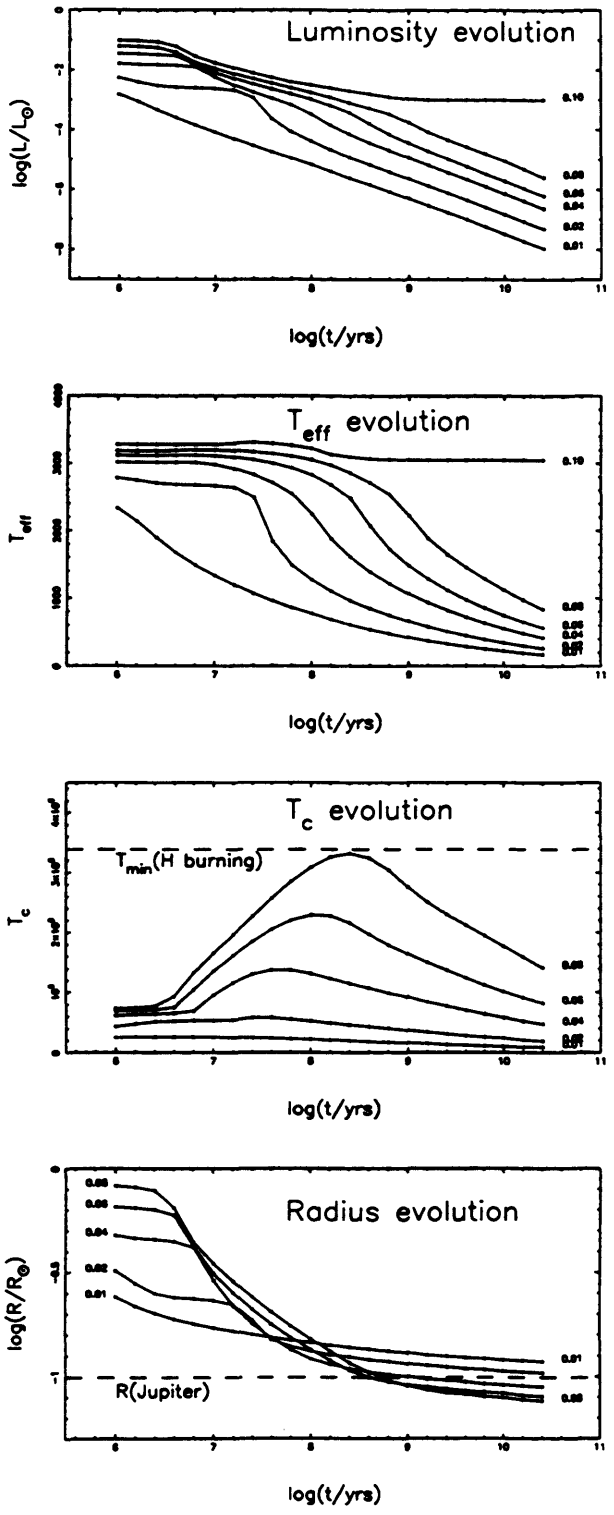

Figure 2.1: The evolution of the luminosity, T_e, T_c and radius of a brown dwarf using the models of Nelson, Rappaport & Joss (1986), courtesy of Pinfield (1997)

2.2.2 The Presence of Lithium

As stated previously, the interior of a VLMS or brown dwarf is fully convective. This means that elements such as lithium (Li) are well mixed at an early evolutionary stage, over relatively short time scales. Li ignites at temperatures above 2.4x10^6K and follows the reactions :

$$\begin{aligned} Li^6 + H^1 &\rightarrow He^3 + He^4 \\ Li^7 + H^1 &\rightarrow 2He^4 \end{aligned} \tag{2.1}$$

If the central temperatures exceed 2.4x10^6K, then Li will be depleted. Conversely, if Li is detected in the spectra of a brown dwarf candidate, then its central temperature must be below this. Ignition of hydrogen will not have occurred and one will have further confirmation towards identification of a sub-stellar object. A brown dwarf with mass below 0.06$M_\odot$ will never burn its lithium. This spectroscopic test, first proposed by Rebolo, Martin & Magazzu (1992), requires observations of the Li line at 670.8 nm. Observing a spectroscopic line in the optical may not sound like the most effective use of observing time for a brown dwarf that emits most of its flux at infrared wavelengths. Unfortunately, due to the low temperatures of these objects, the lower levels of the infrared Li lines are underpopulated with respect to the ground level making them much weaker than the 670.8 nm resonance doublet. Successful observations of this doublet have been made and are described in further detail later on in this chapter. At this stage it is worth noting that the detection of Li not only aids the identification of an object's sub-stellar nature, but depending on the relative abundance of this element, it is possible to infer an age. Basri, Marci & Graham (1996) use this "lithium dating" technique to estimate an age for the Pleiades and Figure 2.2 shows how they do this. The time scale for depletion of Li is relatively small and so using good models of stellar evolution one an determine an age quite accurately. Figure 2.2 shows the position of HHJ3 and PPL15 (see section 2.3.2) in the log luminosity, age diagram. The authors have plotted the mass isochrones and lithium depletion boundaries from the models of Nelson, Rappaport & Chiang (1993). The error bars on both HHJ3 and PPL15 are large in the log luminosity axis as a direct result of the difficulty in calculating luminosity from observable quantities such as magnitudes. However, the positions of both objects indicate the most conservative determination for the cluster age. As no abundance of lithium was detected in HHJ3, the bottom of the error bar could in theory be placed within the shaded "Lithium Depletion Region" on the diagram, thus narrowing the

age range of the cluster. By presenting the diagram as they have, the authors have determined the largest possible age range.

2.2.3 Atmosphere

A brown dwarf atmosphere is particularly difficult to model. The effective temperature of such an object can be anything below about 3500K and so the presence of molecules in the atmosphere causes all kinds of problems for the theoretician. Molecules such as TiO, H_20 and in lower temperature objects, CH_4, dominate, leading to complicated and extensive opacity tables. In the lowest mass, and coolest objects, the condensation of certain molecules into 'grains' has been predicted; see Allard *et al.* (1997) for a comprehensive review of our current understanding of the atmospheres of these objects. The presence of grains complicates the model even further. It is not reasonable therefore to model the flux from a brown dwarf using a simple blackbody. The spectrum of a brown dwarf or VLMS shows no real evidence of a true continuum and so there are no real 'anchor' points for such a treatment. Molecular absorption coefficients are highly wavelength dependent, so using a grey (non-wavelength dependent) approximation to model the atmosphere is no longer valid. Pioneering work by Allard (1990) and the work on dust formation by Tsuji, Ohnaka & Aoki (1996), have substantially improved our understanding of these very low-temperature atmospheres. Using the latest 'NextGen' models of Allard & Hauschildt (1997), Chabrier & Baraffe (1997) present evolutionary calculations for non-gray atmospheres at various different metallicities which include the most up to date and complete line lists for H_2O, the dominant opacity source in the infrared. The work of Allard and her collaborators has coupled the inner structure and atmospheric models together and incorporates a much better treatment of molecules such as Ti0 and H_2O. The new models produce theoretical spectra which allow the direct derivation of important observable quantities such as magnitudes and colours.

2.2.4 From Models to the Observational Plane

Prior to the latest model calculations it was standard practice to take the model parameters such as T_e and luminosity and use bolometric corrections and colour temperature relationships to estimate masses for any VLMS or brown dwarf candidates discovered observationally. This was a particularly tricky process as the models always appeared to over estimate the temperatures of these very low-mass objects. The work of Chabrier & Baraffe (1997) and Allard *et al.* (1997) however

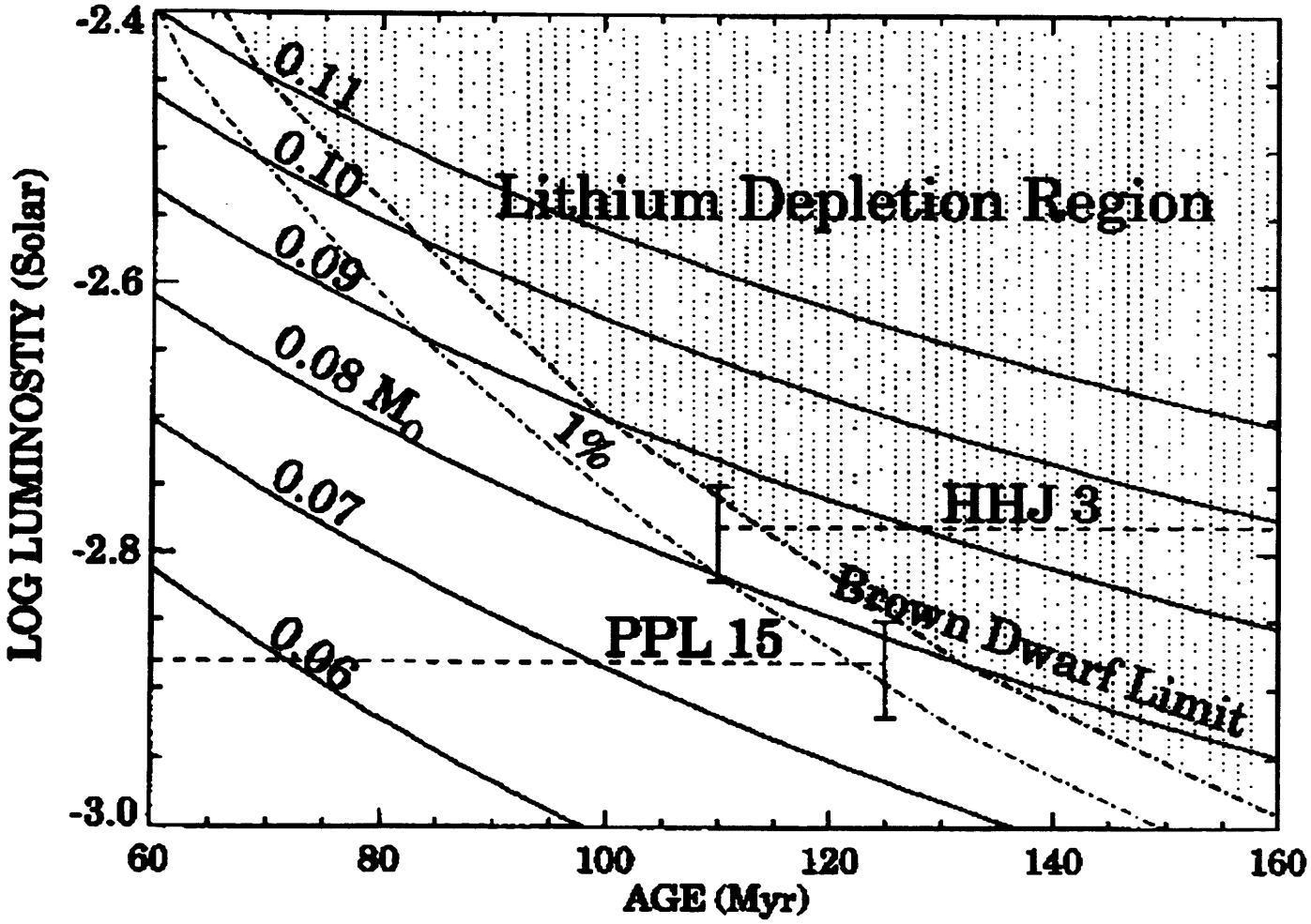

Figure 2.2: Determining the age of The Pleiades from measurements of the lithium abundance of two objects, PPL15 and HHJ3, the former showing partial depletion of lithium and the latter showing no evidence of the element. Using the models of Nelson, Rappaport & Chiang (1993) to plot the various mass isochrones, one can use the Li abundance observed (the depletion boundary and 1% level shown) and object luminosity to determine an age for the cluster. Courtesy of Basri, Marci & Graham (1996). Since this work, it has been found that PPL 15 is in fact a binary system. This changes the position of PPL 15 on the above figure, but does not affect the method behind the age determination.

has removed these problems in that their models provide absolute magnitudes for a complete range of masses for a range of different ages. Of course the observer must still determine an accurate distance and age for his/her observational sample, but by surveying in nearby clusters (see below) these parameters can be determined to some accuracy.

2.3 The History of Brown Dwarf Research

2.3.1 As Companions to Other Stars

Arguably, one of the first survey techniques, was the search for very low-mass companions to other stars. Some surveys have been more successful than others. Jameson, Sherrington & Giles (1983) surveyed areas around 21 nearby stars using both the United Kingdom Infrared Telescope (UKIRT) and the Anglo Australian Telescope (AAT), but failed to make any positive detections. They concluded that any companions must be rare unless they were closer than 10 arcsec from the primary star.

McCarthy, Probst & Low (1985), using speckle interferometry, claimed to have found a companion to VB8. For some time this was believed to be final evidence of the existence of sub-stellar objects and even resulted in an international conference on brown dwarfs. Unfortunately, the brown dwarf did not actually exist, and was dismissed after almost 2 years of astronomers claiming to have seen it.

Becklin & Zuckerman (1988), Zuckerman & Becklin (1988) and Zuckerman & Becklin (1992) used infrared photometric techniques to survey 200 white dwarfs. They found 21 low-mass companions and one brown dwarf candidate GD165B. Using the models of Nelson, Rappaport & Joss (1986) and D'Antona & Mazzitelli (1985), they estimated a temperature of 2100K, (from its highly unusual optical spectrum), and mass in the range 0.06 $M_\odot$ to 0.08 $M_\odot$. From these results they concluded that the initial mass function was flat or increasing down to 0.10 $M_\odot$ but suspected a rapid decline below 0.08 $M_\odot$.

Skrutskie, Forrest & Shure (1989) searched for faint infrared companions to 55 stars in the solar neighbourhood. Using an infrared K-band array and covering a 14 arcsecond field of view around each target star, they discovered one red companion to Gliese 569. The infrared colours of this object suggested that the companion had a mass in the range 0.06 $M_\odot$ to 0.09 $M_\odot$. The very low success rate from this survey

led the authors to conclude that the mass function (see section 8.1.1), was flattening below 0.20 $M_{\odot}$.

Kirkpatrick *et al.* (1994) derived a mass, spectral type relationship for very late M dwarfs. In this work, the authors use speckle and infrared photometry, parallax measurements and obtain spectra for a number of suspected low-mass components to binary systems. They concluded that objects of spectral type M7 and later are sub-stellar, but conceded that they can only be sure of this result when a low-mass binary system with dynamically determined masses, is studied in the same way.

One of the most exciting discoveries to date is documented by Nakajima *et al.* (1995) who are surveying all nearby stars less than 15pc away using both optical coronagraphic and direct infrared imaging methods. They have discovered a companion to the nearby (approximately 5.7pc away) M1V star GL229. The point to note regarding this important discovery is the appearance of methane (CH_4) in the infrared spectrum of this object, similar to that seen in the spectrum of Jupiter. This object presently holds the record for the lowest temperature brown dwarf / giant planet known outside our own solar system. The orbital period of the system is of the order of 10 years and so a dynamical mass estimate has yet to be determined. Based on kinematical arguments that GL229A is a young disk population star of low space motion, the age was inferred to be less than our Sun, but because of the absence of Hα in GL229B's spectrum, an age greater than 0.5 Gyrs is more likely. As the atmosphere of the object is metal rich, its maximum age is unlikely to exceed 5 Gyrs. Using these two age constraints, the mass of GL229B was determined to be in the range of 20 to 50 Jupiter masses, from the non-gray models of Allard *et al.* (1996). From the very cool atmosphere as seen from the spectrum of GL229B, the latest models predict an effective temperature below 1200K, with a more likely value approaching 900K. GL229B was the only companion to be discovered from the first 100 target stars analysed from the survey. From these kind of statistics, the likelihood of discovering a second GL229B type object in the survey sample is small.

2.3.2 The Pleiades

Many brown dwarf surveys have been conducted in the Pleiades open cluster. The cluster is near enough so that the lower main sequence is not too faint, but far enough away so that the area of sky covered, (approximately 20 sq deg), is not too large. The cluster is young enough so that any brown dwarfs will be relatively bright. A

0.07 $M_\odot$ brown dwarf will have log $L/L_\odot$ ~-2.7 and log T_{eff} ~3.495 (e.g. D'Antona and Mazzitelli 1994).

The first CCD survey for very low-mass stars (VLMS) and brown dwarfs in the Pleiades was conducted by Jameson & Skillen (1989) and covered an area of 125 arcmin^2 at R and I. Using the theoretical models of D'Antona & Mazzitelli (1985) and those of Nelson, Rappaport & Joss (1986) this survey presented 9 low-mass objects with 5 possible brown dwarf candidates. Follow up work found them all to be field objects.

Stauffer *et al.* (1989) surveyed approximately 900 arcmin^2 of the cluster at V and I with interesting candidates followed up at J,H and K, concluding that any low-mass stars in the cluster would make no significant contribution to the mass of the cluster. The limiting magnitude of this particular survey was V=19. Stauffer, Hamilton & Probst (1994) have extended this survey to 0.4 sq deg, (approximately 5% of the cluster), finding 6 brown dwarf candidates in total. As a test for brown dwarf status, one of these candidates, PPL15, has been followed up by obtaining high resolution spectroscopy and infrared photometry Basri, Marci & Graham (1996). The detection of the lithium absorption feature at 670.8 nm in PPL15 supports its identification as a brown dwarf candidate. The detection of this lithium absorption feature is a very significant discovery. The partial depletion of lithium in PPL15 suggests that it may be some kind of 'transition' object and is discussed in more detail in chapter 6.

200 arcmin^2 of the cluster was imaged by Simons & Becklin (1992) at I and K. Claiming to be the most sensitive survey to date, an upper limit of 22 objects were found. Spectra of these objects have yet to be published.

A survey of the cluster was carried out by Hambly, Hawkins & Jameson (1991) by obtaining R and I Schmidt plates that covered essentially the whole cluster. The COSMOS automatic measuring machine at the Royal Observatory, Edinburgh, was used to measure the plates. Assuming an age of 63Myrs for the cluster, this work presented 30 brown dwarf candidates and concluded that the resultant mass function was flat at the lowest masses. This work continued with a deep proper motion survey of the cluster. Hambly, Hawkins & Jameson (1993) presented a proper motion membership list for the mass range $0.08 < M_\odot < 0.50$, based on a $\sim$ 25 square degree area. A list of all members with coordinates, R and I photometry and proper motion, was given along with a finding chart for each candidate. The difference in time between first and second epoch plates in this survey was of the order of 40 years. The members from this survey have been termed HHJ stars. Steele,

Jameson & Hambly (1993) followed up the proper motion survey by obtaining JHK photometry for 48 of the HHJ stars. By obtaining R,I CCD photometry for 15 of the stars, the authors were able to estimate the errors of the R,I photographic photometry from the original survey. Using an upper limit of 70Myrs for the age of the cluster, 22 cluster members are presented with masses believed to be below the sub-stellar limit of 0.08 $M_{\odot}$. Based on the I versus I–K diagram that resulted from this work, a number of candidates were thought to be binary systems. Steele *et al.* (1995) obtained infrared spectroscopy, using CGS4, for a number of targets in the photometric sample. One object HHJ54 did show signs of binarity from investigation of infrared spectral features, suggesting that its companion may have a mass as low as 0.035 $M_{\odot}$. They also found that Pleiades objects have slightly lower surface gravities than main-sequence objects of the same temperature, which supported their identification as pre-main-sequence cluster members. The two faintest HHJ stars, 2 and 3, still remained as good brown dwarf candidates. The work of Marcy, Basri & Graham (1994) however removed the tenuous brown dwarf status from these 2 candidates, after lithium was found in the candidate PPL15 (see earlier), but not in HHJ3. This was a crucial result, in that the sub-stellar limit within the Pleiades cluster had now been identified, and the fine line between stars and brown dwarfs could now be drawn. It was not long before a brown dwarf was found within the cluster that showed no signs of any lithium depletion. Rebolo, Zapatero-Osorio & Martin (1995) discovered Teide 1 from a CCD survey of the cluster using the R and I filters. The survey determined the proper motion of the candidate by using CCD images taken in 1986 at the Isaac Newton Telescope (INT). The presence of Teide 1 on the 1986 images was missed by the investigators at that time, see Jameson & Skillen (1989). With a proper motion and radial velocity consistent with the cluster, Hα in emission, and a good optical spectrum showing the dominant TiO and VO molecular bands, Teide 1 achieved the brown dwarf status. Using the theoretical evolutionary tracks and isochrones from Burrows *et al.* (1993), an upper limit of 50 Jovian masses was determined for the mass of Teide 1 and log $L/L_{\odot}$=-2.7.

The Pleiades has always been a popular hunting ground, but with the discovery of Teide 1 and the identification of the sub-stellar limit somewhere between PPL15 and HHJ3, brown dwarf searches within the cluster became more and more common. The follow-up survey to Rebolo, Zapatero-Osorio & Martin (1995) was undertaken by Zapatero-Osorio, Rebolo & Martin (1997) and found a total of eight brown dwarf candidates. One of these was shown to be a foreground object contaminating the sample and one, a Pleiades brown dwarf (confirmed after low-resolution spectroscopy,

detailed in Martin, Rebolo & Zapatero-Osorio 1996, and given the name Calar 3). By obtaining J,H and K photometry for a number of VLMS and some of the brown dwarf candidates discovered previously, Zapatero-Osorio, Martin & Rebolo (1997) attempted to identify the differences between stellar and sub-stellar objects from their infrared colours. This was achieved by careful consideration of the positions of cluster members compared to non-members on a number of two colour diagrams. Rebolo *et al.* (1997) presented 10m Keck spectra of both Teide 1 and Calar 3. Both spectra show clear detections of the lithium line at 670.8 nm. As a result, regardless of the cluster age, both objects with their very low luminosities and lithium detections, lie well into the cluster's brown dwarf realm.

Using the Hale 200 inch telescope, Williams *et al.* (1996), in continuing the early survey work of Stauffer, Hamilton & Probst (1994), identified a small number of faint red stars in the optical. With infrared images taken using the Steward Observatory 2.3m telescope, they present a V versus V–K colour-magnitude with one potential brown dwarf candidate. Many surveys use photometric identification of sub-stellar candidates as the first step before following up with infrared photometry, optical and infrared spectroscopy, proper motion measurements and if possible, the detection of lithium using high resolution optical spectroscopy. The initial photometric identifications outlined in the above surveys relied on the fact that VLMS appear red in V–I, R–I, V–K and so on. The surveys that are described below were the first to use the I–Z colour as a detection discriminant. An outline of the advantages of using this colour is described in chapter 5 and will not be presented here. However, it is important to point out here that the first I, Z survey of the Pleiades cluster was conceived and undertaken by the Leicester Astronomy group. In Cossburn *et al.* (1997) a small I, Z survey was carried out using the INT on the island of La Palma. Initially the project was designed to cover as large an area of the cluster as possible but due to extremely poor weather conditions during the run, only 900 arcminutes^2 were imaged in the two filters. The specifics of the run and the subsequent data reduction are described in chapter 6. One brown dwarf, PIZ 1, was identified after follow-up infrared photometry and spectroscopy. Its estimated effective temperature and mass are 2300K and 48 Jupiter masses respectively. A proper motion measurement is essential to establish cluster membership. Shortly after the discovery of PIZ 1, a much larger CCD I, Z survey of the Pleiades was carried out by the International Telescope Project (ITP); a collaboration between the Instituto de Astrofisica de Canarias (IAC) and the Leicester group. A total area of approximately 1 deg^2 in the central region of the cluster was surveyed. More than 40

faint (I≥17.5) red (I–Z≥0.5) objects were detected. Intermediate to low-resolution spectroscopy of 7 of these candidates showed that 5 were likely cluster members, see Zapatero-Osorio *et al.* (1997).

As the lack of flux in the V and R bands became more apparent for objects of such low-mass, surveys began to use filter combinations centred further into the infrared. Festin (1997) surveyed 180 arcminutes^2 of the cluster using the I,J and K filters, down to a completeness limit of I=21.6. From this relatively small survey area only one new candidate was found, with a likely mass of 0.08 $M_{\odot}$. Using the R,I,J and K filters and covering a larger 850 arcminutes^2 of the cluster, Festin (1998) finds 8 new candidates, four of which are below the brown dwarf limit. The faintest has a mass of just 0.04 $M_{\odot}$.

From optical and infrared photometry that places it on the cluster sequence slightly below the sub-stellar limit, a new candidate, Teide 2, has been the subject of a recent spectroscopic observation by Martin *et al.* (1998). The lithium line has been detected and Hα is seen in emission. Objects in this very narrow region between stars that burn their hydrogen and those that are sub-stellar that don't, play a crucial role in determining the age of the cluster. Recently Stauffer, Schultz & Kirkpatrick (1998) have observed a number of these 'transition' objects by resolving the lithium line and determining the level of depletion. Basri, Marci & Graham (1996) showed how the cluster age could be found if an accurate measurement of the strength of the lithium line was made, see Figure 2.2. In the same way, these new observations have constrained the cluster age to be between 100 and 120 Myrs. The paper also supports the conclusion of Martin *et al.* (1998) that Teide 2 is a Pleiades member.

Finally, at the time of writing, two further surveys are about to be published. A 2.5 deg^2 survey of the cluster at R and I by Bouvier *et al.* (1998) finds 26 objects whose position on the I, R–I colour-magnitude diagram make them likely cluster members. The second survey by Hambly *et al.* (1998) presents 8 new brown dwarf candidates selected because they had both very red photographic colours and had proper motions consistent with cluster membership. The candidates all lie around the sub-stellar boundary within the cluster, with I magnitudes around 18.0.

2.3.3 Praesepe

The Galactic open cluster Praesepe is much older than the Pleiades. As a result of the difference in age, any brown dwarfs in this older cluster will have cooled over a

longer time scale and will have fainter apparent magnitudes as a result. Searches for sub-stellar objects therefore require long exposures to obtain the deepest image possible, and increase the chance of a positive detection.

Williams *et al.* (1994) obtained spectral types, Hα equivalent widths, and optical photometry for a sample of late K and M dwarfs, believed to be candidate members of the cluster from their position on a colour-magnitude diagram. From their position on the V versus V–I diagram seven candidates were identified as probable non-members. The latest spectral type of the photometrically identified members is M4. A deep proper motion and photometric survey of a 19 deg^2 area of the cluster was undertaken by Hambly *et al.* (1995a). Objects with photometry and proper motions consistent with the cluster were termed HSHJ stars, and over 500 were identified. Candidates were cross referenced with previous surveys, with finder charts, photometry and proper motion measurements presented. The survey extended any previous search by between 3 and 4 magnitudes at R.

Applying the R, I and Z filter combinations to a Praesepe survey, Pinfield *et al.* (1997) covered a central region of approximately 1 deg^2. Twenty six new photometric candidates were identified with I>17.8. By extending the cluster main sequence to I=21.5, nineteen new brown dwarf candidates were found, with a possible two binary systems in the sample. Follow-up observations of a number of these candidates were undertaken on a recent observing run at UKIRT, the results of which are outlined in chapter 7. The first likely identification of a brown dwarf in the cluster was made by Magazzu *et al.* (1998). The object, Roque Praesepe 1 (RPr 1), has an I magnitude of 21.01 and I–K colour of 4.57. From the low-resolution spectrum presented in this paper, it is immediately obvious that RPr 1 is a very late object. The mass range estimated for this object is between 0.063 and 0.084$M_{\odot}$. The authors also estimate the likelihood that RPr 1 is a late M field dwarf contaminating their sample. From their analysis, RPr 1 has a 4 times higher probability of belonging to Praesepe than of being a field star.

2.3.4 The Hyades

The Hyades lies at a distance of 48 pc and has an approximate age of 6x10^8 years. Its close proximity makes it an ideal cluster for brown dwarf searches but its age means that any brown dwarfs present will have had longer to cool and will therefore be fainter and harder to detect. The first deep photometric survey of the cluster was carried out by Leggett & Hawkins (1988). Leggett, Harris & Dahn (1994) presents

V and I photometry for the low-mass stars in the cluster and reviews the proper motion Schmidt plate surveys of Reid (1992), Reid (1993), Bryja *et al.* (1992) and Bryja, Humphreys & Jones (1994). As a result the main sequence can be traced down to M_I=14.6.

2.3.5 In The Field

Searching for brown dwarfs in the field is a particularly tricky business. In a cluster environment, many of the important characteristics of any cluster members discovered are already known, e.g., the age, distance and metallicity. When searching in the field, none of these parameters are directly available. One can infer an age from an object's space motion, rotation rate and perhaps surface activity. For nearby candidates, obtaining a parallax and thus distance allows a luminosity determination. If lithium is observed and a very low-luminosity is apparent then the brown dwarf status moves ever closer. Jones, Miller & Glazebrook (1994) identified a brown dwarf candidate during an infrared survey for faint red galaxies. However, after follow-up imaging and spectroscopy, discovered that this candidate may have a fainter, extremely red companion. It is not known if JMG 0918-0023 A and B are physically associated. If they are, then JMG 0918-0023 B would be a GD165B type object, with temperature between 1600 and 2262 K, depending on the model used. The suggestion that the luminosity function does not drop rapidly into the brown dwarf regime was also presented.

By digitally stacking Schmidt plates, limiting magnitudes of I=21.5 and R=23 were achieved by Hawkins (1994), for a large area 25 square degree survey. Preliminary follow-up spectroscopy identified one candidate brown dwarf, D04. Its spectrum showing the characteristic features of TiO and VO, typical of late M dwarfs. A detailed report of the plate stacking method and its results can be found in Hawkins *et al.* (1998). A total area of 25 deg^2 was covered using a stack of around 100 plates. Objects with large R–I colours were selected for follow-up observations, which included infrared photometry and optical spectroscopy. 5 candidates were also selected for a parallax programme and found to be at a distance of approximately 45 pc. When plotted on a K versus I–K colour-magnitude diagram, the new candidates lie 3 magnitudes fainter than previously discovered M7 and M8 objects of the same R–I colours, including the Pleiades brown dwarfs, Teide 1 and Calar 3. The authors propose that the presence of dust in very late-type M dwarfs will enhance the R magnitudes of such objects relative to the hotter late-type M dwarfs

in the Pleiades, and thus decrease the R–I colour. Combining this with the possibility that dust formation is gravity dependent, lower gravity Pleiades brown dwarf candidates, will have larger R–I colours. One object, 296A, (Thackrah, Jones & Hawkins 1997), discovered from the Schmidt plate survey, has a photographic R–I colour of 2.54, and was selected for further study as a direct result of its apparent brightness, I=14.57. Spectroscopic observations detected Hα in emission and the lithium absorption line at 670.8 nm. Based on VO absorption features, a spectral type of M6$\pm$0.5V was assigned. Using CaH, Ca II and Na I absorption features, the gravity of 296A was determined and found to be consistent with Pleiads of similar spectral type. A parallax has not yet been determined for 296A, so its absolute properties have yet to be resolved, but the authors believe that it may be a PPL 15 type object. It does take the prize for the first detection of lithium in a field brown dwarf candidate.

Ruiz, Leggett & Allard (1997) discovered a nearby, (10 pc), free floating brown dwarf that also exhibits lithium in its optical spectrum. It shows no sign of TiO or VO in its optical spectrum. From comparison with the latest evolutionary models of Chabrier & Baraffe (1997), Kelu-1, as it has been named, has an effective temperature of around 1900K, and mass below $0.075 M_{\odot}$. Tinney (1998) presents the discovery of lithium in LP944-20 (also known as BRI0337-3535) and infers a mass between 0.056 and 0.064 $M_{\odot}$ and age between 475 and 650 Myr. The identification of free floating brown dwarfs and discovery of lithium at 670.8 nm, is no longer a rarity. The discoveries outlined above mark the beginning of a new era in brown dwarf research. Two major surveys are underway, with preliminary results already available; the DENIS (DEep Near Infrared Survey) survey of the southern sky, and the 2MASS (2 Micron All Sky Survey) survey of the entire sky. Delfosse *et al.* (1997) presents 3 extremely low-mass candidates, one with a lithium detection, another with evidence of methane absorption. Kirkpatrick, Beichman & Skrutskie (1997) presents follow-up spectroscopy of 8 2MASS candidates. Both papers present objects with optical spectra unlike anything previously seen. Many candidates have been tentatively classified as >M10, or L-type objects. The TiO and VO bands that dominate the optical spectra of late M dwarfs are no longer seen, and so the newly proposed L class would include objects with temperatures somewhere between 2000 and 1500K.

2.4 Conclusions

In this review chapter the many varied survey techniques and locations have been outlined. The successes and failures have moved the field on from tentative classifications of brown dwarf candidates on the sub-stellar boundary, to bona fide brown dwarfs in open clusters, as companions to other nearby stars, and as free floaters in the field. The preliminary results from the DENIS and 2MASS surveys have turned up a number of candidates of spectral type L, with completely different spectral characteristics in the optical to late-type M dwarfs. The results of both these large scale surveys are eagerly awaited as they have potentially dramatic consequences in our understanding of the field star luminosity and mass functions.

Chapter 3

Instrumentation and Software Review

3.1 Introduction

In this chapter I will outline the characteristics of the detectors I have used in the different observational programmes undertaken as part of my Ph.D. There then follows a description of all the necessary steps involved in the subsequent data reduction, required to accurately obtain fluxes, magnitudes and reduced spectra from the raw data.

3.2 Charged Coupled Devices CCDs

A CCD is a semiconductor device normally composed of wafers of Silicon (Si). Electrodes are laid down on these wafers in an array structure, called pixels. When an optical photon is incident on the CCD, electrons in the semiconductor are excited into the conduction band and held in place by a small positive voltage applied across the electrode. These pixels therefore act as 'buckets', storing up the electrons. The energy required to excite an electron into the conduction band is relatively small, ($\sim$ 1eV), so without cooling of the CCD, the thermal excitation of electrons into the conduction band is significant. The resultant current is called the dark current, and to keep this to a minimum (less than 10 electrons/hour/pixel) the detector is cooled using liquid nitrogen to temperatures of the order of 150K. When an exposure is complete the CCD is readout by sequentially switching the electrode voltage so that the 'buckets' of charge are moved across the device until they reach a field effect transistor (FET). The voltage from the FET is amplified and stored digitally which

introduces a certain amount of noise, called the readout noise. In the latest CCD devices, this noise is less than 5 electrons per pixel.

It is fair to say that CCDs have revolutionised the field of optical astronomy for a number of reasons. They have a high quantum efficiency compared to photographic plates and photomultiplier tubes. Between 50 and 90% of the incident photons excite electrons into the conduction band of the semiconductor. A CCD is linear at most count rates and has a large dynamic range. They can have up to 2048x2048 pixels and thus cover a significant area of the sky. This in turn allows differential photometry in poor weather conditions. Generally, the sensitivity of a CCD peaks in the red, somewhere between 600 and 800 nm. The blue response can be improved however by coating the device with phosphor.

3.2.1 CCD Data Reduction

The first step in the reduction process is to subtract a bias and dark frame from the CCD image. Modern CCD detectors have minimal dark current and so this may not be necessary in all cases. Indeed for the observations in this thesis using the La Palma CCDs, a dark frame was not subtracted for this very reason. A bias frame is a frame of zero exposure which is subtracted to remove the CCD's electronic bias.

The next step is to 'flatfield' the image. The pixel to pixel sensitivity across the CCD will vary and this has to be taken into account. A 'flatfield' image can be obtained in a number of ways. A short exposure of the illuminated inside of a telescope dome with the telescope defocussed is one method. Alternatively, an exposure of the twilight sky at the beginning or end of the night will suffice and perhaps best of all by median filtering a number of long exposures from one night in each respective filter. Whichever method is employed, the purpose is to adequately illuminate the CCD so that the sensitivity across the chip can be modelled and removed from the target images. The presence of fringes and cosmic rays on a CCD image requires further median filtering techniques for their removal. Normal procedure is to median filter using 5 or more images taken with the same filter. For some observing runs where limited time is available, such as large area surveys, obtaining multiple images of the same field using the same filter is not always possible. The flatfielding and de-biasing outlined here are done using various software packages. In the context of the work carried out in this thesis, the IRAF suite of packages, in particular, the CCDPROC routines were used to perform such tasks.

The extraction of counts from each image is now possible. The IRAF routine

DAOFIND can search an image for point sources with the PHOT package used to determine subsequent instrumental magnitudes. These aperture photometry packages along with the STARLINK GAIA package allow interactive data reduction to take place. The user can vary the aperture, sky background estimate and full width half maximum (FWHM) to accurately obtain resultant magnitudes. The methods employed to calibrate these instrumental magnitudes are outlined below.

3.3 Infrared Arrays

Infrared arrays are semiconductor devices also. IRCAM3 on the United Kingdom Infrared Telescope (UKIRT), on Mauna Kea in Hawaii, is composed of Indium Antimonide, (InSb). IRCAM3 is a cooled 1 to 5 micron camera with a 256 x 256 array and $\sim$ 0.3 arcsec/pixel plate scale. Using the infrared J,H,K,L and M filters, it has a much smaller field of view than a CCD detector and needs to be cooled to temperatures as low as 35K to reduce the dark current. Even at these temperatures the dark current is significant. A 'dark' exposure is taken before a target image to remove the dark current in the later data reduction stages, see below.

3.3.1 Infrared Data Reduction

As a result of the increased dark current associated with the infrared detectors, the accurate subtraction of a dark frame is essential. A dark frame is taken before any target observations are made and the infrared data reduction package IRCAMDR makes this subtraction automatically. Exposures are taken such that the telescope moves in a 'jitter' pattern taking five different images of the same target. As the sky is so bright at infrared wavelengths, median filtering to produce a flatfield is possible from this jitter pattern of images and again, the IRCAMDR package automatically does this. Once the dark frame has been subtracted and the image has been flatfielded using the median filtering outlined above, aperture photometry can take place. The IRCAMDR and GAIA packages provide the tools necessary to perform aperture photometry on both crowded and isolated star fields. Both give instrumental magnitudes that need to be calibrated as outlined in the next section.

3.4 Spectroscopy

My experience of spectroscopic data reduction is limited to the reduction of data taken using the ISIS spectrograph in service time on the William Herschel Telescope (WHT) in La Palma, (see Cossburn *et al.* (1997) for the reduced spectrum of PIZ 1). The use of CCD detectors in modern spectroscopy means that bias and flat field images are needed as with stellar photometry. Obtaining a good flat field image is essential in the removal of the pixel-to-pixel gain variations across the chip.

A simple, schematic diagram of a stellar spectrum is shown in 3.1. This is presented to help explain the following reduction steps necessary to extract and calibrate a spectrum. All software routines referenced are part of the IRAF reduction package.

- Flatfielding.
  Obtaining a good flat field image is essential. A tungsten filament lamp is normally used to illuminate the chip and any pixel-to-pixel variations across the chip can then be removed.

- Finding the spectrum.
  Using the IMPLOT routines, a cut across the spatial axis indicates where the spectrum is by its corresponding peak above the background.

- Define the extraction and background windows.
  Using IMEXAMINE one can examine the number of pixels to the right and left and right of the centre of the spatial profile and thus specify the size of the extraction window. The background window can be specified in a similar manner. This process is iterative and the relative positions and sizes of each window can be adjusted.

- Trace the centre of the spatial profile as a function of the dispersion axis.
  This is necessary because in practice the spectrum is never parallel to the dispersion axis. There are 3 common reasons for this :
  (1) the camera optics introduce a distortion along the dispersion axis;
  (2) the gratings rarely sit exactly square in their cells;
  (3) as a result of atmospheric refraction, the blue end of the spectrum will be

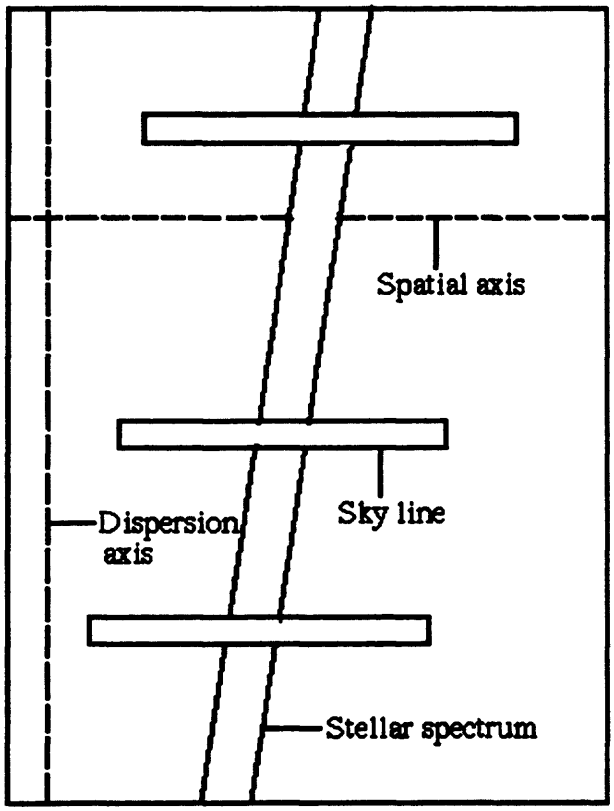

Figure 3.1: A schematic view of a 'perfect' stellar spectrum.

shifted along the slit closer to the zenith than the red end of the spectrum.

- Sum the spectrum within the extraction window and make a sky subtraction. Using the trace, as described in the last point, the spectrum within the extraction window is summed at each point along the dispersion axis. The sky background is subtracted at each point during this process.

- Perform a wavelength calibration.
  This requires a number of steps as outlined below:
  (1) A comparison spectrum observed at the same time as the target object is extracted in the same manner as described above.
  (2) A dispersion solution is determined for the comparison spectrum.
  (3) The dispersion solution is used to put the target object spectrum on a linear wavelength scale.

- Normalize or flux calibrate the spectrum.
  One can flux calibrate the spectrum if one has observed a suitable spectrophotometric standard star. It is possible then to transform the data into either absolute or relative flux units.
  To normalize the spectrum, the simplest method is to fit a smooth function through the continuum and then divide the spectrum by this fit.

3.5 Calibrating the Instrumental Magnitudes

The previous sections have outlined the way in which photons are collected and the steps necessary to obtain instrumental magnitudes and reduce spectroscopic observations using the available data reduction packages. In this section I will outline how one transforms these instrumental magnitudes into calibrated magnitudes. The first thing to understand about the magnitude scale is that it is logarithmic and defined by Equation 3.1.

$$m_1 - m_2 = -2.5\log_{10}(I_1/I_2) \tag{3.1}$$

In Equation 3.1, I_1 and I_2 are the counts, gathered by the instrument/detector at the telescope, and m_1 and m_2 are the apparent magnitudes of any two stars that one may wish to consider. The distance to a star is not considered in the apparent magnitude. To determine the intrinsic luminosity of an object, one needs to calculate the absolute magnitude, M, defined in Equation 3.2, where d is the distance to the object in parsecs and A is the interstellar extinction measured in magnitudes.

$$m - M = 5\log_{10}\mathrm{d} - 5 + \mathrm{A} \tag{3.2}$$

Before being able to fully calibrate any instrumental magnitudes, one must introduce the quantity known as the zeropoint, which is a function of the instrument, atmosphere and telescope configuration. The zeropoint varies according to the amount of atmosphere that one observes through, or the airmass of the observation. The light from an object close to the horizon will have to pass through a greater proportion of the atmosphere than one that is directly overhead and so the airmass is proportional to sec z, where z is the angle between the object and the zenith. The zeropoint is defined in Equation 3.3 but is also a function of wavelength, as shown in Equation 3.4, where k is the wavelength dependent term.

$$\mathrm{Zeropoint} = \mathrm{m}_1 + 2.5\log_{10}(\mathrm{Counts/second}) \tag{3.3}$$

$$\mathrm{Zeropoint} = \mathrm{ksecz} + \mathrm{Zeropoint}_{(\mathrm{secz}=0)} \tag{3.4}$$

To determine the value of k in Equation 3.4 observations of standards are made throughout a night at various different airmasses. A curve of zeropoint against airmass is plotted (an 'airmass' curve) so that values of k for each filter for each night can be found. Once a zeropoint is determined, the instrumental magnitudes of the targets can be converted into apparent magnitudes using the above equations. It is important to note at this point that k has a dependence, albeit small, on stellar colour. It is vital that this colour correction is taken into account by observing standard stars that are of similar colour to the targets being observed. With an accurate airmass curve in place one can transform instrumental magnitudes into more useful apparent magnitudes.

3.6 Conclusions

In this chapter I have outlined the details of the different detectors used in collecting data at the telescope. These include the optical CCD detectors and infrared arrays. The physical characteristics of both are described in some detail. The data reduction techniques for each type of detector are explained in the context of the data reduction packages that I have used throughout my Ph.D. I have presented a general description of the steps required to reduce spectroscopic data also.

Armed with the raw photometric data, I have explained the basics of the magnitude scale and the necessary steps in the calibration process; from instrumental magnitudes and derivation of airmass curves through to calibrated apparent magnitudes. The advantages of using packages such as IRAF is that many of the stages in the reduction process outlined above may be automated. This greatly speeds up the process, especially during survey work, where one may have up to 100 images per night to reduce.

Chapter 4

HST Search for Brown Dwarfs

4.1 Introduction

The first project that I undertook was the reduction of data obtained prior to the start of my PhD. It is important to explain the background to these observations made using the Wide Field Planetary Camera (WFPC 2) of the Hubble Space Telescope (HST) and their relevance to this thesis.

4.1.1 Previous Work

The brown dwarf research group at Leicester has been carrying out intensive studies into the search for brown dwarfs in open clusters such as The Pleiades and Praesepe for some time. Proper motion surveys have been conducted in both clusters (Hambly, Hawkins & Jameson 1993 and Hambly *et al.* 1995a) identifying many stars down to the brown dwarf limit. Follow-up infrared surveys within the Pleiades cluster (Steele *et al.* 1995) along with spectra showing Hα in emission (Steele & Jameson 1995) reinforced the proper motion's survey conclusion that they are Pleiades members. However, when these objects are plotted on an I versus I–K diagram, they appear to lie on two sequences, a single star and a binary star sequence. With this conclusion in mind, an application was made for high resolution imaging time on the HST (Cycle 5). The idea was to image 8 objects, 6 of which were believed to be binaries, so determining the validity of the photometric test and allowing an estimate of the brown dwarf binary fraction to be made. The implications for the cluster mass function and star formation theory were important consequences of this work.

4.1.2 Why use the HST?

The HST has a resolving power of $\sim$ 0.1 arcsec so that binary separations $>$ 12 AU could be recognised. No ground based telescope could achieve this result since these objects are far too faint for speckle interferometry.

4.2 Observations

8 orbits of HST time in late 1995 were awarded to make high spatial resolution measurements. The observations were carried out using the F702W and F785LP filters. The target sample included the faintest (and reddest) objects from the I versus I–K diagram, as outlined above. The planetary camera PC2 was used to maximise spatial resolution. The F785LP filter was used to give the longest wavelength response consistent with a short exposure time and thus maximising the ability to see a 'cool' companion.

The field of view of the WFPC2 instrument is divided into 4 cameras by a fixed four-faceted pyramid mirror near the HST focal plane. The charge-coupled devices (CCDs) are thick front-side illuminated with a read-noise of 5 electrons (rms). The field of view of the wide field camera is 2.5x2.5 arcminutes and 35x35 arcseconds for the planetary camera. The 8 HHJ stars imaged were HHJ3, HHJ5, HHJ6, HHJ10, HHJ11, HHJ14, HHJ19 and HHJ36. Table 4.1 shows the coordinates and exposure times in each filter for these targets. Table 4.2 details the characteristics of the WFPC 2 instrument.

4.3 Data Analysis

The original data reduction was carried out by Dr. Simon Hodgkin in an attempt to resolve any possible binarity. The details of that analysis will not be outlined in this chapter suffice to say that no evidence for red companions was found for any of the targets. The 3 wide field cameras surrounding the planetary camera probed the Pleiades cluster to a much fainter magnitude than had previously been obtained from ground based telescopes albeit over a very small survey area. The data reduction and analysis that will be outlined in this chapter involved looking for any objects that appeared red in this Wide Field Camera data.

The data was analysed using 2 different methods. Originally, STARLINK software routines were employed to pick out sources from the images in each filter, using

Table 4.1: The coordinates and exposure times for each HST field.

Target Name	R.A. (J2000) (hms)	Dec (J2000) (dms)	F785LP [1] (secs)	F785LP [2] (secs)	F702W (secs)
HHJ 3	3 48 50.41	22 44 29.97	500	500	800
HHJ 5	3 44 35.88	23 34 41.82	500	500	800
HHJ 6	3 41 42.35	23 54 57.23	500	500	800
HHJ 10	3 48 35.17	22 53 42.11	500	500	800
HHJ 11	3 46 0.92	22 12 28.85	500	500	800
HHJ 14	3 45 12.59	23 53 45.22	500	500	800
HHJ 19	3 37 15.68	26 29 31.02	500	299	800
HHJ 36	3 49 15.58	23 22 49.56	500	500	800

Table 4.2: The characteristics of the WFPC 2 instrument

Camera	Pixel and CCD Format	Field of View	Pixel Scale
Wide Field	800x800 x3 CCDs	2.5x2.5 arcminutes	approx 100 milli-arcseconds
Planetary	800x800 x1 CCD	35x35 arcseconds	approx 46 milli-arcseconds

PISA (Position Intensity Shape Analysis) but these routines have certain drawbacks. PISA will search for faint sources where the flux is above some user defined detection threshold. Problems arise when ripples left over from the flat fielding process are misidentified as sources by the search algorithm. The second, more accurate method, involved using the software routines in IRAF. The routine DAOFIND searches for local density maxima with a certain user defined shape, i.e. the user defines the full width at half maximum FWHM. A lower and upper limit to the detection threshold can also be specified by the user. In general, the user has a greater control over the search algorithm and can raise or lower the sigma level of the detection.

4.3.1 Star Galaxy Separation

Using PISA routines to search for faint sources does not remove the problem of differentiating between a stellar shaped profile or a more flattened galactic profile. To help make this distinction the technique of plotting peak counts against total counts was employed. Figure 6.2 shows such a plot where the majority of sources lie in a well defined stellar band on this figure and represent stellar like profiles. Objects that have a more flattened profile, such as galaxies, lie below this band because their peak to total count ratio is not as high as that of a stellar object of the same magnitude. Any cosmic rays detected in the images should lie above the well defined band. This is because they have a particularly high peak count to total count ratio and appear as very well defined spikes on the images. The number of cosmic ray hits in the HST images is particularly high, due to the fact that the telescope is not shielded by the Earth's atmosphere like the more conventional ground based telescopes and detectors. As a result of the large number of cosmic ray events and few number of stellar sources detected, a star galaxy separation using this method is extremely difficult, as the stellar band is poorly defined. A new approach was employed and is described in the next section.

4.3.2 Cosmic Ray Removal

The presence of a large number of cosmic rays on the HST images makes the detection of very faint sources difficult. Two methods of removal were employed. For the reduction method using the PISA routines the algorithm was allowed to run as normal detecting sources above a certain fixed threshold. All three images (the 2 F785LP images and 1 F702W image) were registered so that bright sources common to all images had the same pixel coordinates to better than 1 pixel accuracy. I then

wrote a customised photometry program that identified source coordinates from each output photometry file within a certain pixel radius (1 or 2 pixels) and rejected any source that was not common to both the F785LP output files. This in effect removed any cosmic rays from these files. The program also checked with the output from the F702W file for coincidence in coordinates and followed a similar rejection procedure. The 2 filters used for these observations were similar in wavelength bandpasses to the standard R and I filters. The F785LP being more similar to the I filter and the F702W filter similar to the R filter. It was possible that some sources may have only been detected in the F785LP filters and not in the F702W filter. These would have been extremely red objects, just the kind being searched for. The program used to reject cosmic rays would not reject this type of source because they would appear in both F785LP images and would fulfil the first part of the selection criteria.

The IRAF software package is far more sophisticated when it comes to reducing data from the HST. There is a package specific to reducing this kind of data called STSDAS, and it has a number of routines which help to improve the image quality by mosaicing the wide field and planetary camera images together and then removing the cosmic rays from the resultant image. There is one drawback in this method. The removal of cosmic rays can only be accomplished if there are two images of the same area of sky in the same filter. For the F785LP images this is not a problem, but it means that the removal of cosmic rays from the F702W images is impossible. I have tried to use the software on the F785LP data with limited success, i.e. a better result would have been obtained with more than 2 images. The output image had most (approximately 90 percent) cosmic rays removed, but the background subtraction was not as good as it could have been. The resultant source detection procedures had to be performed interactively so that any spurious background fluctuations could be rejected from the output files.

4.4 Initial Results

4.4.1 The Colour-Magnitude Diagram

From the output of the IRAF analysis, a colour-magnitude diagram was plotted of the F785LP magnitude versus the F702W-F785LP colour. This is shown in Figure 4.1. The 8 HHJ stars are labelled along with 3 other brown dwarf candidates, labelled as HST-1,2 and 3. The cluster sequence is unfortunately very poorly defined due to a problem in the photometry of the HHJ stars. Each HHJ star is saturated on the CCD

in at least 1 pixel so that their position on the diagram is not strictly correct. As a result, any object that sits to the right of the background stars by any significant margin has been identified for follow-up infrared observations. An attempt was made to estimate the magnitude of the HHJ stars in these slightly unusual filters so that a conversion could be made between magnitudes in this system to those in the standard Cousins R and I. To do this a model point spread function (PSF) is needed, constructed from other unsaturated stars on the image. A simple technique in theory, but one that uncovers 2 main problems in practice. These are that there are very few unsaturated stars within the planetary camera image due to the very nature of the extremely small field of view. The other problem is the unusual profile of the PSF in the 'wings' which is incredibly difficult to model with only 1 or 2 stars available. After a number of unsuccessful attempts to model the PSF, the calibration of the filter system using this technique was abandoned.

4.4.2 Possible binary companions

The other significant result from this analysis was the discovery of 2 possible binary companions to HHJ 6 and HHJ 10. Figure 4.2 shows these in more detail. The objects could be faint background stars outside the cluster, but the estimated probability of a chance association is approximately 1 in 1000 for each detection, based on the relatively low number of sources detected in the WFPC2 survey. The candidate companions are approximately 5 to 6 magnitudes fainter than the HHJ primaries and lie at 0.8 and 1.8 arcsecs away from the target stars. If they could be shown to be companions they would be extremely low-mass brown dwarfs/planets. However the companions were not red, as would be expected for very cool brown dwarfs, but had neutral F702W-F785LP colours. To be completely sure about the nature of these objects infrared images were obtained of these HHJ stars.

4.5 Follow up Infrared Observations

4.5.1 Observations of HST-1, HST-2, HST-3

K band observations of HST-1 and HST-2 were obtained in service time at The United Kingdom Infrared Telescope in March 1997. K band images of HST-3 were obtained during a 9 night observing run at UKIRT in November/December 1997. All the data analysis was done using the IRCAMDR software package. The results

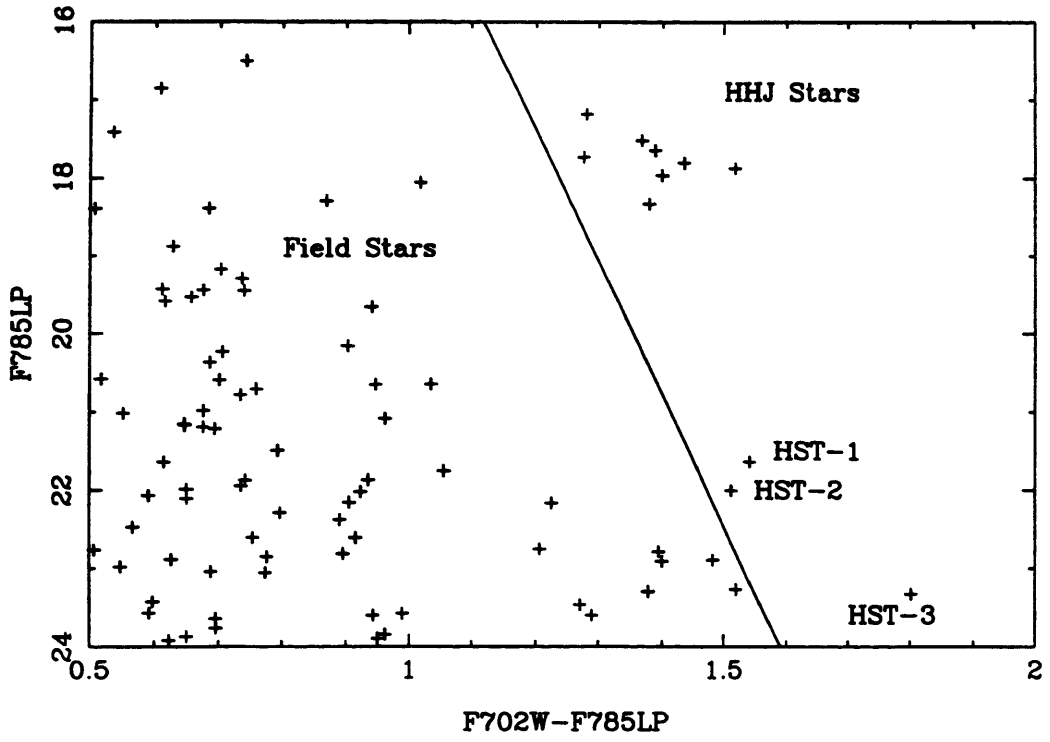

Figure 4.1: The Colour-Magnitude Diagram showing the position of the HHJ Stars and the three brown dwarf candidates, HST-1, HST-2 and HST-3.

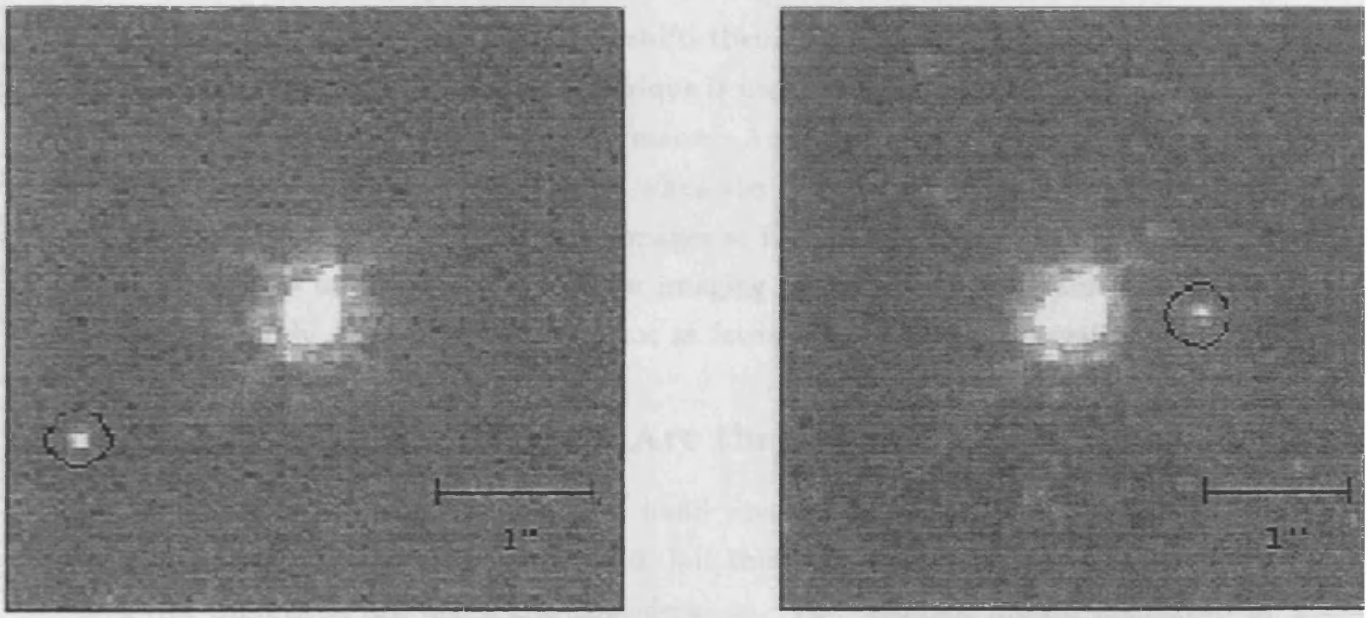

Figure 4.2: The companions to HHJ6 (left) and HHJ10 (right) are indicated with circles in these WFPC2 images (filter F785LP). The HHJ stars are the central stars in both images

showed that only 2 detections were made, HST-1 and HST-2. HST-3 was not detected at all. From the positive detections, HST-2 was not red at all in its F785LP–K colour, and HST-1, the best detection, was not as red as expected for an object of its suspected type.

4.5.2 H band observations of the suspected binaries

The infrared observations were carried out in November 1996 at UKIRT using the shift and add technique to sharpen the images. Shift and add works by taking multiple images of a target and then shifts them to align the peak pixel in a specified region of the image. When this technique is used along with the new tip tilt system (see chapter 3) the results are impressive. According to the latest figures on the UKIRT web page, on a recent night when the seeing was good, the tip/tilt system when used with shift and add, gave images at K with FWHM of 0.33 arcseconds. In theory, these techniques should allow imaging of these extremely faint candidates. Unfortunately, the conditions were not as favourable for these observations.

4.5.3 HHJ6 and HHJ10; Are they binaries?

The subsequent reduction of the H band images showed no direct evidence of a companion to either HHJ6 or HHJ10, but this is not entirely surprising when the awful conditions are taken into consideration. The resultant images are shown in Figure 4.3 As a result of the poor conditions an effort was made to analyse the data to look for any excess counts that could be attributed to a binary companion within the PSF of the primary. A piece of Fortran code was written that divided the PSF of the bright star into 4 quadrants. The number of counts in each pixel in each quadrant were summed and any excess of counts searched for. The completed analysis showed no conclusive evidence of any binary companion to HHJ6 or HHJ10 at a wavelength of 1.6 microns. Thus the companion stars cannot be very red. One must therefore conclude that despite the encouraging statistics, they are not companions and are probably simply very distant stars aligned by chance.

4.6 Conclusions

This chapter has outlined the way that the Hubble Space Telescope has been used to search for free floating brown dwarfs and possible companions to known very low-mass stars in The Pleiades open cluster. The reasons for using the HST and

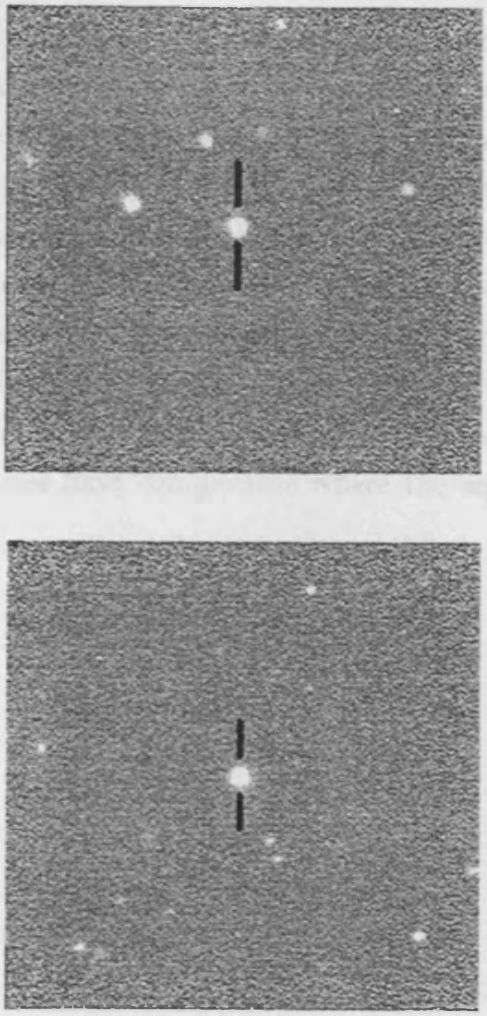

Figure 4.3: H band images of the two HHJ stars; HHJ6 (top) and HHJ10 (bottom). The images cover an area of 1 square arcminute.

the scientific background to this work has also been detailed. This work formed the introduction to my research at Leicester and although 3 free floating candidates and 2 possible binary companions were found in the initial analysis, follow-up infrared photometry indicates that none of the candidates remain as likely brown dwarfs. When one considers the extremely small area of the cluster sampled by the HST it is not entirely surprising that such a null result has been found. The reasons for using the HST to search for very low-mass brown dwarfs and possible planets within young clusters like The Pleiades are still valid, but a large scale survey would be necessary to improve the likelihood of a positive detection. A proposal to do this would be very unlikely to succeed bearing in mind the competition for time on this instrument. Indeed, a follow-up application to use the NICMOS (Near-Infrared Camera and Multiobject Spectrometer) instrument on the HST to image the companions to the HHJ stars was unsuccessful. The photometry that suggested that some of the HHJ stars were binaries is not incorrect as a result of this analysis. It could be that the binaries have companions where the separations are less than ~ 12 AU.

Chapter 5

Calibrating The I-Z Colour

5.1 Introduction

In this chapter I present the results and analysis of an observing run carried out using the Jacobus Kapteyn Telescope (JKT) on the island of La Palma in February 1997. The aim of the work was to provide a calibration of the I–Z colour by observing a complete spectral sequence of M dwarfs from type M0 to M10, some with estimated effective temperatures, using the Harris R and I, (R_H and I_H) and RGO Z (Z_{RGO}) filters. The Harris filters were used as they were the standard filters for R and I available at the JKT. In the following sections I will explain the reasons behind this work along with a description of all the data reduction. The success of the I–Z colour as a detection discriminant is discussed and the implications for future surveys outlined.

5.2 Previous Work

For some time searches for brown dwarfs have been conducted in young open clusters such as the Pleiades. The advantages of hunting in these regions have been outlined in chapter 2. Modern CCD detectors can image large areas of sky (anything from 100 square arcminutes upwards in a single exposure), allowing a significant proportion of a cluster such as the Pleiades to be surveyed in a typical ($\sim$ 5 nights) observing run. The photometric identification of VLMS and brown dwarfs is based on the assumption that objects of late spectral type have large V–I and R–I colours. A review of recent photometric surveys can be found in chapter 2. The sensitivity of these surveys in detecting objects below the sub-stellar limit was relatively poor. A new approach was needed. Large scale optical surveys were still required to improve

the statistical chances of detecting any sub-stellar object, and modern infrared detectors, such as IRCAM 3 on UKIRT, can only image 1 square arcminute at a time, (see chapter 3). Long baseline colours such as V–K pick out cluster members on a colour-magnitude diagram extremely well, but the contamination due to red galaxies is high. This contamination can be removed if careful examination of the objects point spread function is carried out, but in some cases it can only be fully removed after follow-up infrared photometry and optical spectroscopy. A secondary concern in the use of long baseline colours such as R–I and V–I as detection discriminants is highlighted in the long exposure times necessary to achieve a statistically good measurement at shorter wavelengths. This places constraints on the scheduling of telescope time in the need for darktime and therefore makes the project proposal less competitive to the allocation committee. In 1995 in an attempt to remedy the above drawbacks, the Leicester Brown Dwarf Group proposed to use the I and Z filter combination. The advantages of using the short baseline I–Z colour are presented in Chapter 6.

The first small area survey of the Pleiades using this filter combination, (Cossburn *et al.* 1997), led to the discovery of PIZ 1, a brown dwarf of approximately 48 Jupiter masses. The success of this discovery has led others to try our technique. I, Z surveys in Praesepe (Pinfield *et al.* 1997) with follow-up infrared photometry (Hodgkin *et al.* 1998) and the International Telescope Project (ITP) in the Pleiades cluster (Zapatero-Osorio *et al.* 1997), again followed up in the infrared, (Jameson *et al.* 1998) have been extremely successful in discovering a number of VLMS in Praesepe and brown dwarfs in the Pleiades. The success rate from the Pinfield *et al.* (1998) survey is of the order of 50%. However, this success rate is considerably reduced if candidates are selected from the original I, I–Z colour-magnitude diagram at the faintest end of the sample where the errors in the I–Z colour are large. To reduce this problem one must use long exposures at Z. It became apparent that a calibration of the I–Z colour as a function of spectral type was needed. The main objectives of the programme outlined in this chapter were to attempt an effective temperature calibration and to obtain a number of Z observations of standards for future survey work.

5.3 Target Selection

It was necessary to include some target objects with reasonably well defined T_es. Defining T_es for VLMS is a particularly difficult task. Jones *et al.* (1994) used the

water vapour features in the infrared spectra of a number of known VLMS, including GD165B (> M10), to estimate T_e. Targets for this observational programme were selected from this list, as well as from Leggett (1992), Veeder (1974) and Berriman, Reid & Leggett (1992). The T_es derived in Kirkpatrick *et al.* (1993) for targets common to the work of the above authors, were found to be considerably higher. To include the values of T_e from Kirkpatrick's work introduces a systematic error across the data-set. This may be due to Kirkpatrick's use of the models from Bessell (1991). These models predict higher effective temperatures for VLMS and brown dwarfs compared to more recent theoretical predictions. As a result of this systematic error, I have not included Kirkpatrick's temperatures in any further analysis here.

Obtaining Z photometry for a number of the latest spectral type objects known was the second priority. At the time of target selection before this observing run, the results of the DENIS survey (Delfosse *et al.* 1997) and 2MASS surveys (Kirkpatrick, Beichman & Skrutskie 1997) were not available which is rather unfortunate as these surveys discovered a number of objects that have been tentatively classified as > M10 and would have been an ideal test for the I–Z colour. As a result, the latest type objects were taken from Kirkpatrick, Henry & Simons (1995) and included the targets BRI 1222-1222 and the TVLM stars 513-46546 and 868-110639 (Tinney, Mould & Reid 1993). These have been classified as M9, M8.5 and M9 respectively and define the latest spectral type objects in the sample.

5.4 Observations and Data Reduction

All observations were carried out using the TEK4 CCD at Cassegrain focus of the JKT at the Observatorio del Roque Muchachos on the island of La Palma. The observing run took place between the 15th and 23rd of February 1997. The weather was generally stable, but the extinction was unusually high as a direct consequence of high levels of dust in the atmosphere. Observations of standards were made using stars from the lists of Landolt (1992). All images were de-biased, trimmed and flatfielded using the CCDPROC routines in IRAF. For more details of these software packages see chapter 3. Flat fields were taken at the beginning and end of each night in the complete filter set, which included the B,V,R,I and Z filters. The flat field images in each respective filter were co-added to obtain the best resultant flatfield and then normalised to 1.0. The target images were then flatfielded using these normalised flats. In general the flatfielding process produced good, clear images. It was noted though that on few occasions the presence of dust rings, from the

filters themselves, were not being removed from the images correctly. It was soon discovered that this was due to a change in position of the rings on the images with respect to their original position on the flat fields at the beginning of the night. After further investigation I concluded that when changing between filters at certain times during the night, the filter wheel had not locked into position correctly and so the dust rings had appeared to move position. This problem was notable on only a handful of observations during one night and on closer examination I was satisfied that the images concerned contained targets that, due to their position on the image, were not directly affected by this problem.

To obtain instrumental magnitudes from the flatfielded images I used the IRAF routine PHOT in interactive mode. A number of unreddened A0 standards were chosen specifically to calibrate the Z filter, as by definition, the colour of such a star is zero. Observing a complete set of standards in both I and Z would provide sufficient data to calibrate the Z filter. Some of the A0 stars were so bright that even using the shortest exposure time resulted in extensive saturation of the CCD. In an effort to get around this problem, the focus of the telescope was adjusted to 'blur' the image on the CCD and prevent saturation. When these images were later reduced it became apparent that, even using the largest apertures available on these extended sources, there was a reasonably large discrepancy between the obtained magnitudes and those published in the catalogues. The problem persisted even after a complete re-analysis. The possibility that the catalog magnitudes were incorrect remains but the most likely source of error comes from the presence of background stars that were masked on the image by the defocussed standards. As a result, these standard stars were not used to calibrate the target instrumental magnitudes.

To calibrate the target stars the following procedure was adopted. I assumed, see Figure 5.1 that $R_H = R_C$ (R Cousins). I further assumed that I_C (I Cousins)$=I_H=Z_{RGO}$ for unreddened A0 stars since these by definition have zero colours. Airmass curves and aperture corrections (see chapter 3) were then determined in the usual way. I was then able to determine R_H ($=R_C$), I_H and Z_{RGO} for the target stars. The results are summarised in Table 5.1.

Included in the table are the spectral types and I–K colours where available. One target, GL494 does not have an Z magnitude listed in the table. This was due to a corrupt Z image that was only discovered after the observing run had been completed and so a repeat observation could not be made. Also included in this table is the brown dwarf discovered by the DENIS survey, DENIS-PJ1228.2-1547, Delfosse *et al.* (1997). The I and Z photometry for this object was obtained by Matt

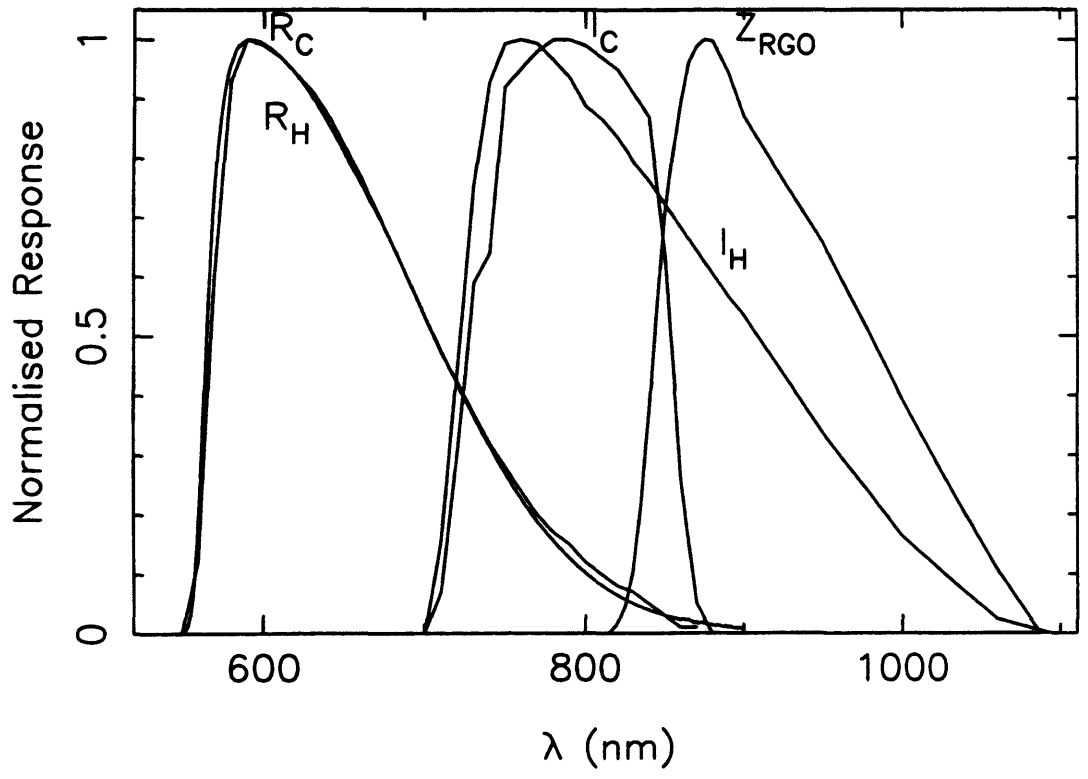

Figure 5.1: The filter profiles convolved with the TEK 4 CCD response. The filters used in this programme were R_H, I_H and Z_{RGO}.

Burleigh and Nigel Bannister, on a recent observing run at the JKT, using the same filter and detector configuration as was used in the original JKT observing run.

5.5 R–I versus I–Z

I have plotted $(R\text{–}I)_H$ against $I_H\text{–}Z_{RGO}$ for all the targets presented in Table 5.1, shown in Figure 5.2 The crosses plotted in Figure 5.2 are non A0 Landolt standard stars observed as target stars. As a result of this calibration I have been able to put together a catalog of Z magnitudes for a range of Landolt standards for future observations in this filter system (see Table 5.2), but must emphasize that repeat observations are necessary to reduce the errors.

Also plotted on this figure is the brown dwarf discovered by the DENIS survey, DENIS-PJ1228.2-1547, (Delfosse *et al.* 1997) shown as a solid circle. The large error in the R–I colour of this object is due to the shortness of the R exposure.

5.6 I–Z versus Spectral Type

Most of the objects included in Table 5.1 have determined spectral types. In the main, these have been obtained from Leggett (1992), but for some of the latest and reddest objects, the spectral types have been taken from Kirkpatrick, Henry & Simons (1995). Figure 5.3 shows the relationship between the I–Z colour and spectral type. Again, one can see the colour smoothly increasing with spectral type. The discovery of a number of objects with spectral types > dM10, (see Kirkpatrick, Beichman & Skrutskie 1997, Delfosse *et al.* 1997 and Ruiz, Leggett & Allard 1997) has led to the proposed L-type classification of these objects, (see Kirkpatrick 1998). Obtaining I and Z photometry for a number of these targets will show whether or not the I–Z colour continues to increase with spectral type. It should be noted that the leftmost points, with spectral types of M1 or earlier, show a slight deviation from a straight line that one could fit to the rest of the data-set. This may be a real effect, in that the I-Z colour is much less sensitive to objects of this spectral type. Further observations are required to confirm this hypothesis.

5.7 Colour Temperature Relationship

One of the key objectives of this observational programme was to derive a relationship between the I–Z colour and effective temperature. There have been many

Object Name	$(R-I)_H$	I_H	±	$I_C^{(a)}$	Z_{RGO}	±	I_H-Z_{RGO}	Sp. Typ.[b]	I-K[c]
Gl 270	0.99	8.11	0.02	8.27	7.88	0.03	0.23	M2.0	1.90
Gl 328	1.00	8.08	0.02	8.22	7.75	0.05	0.33	M0.5	1.80
Gl 319A	1.02	7.70	0.02	7.79	7.39	0.05	0.31	M0.0	1.91
Gl 353	1.08	8.14	0.02	8.27	7.82	0.05	0.32	M0.0	1.93
Gl 464	1.12	8.42	0.02	8.57	8.07	0.05	0.35	K5.0	1.88
Gl 494	1.15	7.55	0.02	7.71				M2.0	2.10
Gl 424	1.17	7.25	0.02	7.42	6.89	0.05	0.36	M1.0	1.87
Gl 524	1.17	8.07	0.02		7.74	0.05	0.33		
Gl 459.3	1.21	8.61	0.02	8.75	8.26	0.05	0.35	M2.0	1.91
Gl 272	1.23	8.35	0.03	8.50	8.09	0.03	0.26	M2.0	2.01
Gl 361	1.26	8.01	0.02	8.18	7.71	0.03	0.3	M2.0	2.01
Gl 393	1.30	7.27	0.03	7.41	6.96	0.02	0.31	M2.0	2.07
Gl 452	1.40	9.42	0.02	9.55	9.04	0.05	0.38		2.10
GJ 347ab	1.41	9.59	0.02	9.72	9.20	0.05	0.39		2.09
Gl 476	1.41	8.99	0.02	9.19	8.67	0.03	0.32	M4.0	2.04
GJ 333-2a	1.45	9.77	0.02	9.94	9.37	0.05	0.4	M4.0	2.17
GJ 333-2b	1.48	10.05	0.02	10.20	9.61	0.05	0.44	M4.0	2.20
Gl 463	1.48	9.05	0.02	9.24	8.59	0.05	0.46	M4.0	2.11
Gl 436	1.67	8.09	0.02	8.28	7.60	0.05	0.49	M3.0	2.18
Gl 299	1.75	9.79	0.03	9.91	9.33	0.02	0.46	M4.0	2.27
GJ 1103A	1.80	10.00	0.07		9.45	0.06	0.55		
Gl 268	1.83	8.29	0.02	8.44	7.81	0.02	0.48	M4.5	2.57
Gl 402	1.83	8.64	0.02	8.86	8.11	0.05	0.53	M4.0	2.44
Gl 285	1.86	8.08	0.02	8.20	7.56	0.05	0.52	M4.5	2.47
Gl 447	2.01	7.90	0.02	8.14	7.32	0.05	0.58	M4.0	2.51
LHS 3003	2.35	12.18	0.02	12.53	11.35	0.03	0.83	M7.0	3.60
LHS 2026	2.39	14.00	0.04	14.27	13.27	0.05	0.73		3.12
LHS 2632	2.46	14.36	0.03		13.58	0.02	0.78	M7.5	
LHS 2645	2.46	14.20	0.05		13.49	0.04	0.71	M7.5	
GL 406	2.48	9.18	0.02	9.50	8.41	0.03	0.77	M6.0	3.31
BRI 1222-1222	2.49	15.12	0.05		14.25	0.03	0.87	M9.0	
LHS 2243	2.52	14.27	0.03		13.51	0.02	0.76	M8.0	
LHS 2471	2.52	13.35	0.04	13.69	12.62	0.05	0.73		3.39
CTI115638.4+280000	2.60	16.42	0.03		15.61	0.03	0.81	M7.0	
LHS 2924	2.62	14.59	0.05	15.21	13.70	0.04	0.89	M9.0	4.54
LHS2065	2.62	14.05	0.03	14.44	13.15	0.03	0.9	M9.0	4.46
VB8	2.62	11.89	0.02	12.24	11.06	0.05	0.83	M7.0	3.42
LHS2397A	2.64	14.51	0.02	14.95	13.61	0.03	0.9	M8.0	4.11
Gl316.1	2.65	13.11	0.07	13.45	12.30	0.05	0.81	M6.5	3.42
TVLM 513-46546	2.82	14.56	0.07	15.09	13.70	0.05	0.86	M8.5	4.32
TVLM 868-110639	2.86	15.37	0.07	15.79	14.47	0.06	0.9	M9.0	4.35
DENIS-PJ1228.2-1547	2.92	17.58	0.04	18.19[d]	16.60	0.10	0.98	>M10	5.46[d]

Table 5.1: The photometry for all the target stars in the sample

[a] The I_C magnitudes were taken mostly from Leggett (1992). Other sources included Tinney (1993) and Kirkpatrick (1995).

[b] Spectral Types are from Leggett (1992) and Kirkpatrick (1995).

[c] K photometry taken from Leggett (1992) and Tinney (1993).

[d] I,K photometry taken from Delfosse et al. (1997).

$(R-I)_C = (R-I)_H + I_H - I_C$

Table 5.2: The Catalog of Landolt Standards with calibrated Z magnitudes

Object Name	R_C	I_C	Z_{RGO}	±
LAN95-96	9.931	9.836	9.72	0.04
LAN95-97	14.296	13.750	13.48	0.04
LAN95-98	13.725	13.106	12.86	0.04
LAN95-100	15.095	14.672	14.46	0.04
LAN95-101	12.241	11.814	11.66	0.04
LAN98-670	11.207	10.555	10.27	0.04
LAN98-671	12.810	12.314	12.06	0.04
LAN98-675	12.316	11.313	10.79	0.04
LAN98-676	12.385	11.716	11.39	0.04
LAN98-682	13.383	13.032	13.05	0.04
LAN98-685	11.664	11.384	11.27	0.04
RU-149B	12.268	11.914	11.79	0.04
RU-149D	11.459	11.451	11.42	0.04
RU-149E	13.397	13.081	12.69	0.04
RU-149F	12.877	12.339	12.13	0.04
RU-149G	12.507	12.184	12.08	0.04
PG0918+029	13.456	13.615	13.68	0.05
PG0918+029A	14.165	13.829	13.66	0.05
PG0918+029B	13.546	13.176	12.96	0.05
PG0918+029C	13.170	12.815	12.72	0.05
PG0918+029D	11.697	11.164	10.92	0.05
101-262	13.855	13.468	13.28	0.04
PG1323-086	13.529	13.608	13.60	0.04
PG1323-086A	13.339	13.085	12.87	0.04
PG1323-086B	12.980	12.573	12.37	0.04
PG1323-086C	13.608	13.244	13.06	0.04

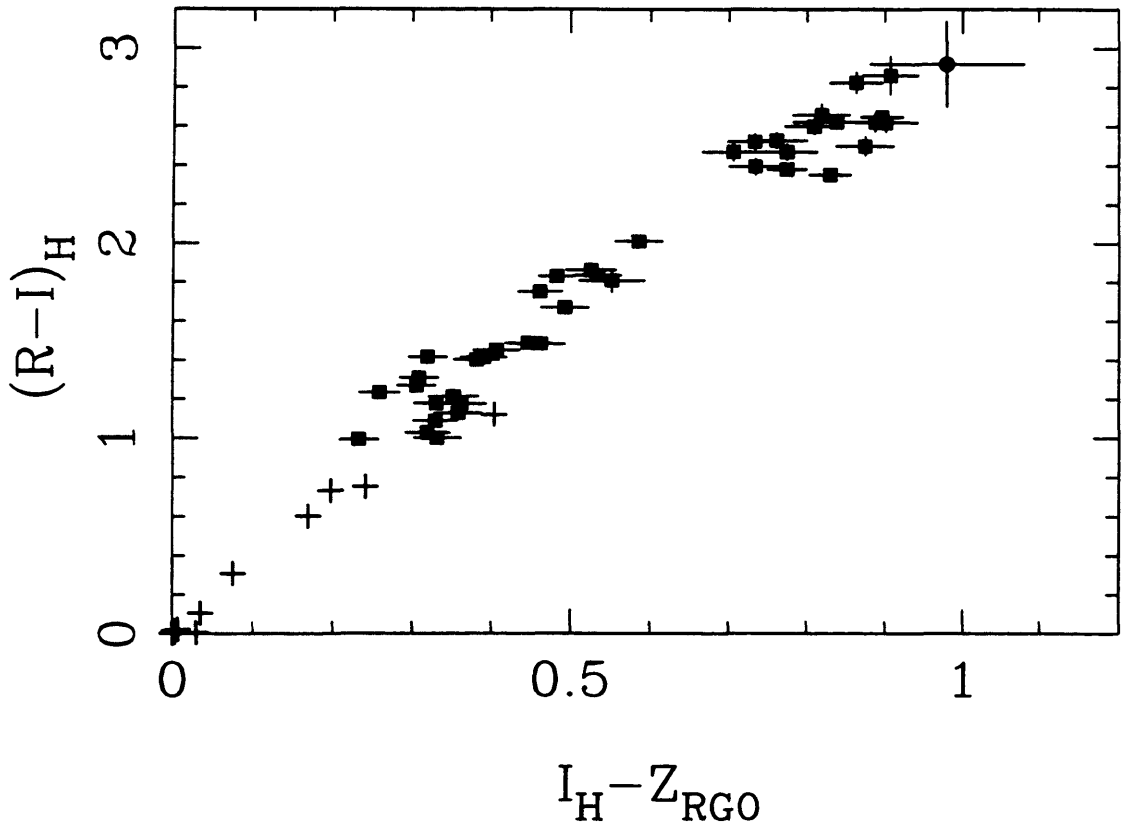

Figure 5.2: The R–I versus I–Z diagram showing the target objects (solid squares), the standard stars (crosses) and the DENIS brown dwarf, DENIS-PJ1228.2-1547, plotted as a solid circle.

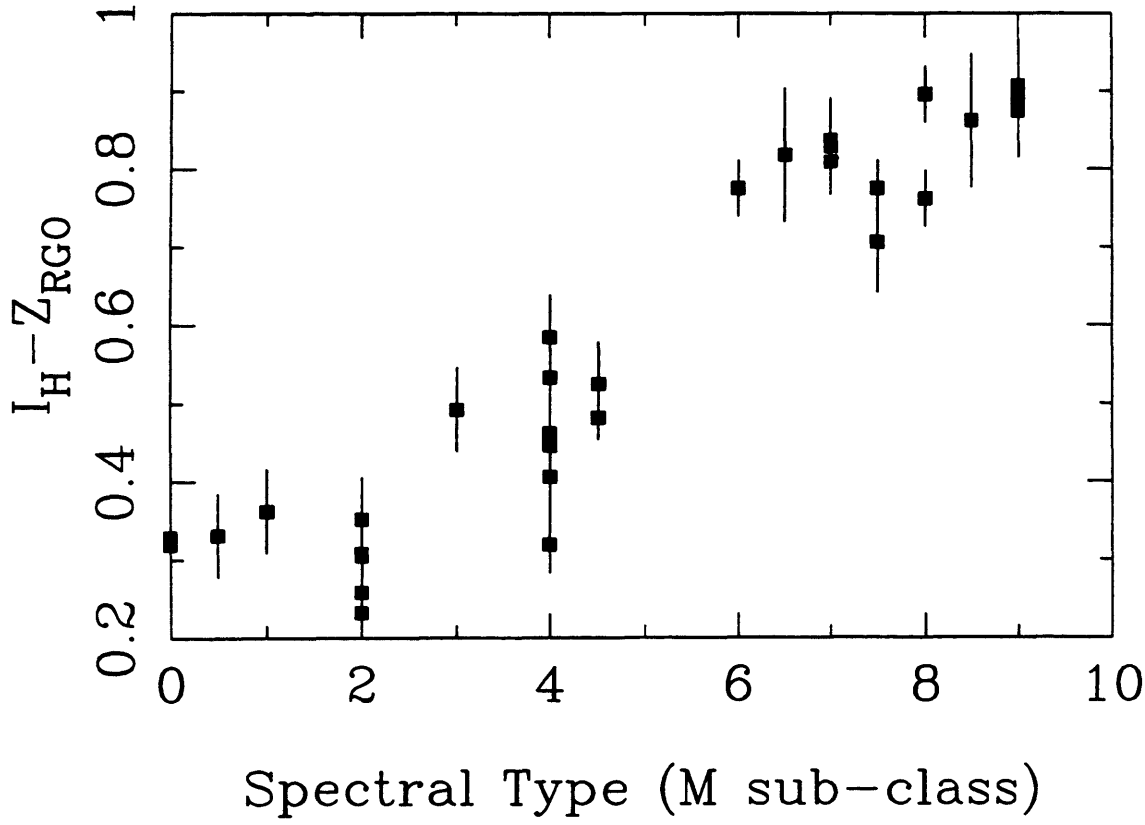

Figure 5.3: The relationship between the I–Z colour and published spectral type, for the target objects given in Table 5.1

Object Name	I–Z	±	Sp. Typ.	T_{eff} (K)	±
GL268	0.665	0.022	M 4.5	3100	100
GL299	0.640	0.027	M 4.0	3150	50
GL447	0.694	0.054	M 4.0	3200	100
GL406	0.862	0.033	M 6.0	2573	90
LHS2924	1.088	0.066	M 9.0	2219	100

Table 5.3: The five targets used with known T_e to calibrate the I–Z colour.

attempts to derive T_e for VLMS and brown dwarfs by a number of different authors. The difficulties in deriving T_e are due to the difficulty in modelling the atmospheres of such objects, due to the complex nature of the molecular and dust opacities. The T_e of LHS 2924, taken from Jones *et al.* (1994) is the lowest measured temperature of all the objects in this target sample. Temperatures for the other targets have been taken from Veeder (1974), Berriman, Reid & Leggett (1992) and Leggett *et al.* (1996). All the data used is presented in Table 5.3. Figure 5.4 shows the I–Z versus T_e diagram. The errors arise from the differences in individual measurements. I have determined a cubic fit to this data which is given in Equation 5.1.

$$\begin{gathered} T_e = 9700 - 30200(I-Z) + 45800(I-Z)^2 - 24100(I-Z)^3 \\ (0.5 < (I-Z) < 0.9) \end{gathered} \tag{5.1}$$

The cubic fit presented here also passes through (I–Z)=0, for an A0 star. The downward trend beyond I–Z of 0.9 is significant in that it is possible that the colour is already beginning to saturate at this point, see below. As a result of the difficulty in deriving the T_e for such cool objects, the inherent errors are large. The relationship derived above therefore merely demonstrates the effectiveness of the I–Z colour as a discriminant for objects with effective temperatures down to approximately 2000K. For the temperature range presented, a least squares fit to the data has also been determined and this is presented below, in Equation 5.2.

$$\begin{gathered} T_e = 4200 - 410(I-Z) \\ (0.5 < (I-Z) < 0.9) \end{gathered} \tag{5.2}$$

5.8 Relationship between I–Z and I–K

For some time it has been known that the I–K colour is a good indicator of T_e for late type M dwarfs. This can be seen to good effect in Jones *et al.* (1994) where the

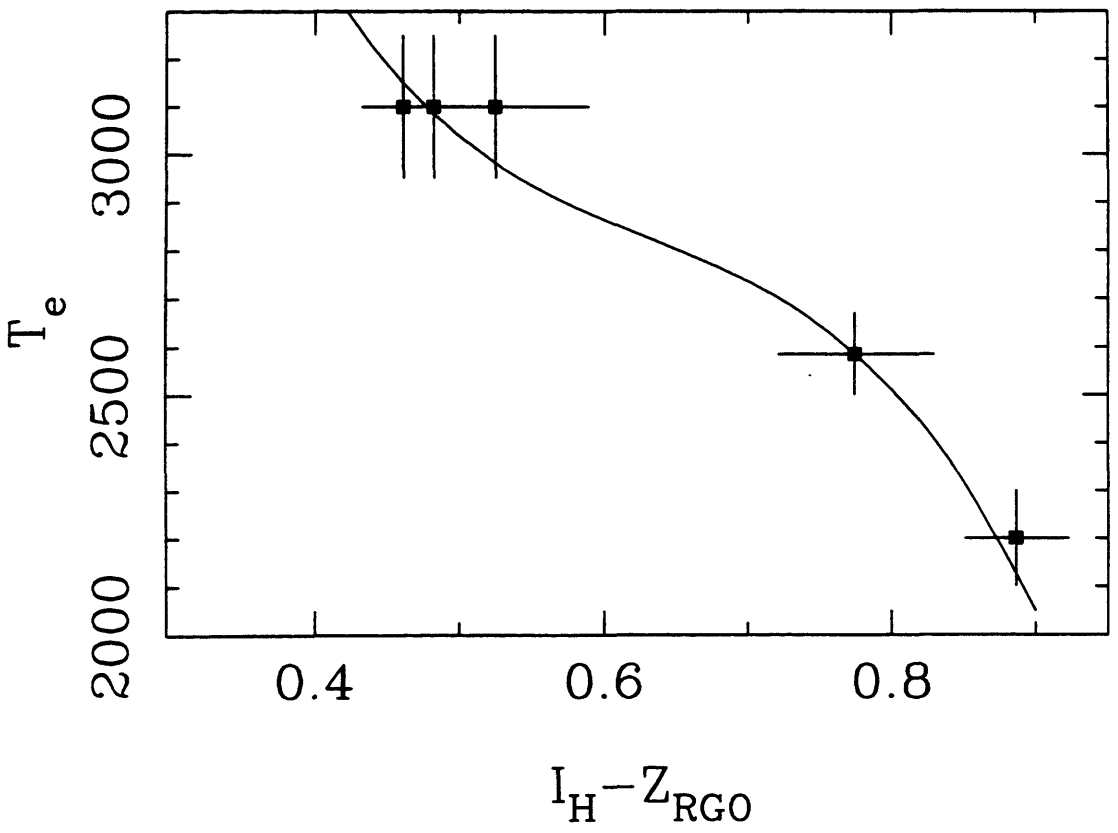

Figure 5.4: The relationship between I–Z and T_e for the objects listed in Table 5.3

strength of a number of spectral features identified in late type objects are plotted against T_e. From the previous section I have shown that the I–Z colour correlates well with T_e. Using the available K photometry, included in Table 5.1, taken mainly from Leggett *et al.* (1996), I have plotted I–K against I–Z, shown in Figure 5.5 I have also plotted the DENIS object on this figure. For objects with large I–K colours it appears that the I–Z colour begins to saturate. This has implications for the use of the R–I colour in VLMS and brown dwarf survey work also, as it too must also be saturating, see Figure 5.2. A close look at Figure 5 of Bouvier *et al.* (1998) reinforces this conclusion. At the limit of their survey using the CFHT, the VLMS and brown dwarf sequence appears to fall off dramatically as the R–I colour saturates.

5.9 Transformation from the Harris to Cousins System

As most of the targets listed in Table 5.1 have published Cousins I photometry, (Leggett 1992) it is possible to derive a conversion between the Harris and Cousins system. I have plotted I_C–I_H against $(R–I)_H$ and I_H–Z_{RGO} in Figure 5.6. I have derived fits to these plots, given in Equation 5.3 and Equation 5.4 shown below.

$$I_C - I_H = 0.0788(R-I)_H + 0.0219(R-I)_H^2 \quad (0 < (R-I)_H < 2.9) \tag{5.3}$$

$$I_C - I_H = 0.298(I_H - Z_{RGO}) + 0.1401(I_H - Z_{RGO})^2 \quad (0 < (I_H - Z_{RGO}) < 0.95) \tag{5.4}$$

The objects plotted as solid squares in these two figures are TVLM 513-46546 and LHS 2924. They show a larger deviation in I_C - I_H than expected which could be attributed to variability. As a result, these 2 objects were not used to determine the above fits. The suggestion that TVLM 513-46546 shows signs of variability has already been proposed in Tinney (1993). Further observations of both objects are essential to confirm this hypothesis.

5.10 Conclusions

This chapter has outlined the validity of using the Z filter in the search for VLMS and brown dwarfs in open clusters and in the field. The I–Z colour continues to increase for very late type objects and evidence of this is presented. I have attempted to

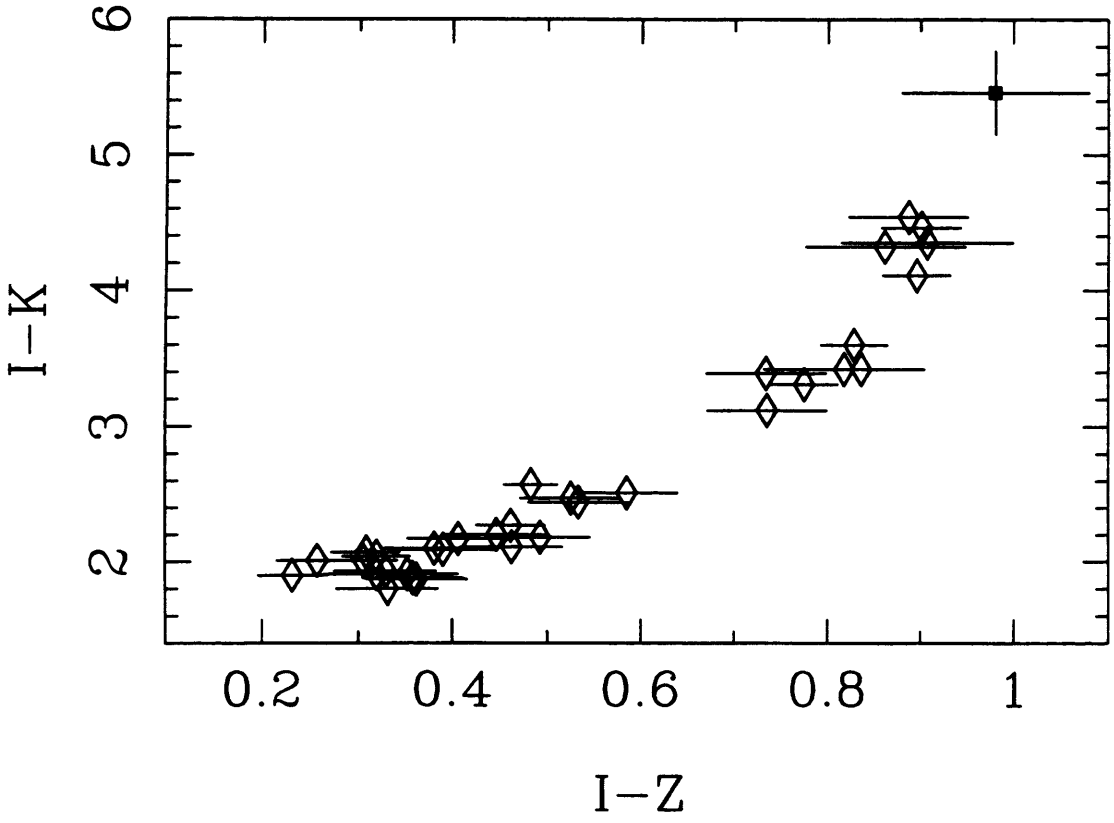

Figure 5.5: The I–K versus I–Z diagram for all the target objects (shown as open diamonds) including the DENIS brown dwarf, DENIS-PJ1228.2-1547, (shown as a solid symbol).

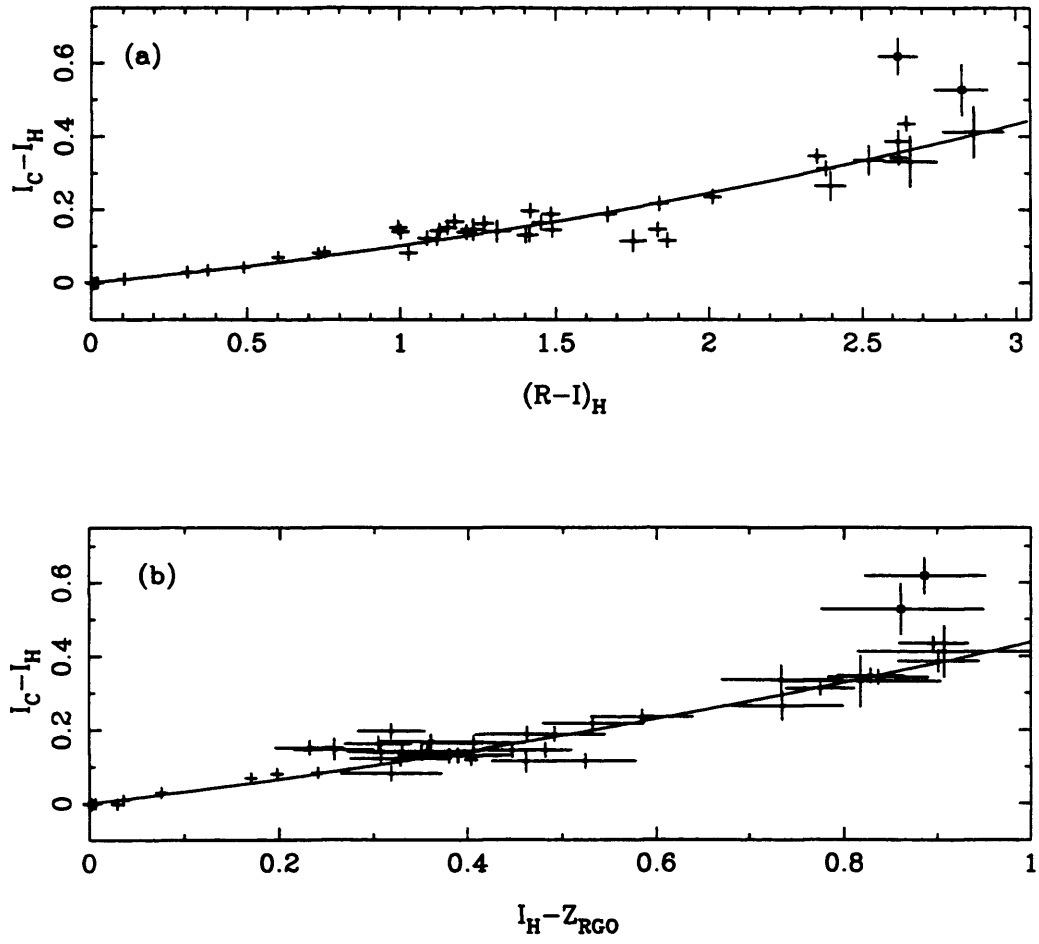

Figure 5.6: The relationship between I_C and I_H as a function of (a) $(R-I)_H$ and (b) I_H-Z_{RGO}. The objects plotted as solid squares were rejected from the data set used to derive the fits given in Equations 5.3 and 5.4, (solid lines), because they show possible signs of photometric variability, (see text for more details).

define a relationship between I–Z and effective temperature (T_e). This relationship is somewhat limited as a direct result of the difficulty in estimating temperatures for these type of objects. As the modelling of VLMS atmospheres improves, these temperature estimates will hopefully become more accurate, and relationships like the one derived here should improve. The ability to transform from the Harris to Cousins system is vital. For very red objects like the targets from this observational programme, the difference between the systems is very significant. When carrying out large scale surveys for brown dwarfs in clusters or the field, this offset must be included in any subsequent analysis of the data. For future surveys using the I and Z filter combination, there is now a list of Z standards in place. These standards cover stars that are non-A0 but repeat observations of these stars are necessary, preferably in photometric conditions, to reduce the errors.

Chapter 6

Discovery of a Brown Dwarf in The Pleiades

6.1 Introduction

In this chapter I present the results of a small area, optical survey in the Pleiades open cluster. The highlight of this work was the discovery of a brown dwarf in the cluster, PIZ 1, of approximately 48 Jupiter masses, which led to the publication of Cossburn *et al.* (1997) in Monthly Notices of the Royal Astronomical Society. It is also important to point out that this was the first I,Z survey of the cluster by the Leicester group. For some time now, the Leicester Group has been involved in the search for VLMS and brown dwarfs in open clusters, and by adopting the new technique of using the I–Z colour as a detection discriminant, objects below the sub-stellar boundary have now been identified. A summary of previous photometric and proper motion surveys is outlined in Chapter 2. The observational test of the I–Z colour is described in Chapter 5. Below I present details of the original observing run at the Isaac Newton Telescope (INT) in La Palma and then describe the work carried out following the initial candidate selection. I end the chapter with a summary of the observations and results, and present ideas for future work.

6.2 Observations

The profiles of the I Kitt Peak, (I_{KP}), and Z RGO, (Z_{RGO}), filters used in this survey have been plotted in Figure 6.1, overlaid on the spectrum of a VLMS to remind the reader of the narrow baseline of the I–Z colour, and also to clearly show the steepness of the spectrum in this region. The spectrum rises from about 10% to

almost 100% of its peak flux in the wavelength region defined by the I and Z filters. The short baseline of the I–Z colour is compensated by the increased brightness of a VLMS / brown dwarf at these wavelengths. As the sky is already bright at I and Z due to OH airglow bands there is little penalty in sensitivity in using bright time, and therefore greater flexibility in scheduling for the proposal.

The observations at I and Z were carried out in December 1995 using the TEK3 CCD at the prime focus of the INT at the Observatorio del Roque de los Muchachos on the island of La Palma. The survey included 9 fields covering a total area of approximately 900 arcmin^2. The nine field centres and exposure times are listed in Table 6.1. The observing run took place during bright time and with the poor weather, leading to particularly difficult observational conditions. The nine fields described here were taken when the cloud cover temporarily lifted, but as a result, it was extremely difficult to obtain accurate standards for each field for calibration purposes. To help resolve the calibration problem the following procedure was employed. During the run, fields were imaged that overlapped two or more of the 9 fields, and short exposures taken. The plan was to observe these overlapping fields in better conditions and calibrate the target fields indirectly. Images at I and Z of the overlapping fields were obtained at Leicester University's Oadby 0.4m telescope during February 1996. This telescope uses P8600 CCD with 395 x 578 pixels. Observations of standard stars at I and Z were also taken. These included LHS2924, VB10 and α Lyrae. The conditions during the Oadby run were very near photometric.

6.2.1 Data Reduction

The INT images were reduced using the software package IRAF running on the Leicester University STARLINK system. All the images were bias subtracted, flat-fielded and trimmed using the CCDPROC routines within IRAF. DAOFIND was then used to search for point sources and magnitudes derived using the DAOPHOT aperture photometry routines. See chapter 3 for more details of these software packages. The Oadby images were reduced using an Archimedes based system.

Magnitudes were derived for a number of stars on the overlapping fields that were not saturated on the INT images. To differentiate between stellar sources and faint red galaxies, a star-galaxy separation procedure was performed, in which all the sources were plotted on a a $\log_{10}$(peak counts) versus $\log_{10}$(total counts) diagram, see Figure 6.2. Points that lie above the top solid line in this plot have a higher peak count to total count and are likely to be cosmic rays. Objects lying

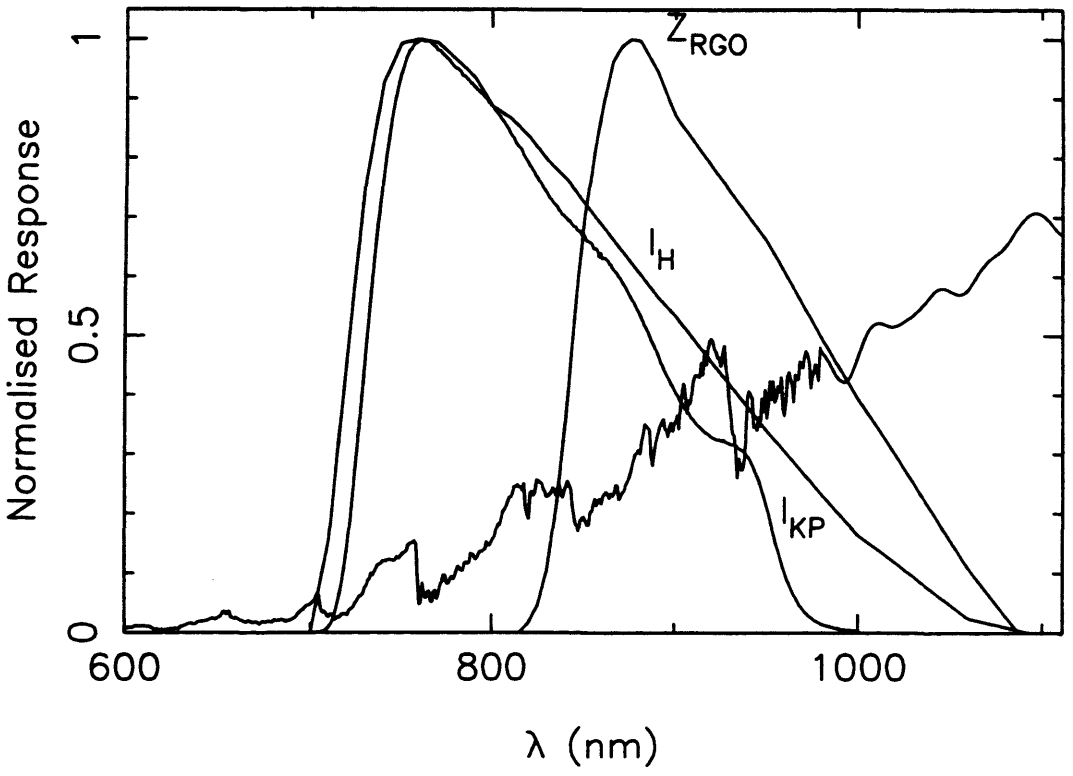

Figure 6.1: The profiles of the normalised bandpasses for the I (Harris and Kitt Peak) and Z (RGO) filters used in the small area survey of the Pleiades. Also plotted is the spectrum of the VLMS, HHJ3 (Hambly, Hawkins & Jameson 1993)

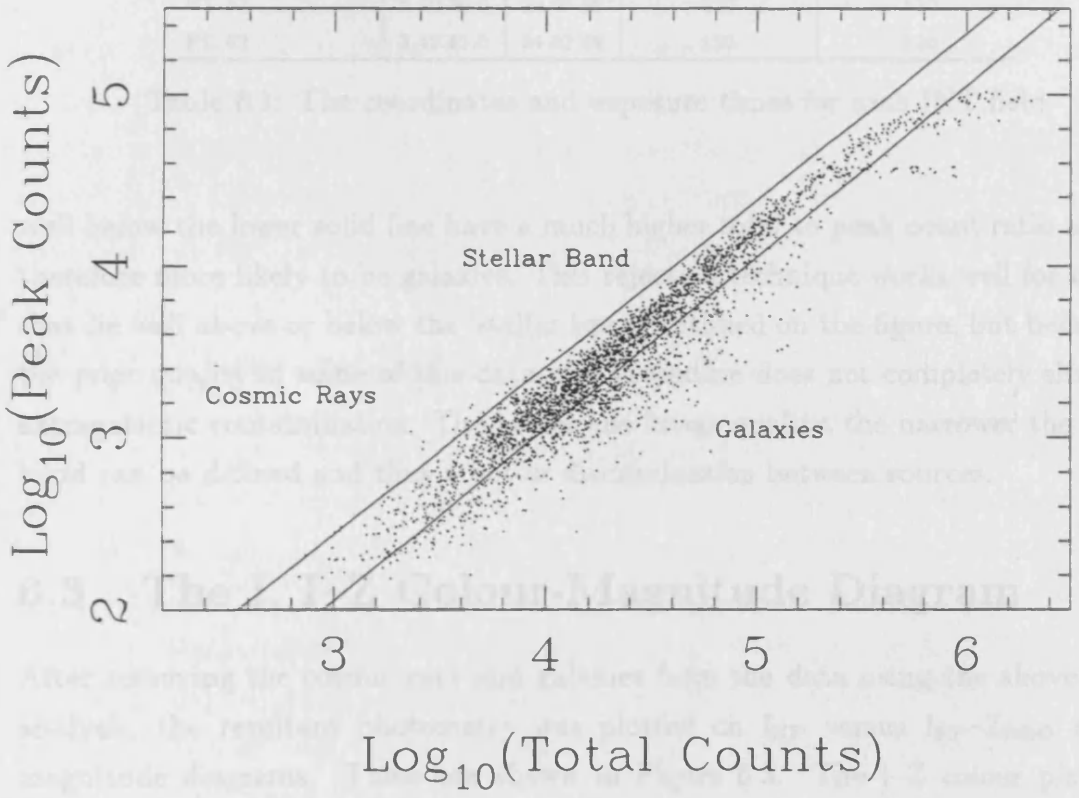

Figure 6.2: Log peak counts versus log total counts at I, for the INT survey. Sources lying above the stellar band are cosmic rays and those below it are galaxies.

Field Name	R.A. (J2000)	dec (J2000)	I Exposure Time (seconds)	Z Exposure Time (seconds)
PL 1	3 49 50.2	24 31 07	240	800
PL 2	3 49 10.2	24 30 40	500	940
PL 3 (PIZ 1 field)	3 48 31.9	24 30 40	500	640
PL 4	3 47 53.0	24 30 39	180	300
PL 27	3 48 38.0	24 00 39	400	600
PL 28	3 47 59.0	24 00 39	240	300
PL 29	3 48 15.0	23 51 00	480	540
PL 53	3 50 30.0	24 03 59	120	520
PL 63	3 49 51.0	24 03 59	120	120

Table 6.1: The coordinates and exposure times for each INT field

well below the lower solid line have a much higher total to peak count ratio and are therefore more likely to be galaxies. This rejection technique works well for objects that lie well above or below the 'stellar band' outlined on the figure, but because of the poor quality of some of this data, the procedure does not completely eliminate extragalactic contamination. The better the image quality, the narrower the stellar band can be defined and thus a better discrimination between sources.

6.3 The I, I–Z Colour-Magnitude Diagram

After removing the cosmic rays and galaxies from the data using the above shape analysis, the resultant photometry was plotted on I_{KP} versus I_{KP}–Z_{RGO} colour-magnitude diagrams. These are shown in Figure 6.3. The I–Z colour picks out the brown dwarf candidates in these colour-magnitude diagrams well, (shown as larger black dots). These candidates were selected for follow-up infrared observations. However, at this point I became involved in the International Telescope Project (ITP) in collaboration with the Instituto de Astrofisica de Canarias (IAC), in a large area, I_H,Z_{RGO} survey of the Pleiades, (This work has now been published in Zapatero-Osorio *et al.* 1997). My role was to undertake the preliminary data reduction of approximately 1 square degree of data, taken in near photometric conditions at the INT in September 1996. Fortunately, a number of the ITP fields overlapped some of the nine fields already covered by the small area survey. I was able to cross check some of the 10 brown dwarf candidates with this new data. Not surprisingly, I found that a number of them were not as red as the initial data had suggested

R.A. (J2000)	Dec (J2000)	m_I	m_Z	m_K	I–Z	I–K
3 48 31.4	+24 34 37.7	19.64	18.31	15.5	1.33	4.1

Table 6.2: A summary of the photometry for PIZ 1. Coordinates have been measured to sub-arcsecond accuracy.

and were therefore rejected from any follow-up proposal. The five candidates that remained after this analysis were put into a service proposal at UKIRT, to obtain K band images, the results of which are described below. It should be pointed out at this stage that the I_{KP}–Z_{RGO} colours of the brown dwarf survey outlined in this chapter are significantly larger than those using the I_H–Z_{RGO} colour. A quick glance at Figure 6.1 shows that the I_H filter profile extends further into the red than the I_{KP}. The resultant I_H magnitudes are brighter making the I–Z colour smaller.

6.4 Follow-up Infrared Photometry

K band photometry for 3 of the 5 candidates was obtained in UKIRT service time on 22 October 1996 using IRCAM3. The infared photometry was reduced using the STARLINK package IRCAMDR. Of the three targets imaged, only one, PIZ 1, remained red in I–K, (I–K larger than 3.5). The other two had I–K colours less than 3.0. (The remaining two candidates were followed up at J,H and K at UKIRT on a nine night observing run in November 1997, see chapter 7.) The K band photometry for PIZ 1 has been used to place it on an I versus I–K diagram, shown in Figure 6.4. Other Pleiades brown dwarfs, Teide 1, Calar 3 and PPL 15 have been plotted and PIZ 1 clearly extends this infrared sequence. Figure 6.5 shows the finder charts for PIZ 1 at I and K, with coordinates and photometry given in Table 6.2.

6.5 Optical Spectroscopy

The large I–K colour of PIZ 1 was encouraging but an optical spectrum was essential to completely eliminate the possibility of it being extragalactic. A service proposal was submitted and the spectroscopy was carried out in service time on the 4.2m William Herschel Telescope (WHT) on 30 November 1996. The ISIS double arm spectrograph and R158R grating were used together with the TEK 1124x1124 chip.

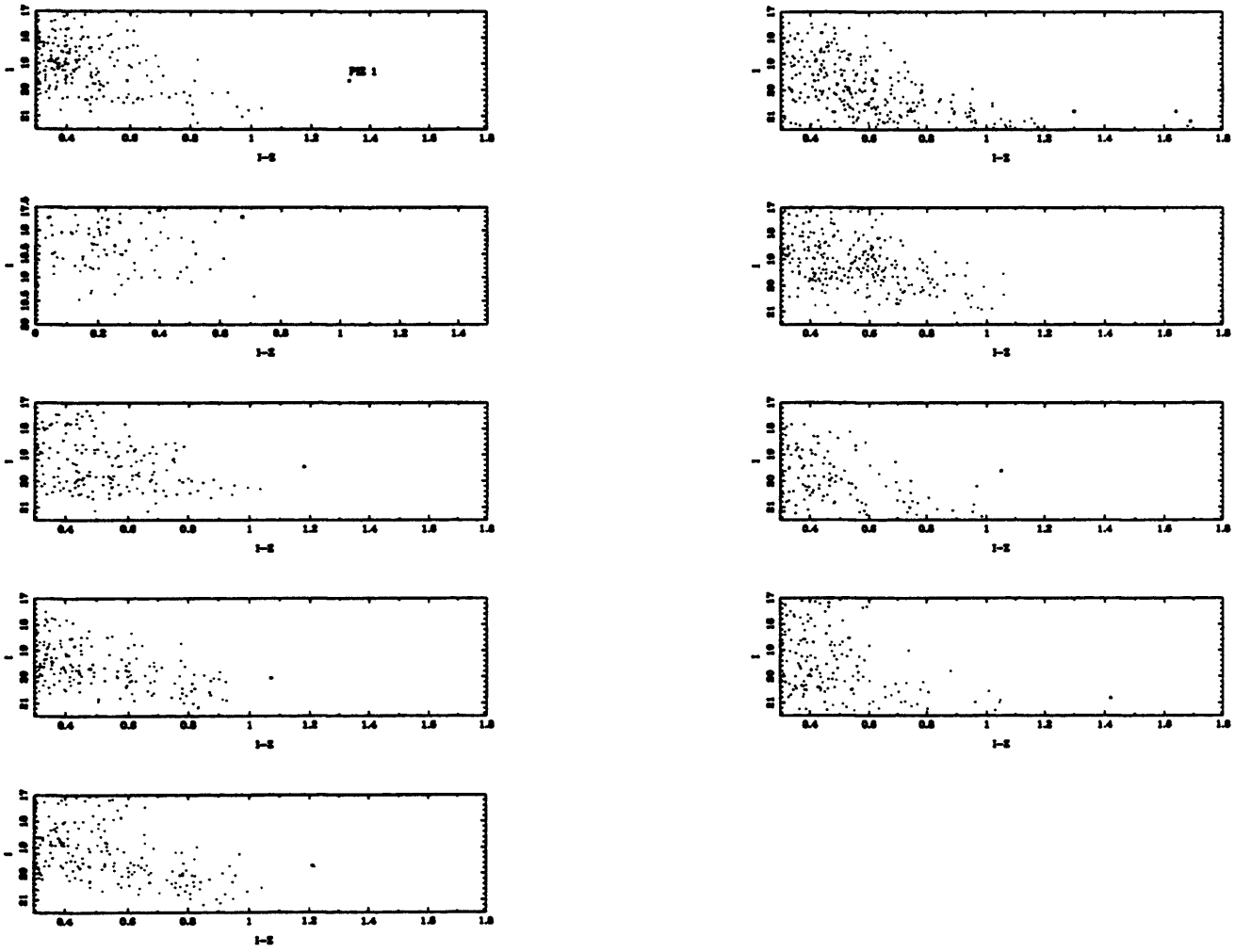

Figure 6.3: The I versus I–Z colour-magnitude diagrams for the 9 fields observed. The 10 brown dwarf candidates have been highlighted as larger black dots.

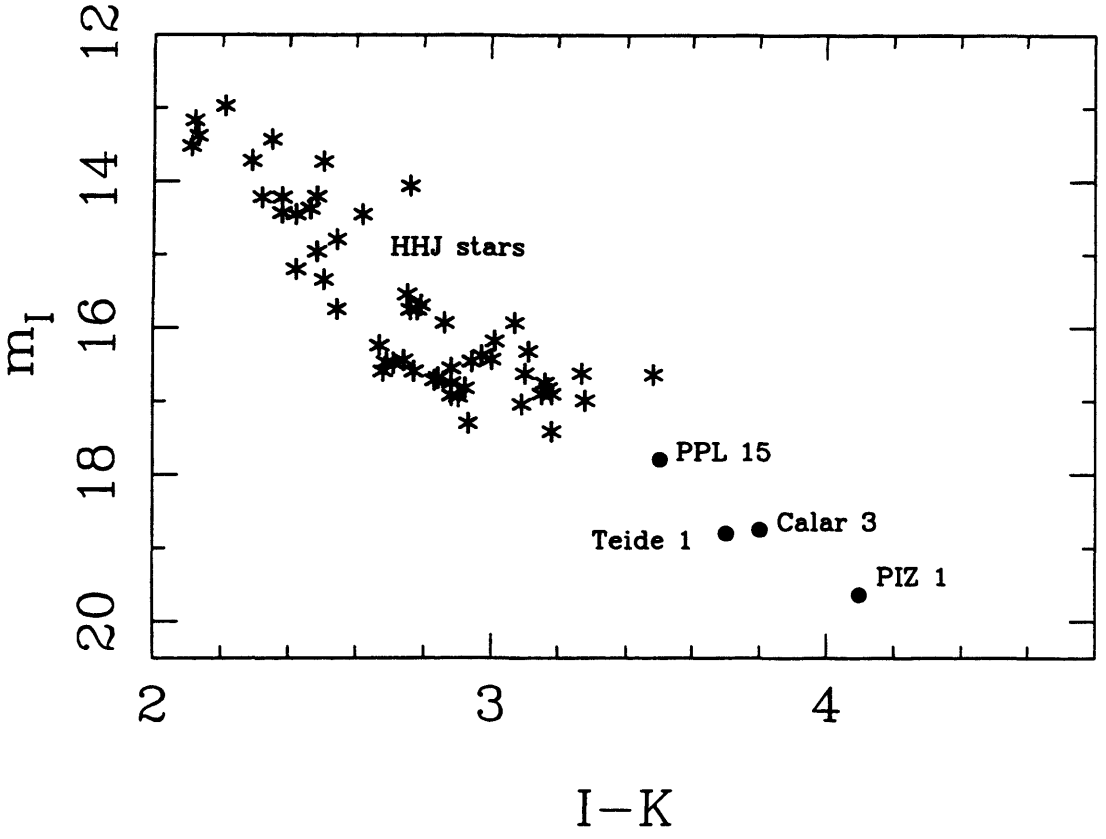

Figure 6.4: The I versus I–K colour-magnitude diagram for the Pleiades showing the low-mass HHJ stars (Hambly, Hawkins & Jameson 1993), the brown dwarfs, PPL 15, Teide 1 and Calar 3, and the object PIZ 1.

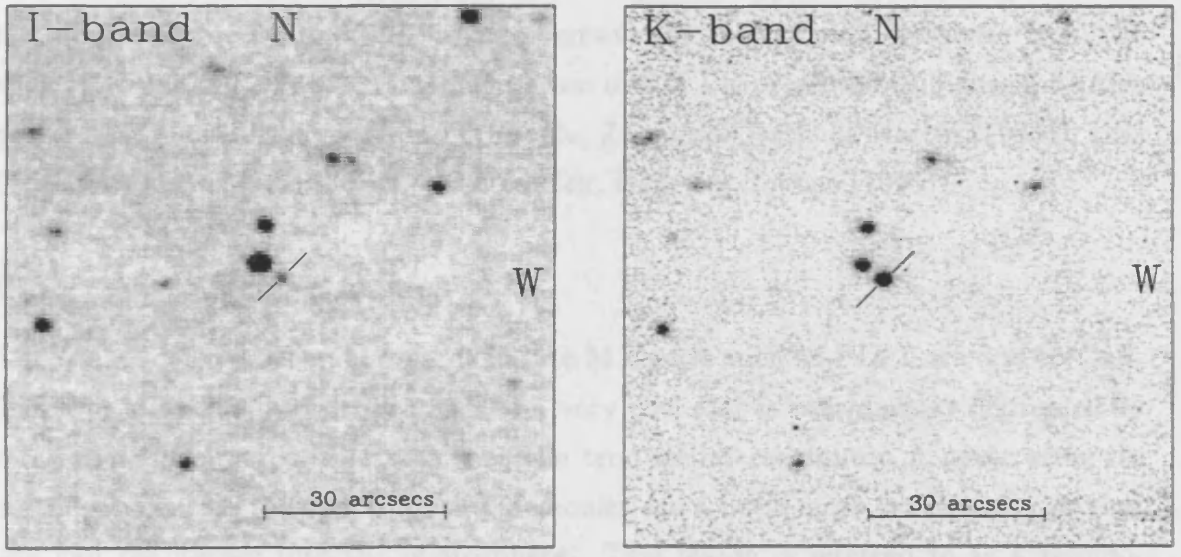

Figure 6.5: Finder charts for PIZ 1 at I and K. Coordinates and photometry are given in Table 6.2.

PC index	Numerator	Denominator
PC3	823.5-826.5	754.0-758.0
PC4	919.0-922.5	754.0-758.0

Table 6.3: Pseudo-continuum integration limits (nm).

Five 30 minute integrations were carried out covering 6500 to 9500 Å. The spectrum was reduced using IRAF software. This included bias subtraction, flatfielding, optimal extraction and wavelength calibration, (for more details see chapter 3). The star nearest to PIZ 1 has been identified as spectral type G5 from its optical and infrared photometry, and was used to remove the instrumental response from the spectrum of PIZ 1. The extracted spectrum of PIZ 1 is presented in Figure 6.6. Also plotted are the spectra of Teide 1, (Rebolo, Zapatero-Osorio & Martin (1995)), BRI 0021-0214 and 2MASP-J0345, (Kirkpatrick, Henry & Simons (1995)).

6.5.1 Spectral features

The main molecular bands present in late M dwarfs such as PIZ 1 are due to CaH, TiO and VO. The overall spectrum of a very cool star is considerably depressed by molecular opacity to the extent that the true stellar continuum is never seen. In certain regions of the spectrum the molecules are a little more transparent so that one can see deeper into the photosphere. This region is referred to as a pseudo-continuum and is used to classify the spectral type of very cool objects such as PIZ 1. To determine the spectral type of PIZ 1, I have used the pseudo-continuum spectral ratios, PC3 and PC4, as defined by Martin, Rebolo & Zapatero-Osorio (1996). Table 6.3 shows how these two spectral ratios are defined. Using both PC3 and PC4 I have classified PIZ 1 as M9. This was done using equations 6.1 and 6.2, again taken from Martin, Rebolo & Zapatero-Osorio (1996).

$$SpT = -8.009 + 14.080 \times PC3 - 2.810 \times PC3^2 \quad (6.1)$$

$$SpT = -0.944 + 4.663 \times PC4 - 0.515 \times PC4^2 \quad (6.2)$$

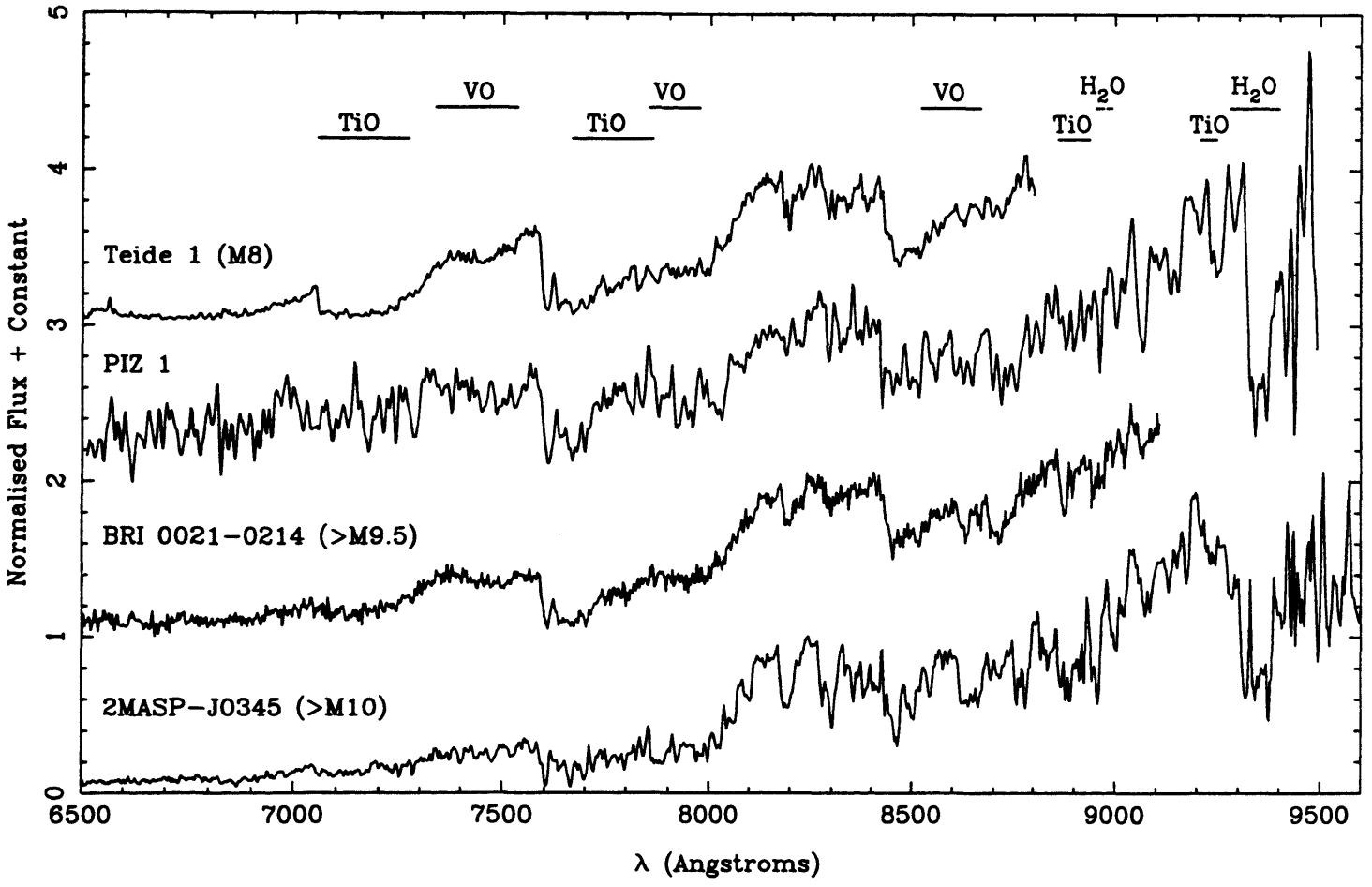

Figure 6.6: The spectra of Teide 1, PIZ 1, BRI 0021-0214 and 2MASP-J0345 ordered by increasingly late spectral type from top to bottom.

There are similarities between PIZ 1 and 2MASP-J0345 in the wavelength region 9300 to 9400 Å. The blueward edge of this feature is a result of H_2O absorption in the atmosphere of PIZ 1. The redward edge also has a contribution from terrestrial atmospheric absorption by H_2O which has not been properly removed. TiO absorption at 9208, 9230 and 9248 Å, in the spectrum of 2MASP-J0345 appears considerably stronger than in PIZ 1, indicating that 2MASP-J0345 is cooler. Kirkpatrick, Henry & Simons (1995) argue that the heights of the pseudo-continuum points at 7550 and 8250 Å decrease moving to objects of later spectral type as a result of increased VO opacity. The VO bands lie on the blueward side of these features, and the effect can be seen in PIZ 1 at 7550 Å. However, at 8250 Å, the effect is less noticeable. Hα appears to be present but the errors are large. Hα emission is also found in Teide 1, Calar 3 and other low-mass stellar Pleiads, but has not been detected in some of the latest spectral type objects found within the Pleiades cluster from the ITP survey, (Zapatero-Osorio *et al.* 1997).

6.6 The Effective Temperature of PIZ 1

It is useful to compare this object with the low-mass stars and brown dwarfs already identified in the Pleiades cluster. Figure 6.4 shows the low-mass HHJ stars and the three brown dwarfs, PPL15, Teide 1 and Calar 3. PIZ 1 has been plotted and its position indicates that it is significantly redder than Teide 1. PIZ 1 has a K magnitude of 15.5 giving an I–K colour of 4.1 . If the data from Jones *et al.* (1994) is combined with the models of Chabrier, Baraffe & Plez (1996) one can determine a relationship between the I–K colour and effective temperature (T_e). This relationship is shown in 6.7 and fit to the data given in 6.3. Using this relationship I found the T_e of PIZ 1 to be approximately 2300K.

$$(I-K) = (5.2273 \times 10^{-10})T_e^3 - (3.8873 \times 10^{-6})T_e^2 + (7.3493 \times 10^{-3})T_e + 1.415$$
$$(1700K \leq T_e \leq 3700K) \tag{6.3}$$

6.7 Cluster Membership

Photometrically PIZ 1 is a good candidate for membership of the cluster. Both optical and infrared point spread functions are stellar when compared to other objects in the field, indicating that PIZ 1 is not a galaxy, but the conclusive proof is the

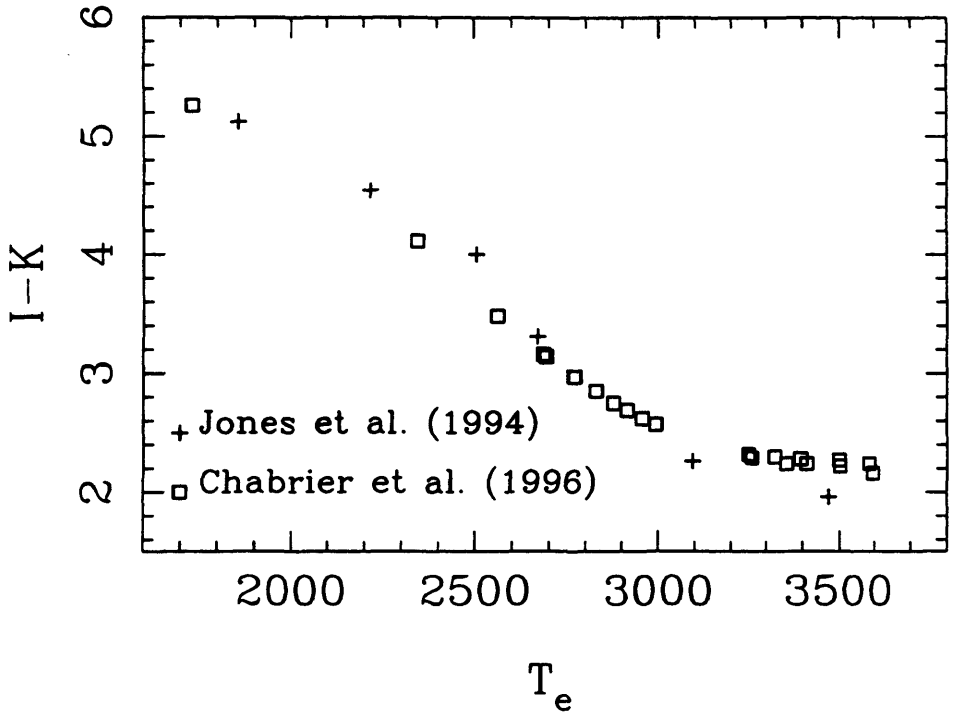

Figure 6.7: The I–K versus T_e diagram used to estimate the T_e of PIZ 1.

spectrum, clearly that of a late M dwarf. There is a remote possibility that PIZ 1 is a rare field star that coincides with the cluster main sequence. An old field star of the same effective temperature as PIZ 1 is from theory 0.4 magnitudes fainter than PIZ 1. Thus to mimic a brown dwarf Pleiad it must be in the distance range of approximately 60 to 130 pc. A field of 100 arcmin^2 then corresponds to a volume of 5.29 pc^3. Both Tinney, Mould & Reid (1993) and Kirkpatrick *et al.* (1994) find $\Phi \approx 10^{-2.3}$ stars per pc^3 of M_I=13.25 to 14.25. Thus the expected contamination of the survey sample of stars is of the order of 0.027 field stars per 100 arcmin^2. The luminosity functions from both Tinney and Kirkpatrick are local to the Sun.

Unfortunately there is no information on the scale height of the luminosity function for very faint field stars. Furthermore the Sun maybe 10 to 40 pc above the plane Kirkpatrick *et al.* (1994) and the Pleiades (galactic latitude -24°) therefore 40 to 10 pc below the plane, so it would be difficult to use scale height information even if it were available. Unless the field star luminosity function rises steeply at fainter magnitudes than Teide 1 the contamination would not increase substantially. The likelihood of the field star luminosity function increasing without an increase in the cluster luminosity function is small.

6.8 The mass of PIZ 1

The first step in estimating the mass of PIZ 1 is to estimate the age and distance to the Pleiades cluster. Stauffer, Schultz & Kirkpatrick (1998) has recently observed the lithium line at 670.8 nm in a number of candidate brown dwarfs discovered using the CFHT in a Pleiades survey carried out by Bouvier *et al.* (1998). By obtaining lithium abundances for a number of objects that have partially depleted this element one can infer the age of the cluster (see Basri, Marci & Graham 1996). Using this method an age of 125±5 Myrs was determined. Taking a distance modulus of 5.65 (Steele & Jameson 1995) one can use the latest models of Chabrier & Baraffe (1997) to estimate the mass of PIZ 1. I find the mass of PIZ 1 to be 48±3 Jupiter masses.

6.9 Future Work

PIZ 1 is a very interesting object. Its very late-type spectrum presented in this chapter is a little noisy. The need to obtain a better spectrum of the object is essential. A better quality spectrum would perhaps resolve the question as to whether Hα is seen in emission or not. One could also measure the radial velocity and take a closer look at some of the more gravity and temperature sensitive features. Both of these are important in defining cluster membership. A proper motion measurement of this object would add major credence to this argument. The Pleiades has a proper motion of around 5 milliarcseconds per year. If a good sampling of the point spread function is undertaken, (i.e. a good quality CCD image obtained, with similar pixel scale to the original INT image), then a likely time baseline of around 10 years would be sufficient to determine the proper motion. A better spectrum of PIZ 1 has been taken using the William Herschel Telescope (WHT) in October 1997. The radial velocity measurement is possible from this new data but due to time constraints could not be included in this thesis.

6.10 Conclusions

In this chapter I have outlined the first observational project of my Ph.D. This small area survey using the I and Z filters at the INT discovered an extremely red object, PIZ 1. As a result of the very poor observing conditions, I have outlined the necessary steps undertaken in the data reduction procedure. The follow-up infrared photometry obtained at UKIRT is also presented and the optical spectrum obtained

in WHT service time is shown. The spectrum shows a number of features that one would expect to see in a very cool M dwarf. The presence of TIO and VO molecular bands are very evident. Using the pseudo-continuum ratios outlined in Martin, Rebolo & Zapatero-Osorio (1996) I have assigned a spectral type of M9 for PIZ 1. I have discussed the methods employed to estimate both the effective temperature and the mass of PIZ 1 and outlined the steps required to fully confirm the identity of PIZ 1 as a Pleiades cluster member. PIZ 1 has T_e ~2400K and a mass of approximately 48 $M_{Jupiter}$. I have presented the argument against PIZ 1 being a foreground or reddened background object, the likelihood of this within the survey area being less than 2%. The discovery of PIZ 1 is a very significant result. This INT survey was the first to use the I, Z filter combination and PIZ 1 has become the first of many brown dwarf discoveries in the cluster using this technique.

Chapter 7

Infrared Follow Up Photometry

7.1 Introduction

In this chapter I present the results of observations carried out at UKIRT in November and December 1997 using IRCAM 3. The target list included many brown dwarf candidates and VLMS from a number of different surveys. I will describe the initial surveys, outlining the key results from each. The results from the UKIRT run are then presented and discussed. The implications to the luminosity and mass functions as a consequence of these results will be described in more detail in chapters 8 and 9.

7.2 Review of Initial Surveys

7.2.1 The International Time Project (ITP)

Arguably the most comprehensive I, Z survey of the Pleiades cluster published to date, the ITP survey involved collaboration between members of the Leicester Group, the IAC and astronomers based in the U.S.A. Observations of approximately 1 square degree of The Pleiades were made at I and Z using the INT telescope in La Palma. The survey covered the central region of the cluster in a magnitude range of 17.5 to 22 at I. This corresponds to a mass range of 0.08 to 0.03 $M_{\odot}$. The reduction of the I, Z photometry was undertaken by myself as part of my research. An analysis by Maria Rosa Zapatero Osorio at the IAC was performed at the same time and the subsequent candidate lists compared. More than 40 faint, very red objects were detected with positions on the I, I–Z colour-magnitude diagram suggesting cluster membership. It was these candidates that formed an important component of the

target list for the UKIRT follow-up survey. The ITP survey is significant because of the possible effect its results may have on the luminosity and mass functions of the cluster below the sub-stellar limit. This is discussed in more detail in the next chapter.

7.2.2 The INT Survey

This survey, carried out using the INT on the island of La Palma, was the first I, Z survey conducted in the Pleiades and Praesepe by the Leicester Group. It began in late December 1995 and formed the first observational run of my Ph.D. The conditions during the run were extremely poor with only glimpses of clear sky at the best of times. From an analysis of this data, see chapter 6, 1 brown dwarf was discovered, PIZ 1, see Cossburn *et al.* (1997). A handful of candidates still required infrared follow-up photometry, and these were among the targets observed at UKIRT in 1997. The INT survey was attempted exactly one year later in December 1996, but the conditions were worse than the previous year and the telescope dome was shut on 5 nights out of 7. The third attempt took place in December 1997 to January 1998 using the new Wide Field Camera on the INT in much better conditions. Data from this run is still being reduced and as it took place after the UKIRT run no candidates were available for follow-up.

7.2.3 The Double I Survey

Using I band Schmidt plates taken over a 7 year time baseline, this survey covered a 6 x 6 degree area centred on the Pleiades and employed the new, high precision microdensitometer SuperCOSMOS at the Royal Observatory, Edinburgh. By measuring proper motions this survey goes deeper than the original HHJ survey which used R plates, since VLMS and brown dwarfs are brighter at I. This is compromised by the relatively short timescale between epochs of 7 years compared to approximately 30 years in the HHJ survey. R plates are still needed to confirm a very red colour, where an object may be detected at I but no evidence of a source detected at R. Candidates for the UKIRT observing run were selected on the basis of having extremely red photographic colours and proper motions consistent with cluster membership. The target list included many candidates with similar characteristics to PPL 15. The faintest candidate was 0.3 magnitudes fainter than PPL 15. The initial survey, the infrared photometry and the consequences of the results on the

Pleiades mass function have recently been accepted by MNRAS in Hambly *et al.* (1998).

7.2.4 RIZ Survey of Praesepe

This RIZ survey of the older cluster, Praesepe, included the optical data taken from Pinfield *et al.* (1997). They present 26 candidate cluster members of which 19 were believed to be new brown dwarfs. Possible binary or multiple systems were also identified. Pinfield *et al.* (1997) describes the criteria used for candidate selection.

7.2.5 The Kitt Peak Surveys; Praesepe, The Pleiades and The Hyades

These surveys used the Burrell Schmidt Telescope on Kitt Peak in Arizona to survey as large an area of the three open clusters as possible. The Burrell Schmidt has a 0.61m aperture with a 2048x2048 pixel CCD. The field of view is slightly greater than 1 square degree, which in theory is ideal for such large scale observational projects. The disadvantages are that the small aperture means increased exposure times are necessary, and with a scale of 2 arcseconds per pixel, shape analysis is difficult to carry out. Any source that is closer than 2 arcseconds from a bright star will also be impossible to detect. The characteristics of The Pleiades and Praesepe have been outlined in chapter 2, so I here will just summarise the basic characteristics of The Hyades for completeness. Having approximately the same age as Praesepe, $\sim$0.9Gyrs, The Hyades cluster is much closer at 48pc. As a direct result of the close proximity of the cluster, the depth to distance ratio is large. This causes a widening of the main sequence on a colour-magnitude diagram by about $\pm$1 magnitude. The Kitt Peak observations were carried out in December 1996 with generally good weather. Typical exposure times for Praesepe and The Pleiades were 1 and 2 hours at I and Z respectively, with 0.5 and 1 hours at I and Z respectively for the Hyades cluster. For a complete review of the survey and the data reduction see Pinfield (1997). For the purpose of this chapter, the surveys identified 96 brown dwarf candidates in The Pleiades, 141 VLMS in Praesepe, and 33 candidate brown dwarfs in The Hyades.

7.3 The UKIRT Observations

The observations took place over a nine night observing run in November and December 1997 at UKIRT on Mauna Kea, Hawaii. The weather was variable with both thick and thin cirrus and good photometric conditions. Using the IRCAM 3 infrared array (see chapter 3), 1 square arcminute images were taken. During good conditions, rough calculations were done at the telescope after readout of the image to identify any objects that remained red in I–K. In poorer conditions, the same process was undertaken relative to other stars on the image. By identifying the bluer field stars on the original I and Z images it was possible to roughly predict how red one would expect the targets on the infrared images to be. If the targets were found to remain red with respect to the other field stars they were highlighted and reobserved during better conditions. If the targets appeared bluer than the field stars or did not change relative to their neighbours then they were rejected at this stage. This process allowed the maximisation of observing time, necessary considering the number of VLMS and brown dwarf candidates targeted for this survey, and the general unpredictability of the weather from night to night. The STARLINK package IRCAMDR was used to reduce this infrared data, using procedures outlined in Chapter 3.

7.4 The I, I–K results

The greater sensitivity of the I–K colour to effective temperature (T_e) over the R–I and I–Z colours means that the I versus I–K colour-magnitude diagram is useful in discriminating between members and non-members for the above surveys. A colour-magnitude diagram of this type is of greater value if one can identify where the cluster sequence should sit from theory. To do this one must use a theoretical model of which there are a number available. In this chapter I have presented the results of the UKIRT survey on I versus I–K diagrams and over-plotted isochrones from the models of Chabrier & Baraffe (1997). Each survey has been plotted individually. I have included the original I versus I–Z diagram showing the positions of the I, Z candidates. The I, K selection of brown dwarf candidates will now be described for each individual survey.

7.4.1 The ITP Survey Results

The I, I–Z and I, I–K colour-magnitude diagrams are shown in Figure 7.1. Plotted on the I, I–K diagram is the 5 Gyr isochrone at the distance of the Pleiades, taken from the models of Chabrier & Baraffe (1997). In an ideal situation one would find a gap between background field objects and cluster members on this diagram. In practice, this is rarely seen and so some kind of selection criteria needs to be employed. An isochrone of age 5 Gyr has been used to identify the position on this diagram of where one would expect to find the field star sequence. Objects that lie on this line or to the right of it are possible cluster members, with objects to the left being background field stars. There is of course a probability that some objects that I have classed as possible members using this criteria are in fact foreground field objects. One cannot estimate the probability of contamination from such a diagram at this stage but must rely on further observations, including optical and infrared spectroscopy and proper motion measurements to help confirm cluster membership. Table 7.1 presents the optical and infrared photometry for the ITP survey with a yes or no flag (y/n) as to cluster membership based on the above selection criteria. Where candidates have not been followed up at K, a question mark has been included in this table. The original I, Z survey employed the I Harris filter (I_H) whereas the model isochrone photometry is in the Cousins system, I_C. For very red objects the difference is significant and so I have used the relationships I derived in Chapter 5, to convert the I_H magnitudes into the Cousins system for the figure only. The photometry in 7.1 is in the original I_H filter system.

7.4.2 The Kitt Peak Survey Results

The Kitt Peak data covers 3 clusters, The Pleiades, Praesepe and The Hyades. I shall present the results in this order, starting with The Pleiades. In Figure 7.2 I again show the I, I–Z and I, I–K colour-magnitude diagrams for this survey. The 5 Gyr isochrone plotted to select candidates. There is an important point to note about the I photometry used in these diagrams. The original filter system used in this survey included the Kitt Peak I filter (I_{KP}) which, for very red objects, results in significantly different I magnitudes than I_C. As with the previous section, a conversion is required before an isochrone can be plotted. By convolving the TEK CCD response with the Kitt Peak and Cousins I, and Z RGO filter profiles, D. Pinfield (private communication) derived theoretical magnitudes for a number of very red, late-type stars, including GL406 and LHS 2924. Using these calculations I

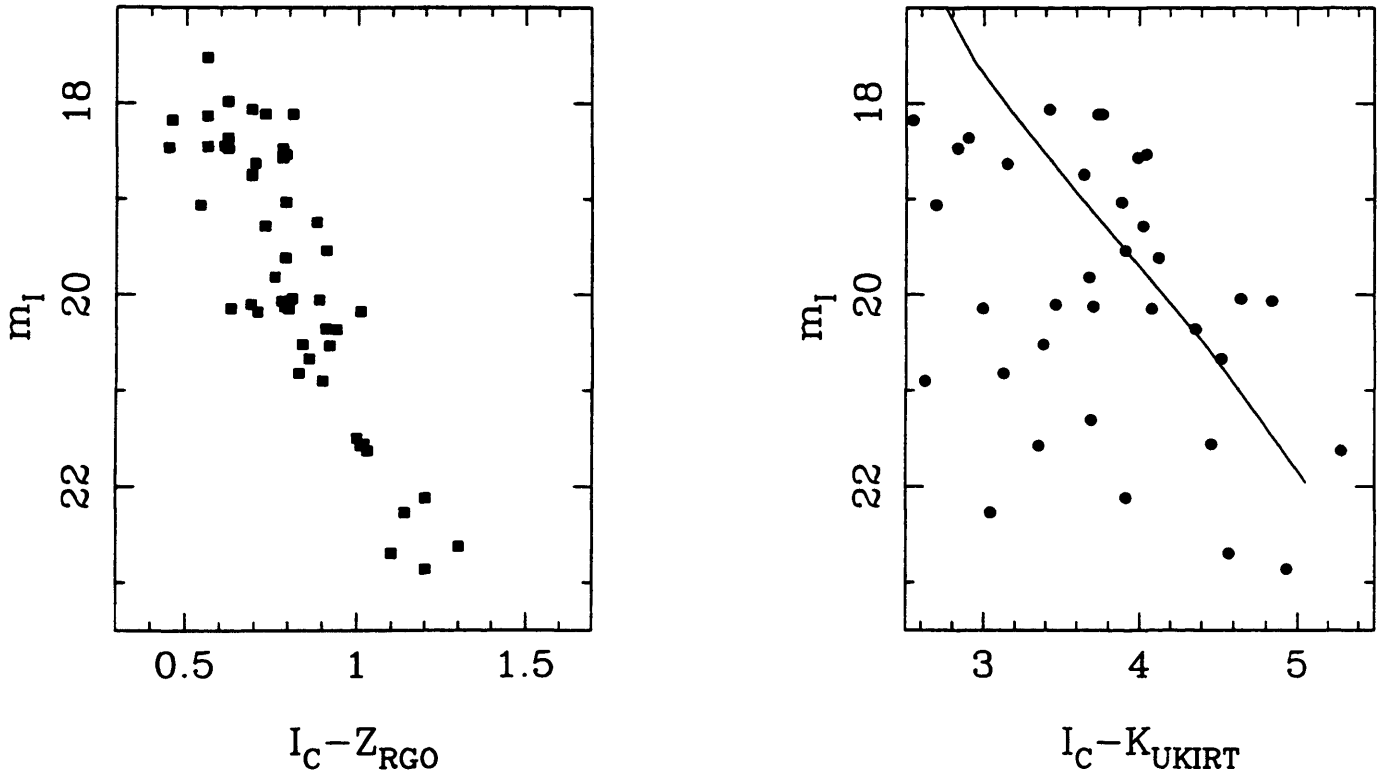

Figure 7.1: The I, I–Z and I, I–K diagrams for the ITP survey. The 5 Gyr isochrone (from Chabrier & Baraffe 1997) is plotted on the I, I–K diagram to show the position of the field star sequence shifted to the distance of the Pleiades. Objects that lie on this line or to the right of it have been considered to be possible cluster members at this stage.

Name	R.A. J2000	DEC J2000	I_H	I_H–Z_{RGO}	K_{UKIRT}	Flag
Roque48	3 47 41.3	22 44 33	17.31	0.56		?
Roque47	3 49 04.8	23 33 39	17.74	0.62	14.75±0.03	y
Roque17	3 47 23.9	22 42 38	17.78	0.81	14.38±0.05	y
Roque16	3 47 39.0	24 36 22	17.79	0.69	14.64±0.03	y
Roque15	3 45 41.2	23 54 11	17.82	0.73	14.35±0.03	y
Roque45	3 49 42.8	24 31 11	18.01	0.46	15.63±0.03	n
Roque44	3 47 38.9	22 38 41	18.12	0.62	15.46±0.04	n
Roque42	3 49 39.3	23 34 55	18.21	0.61		?
Roque14	3 46 42.9	24 24 50	18.21	0.79	14.49±0.03	y
Roque41	3 46 44.4	24 35 00	18.23	0.62	15.64±0.04	n
Roque40	3 50 00.3	24 28 15	18.24	0.56	16.22±0.04	n
Roque13	3 45 50.6	24 09 03	18.25	0.78	14.58±0.03	y
Roque39	3 46 08.4	24 45 58	18.30	0.45		?
Roque38	3 46 37.8	24 35 01	18.35	0.70	15.48±0.02	n
Roque12	3 48 19.0	24 25 12	18.47	0.69	15.10±0.10	y
Roque37	3 48 44.2	24 21 18	18.48	0.69		?
Roque11	3 47 12.1	24 28 32	18.71	0.79	15.15±0.04	y
Roque10	3 48 02.0	24 00 03	18.87	0.88	16.82±0.05	n
Roque9	3 46 23.1	24 20 36	18.99	0.73	15.26±0.02	y
Roque8	3 49 21.2	23 34 01	19.15	0.91	15.63±0.04	y
Roque7	3 43 40.3	24 30 11	19.29	0.79	15.49±0.02	y
Roque6	3 49 57.8	23 41 50	19.51	0.76	16.14±0.04	n
Roque5	3 44 22.4	23 39 01	19.71	0.81	15.40±0.10	y
Roque4	3 43 53.5	24 31 11	19.75	0.78	15.23±0.10	y
Roque3	3 44 10.9	23 40 14	19.80	0.79	16.42±0.10	n
Roque36	3 44 20.8	24 39 03	19.82	0.80	16.07±0.03	n
Roque35	3 46 18.5	24 44 41	19.90	0.71		?
Roque33	3 48 49.1	24 20 24	19.97	0.91	16.00±0.03	y
Roque32	3 47 05.8	23 24 51	20.14	0.92	17.00±0.05	n
Roque31	3 50 32.5	24 08 52	20.17	0.84	17.14±0.06	n
Roque30	3 50 15.9	24 08 35	20.31	0.86	16.15±0.03	y
Roque29	3 50 06.0	23 42 15	20.48	0.83	17.70±0.06	n
Roque28	3 50 20.6	24 08 41	20.52	0.90	18.28±0.07	n
Roque18	3 44 12.6	23 43 17	21.11	1.02	17.10±0.08	n
Roque26	3 48 49.3	22 45 50	21.13	1.01	18.22±0.20	n
Roque25	3 48 30.6	22 44 50	21.17	1.03	16.34±0.04	y
Roque24	3 43 21.1	24 34 36	21.56	1.20	18.21±0.30	n
Roque23	3 47 51.0	23 55 48	21.75	1.14	19.23±0.30	n
Roque22	3 43 21.3	24 32 02	22.00	1.30	20.13±0.30	n
Roque21	3 43 27.8	24 33 39	22.20	1.10	18.13±0.20	n
Roque19	3 48 55.0	24 20 10	22.30	1.20	17.93±0.20	n

Table 7.1: The I, Z and K photometry for the ITP survey.

have derived an approximate relationship between I_C and I_{KP} as a function of I_{KP}-Z_{RGO}. Applying these corrections to the dataset has allowed me to plot the 5 Gyr model from Chabrier & Baraffe (1997) onto the I, I–K diagram. The relationship I derived is given in Equation 7.1.

$$I_C - I_{KP} = -0.223(I_{KP} - Z_{RGO}) + 0.805(I_{KP} - Z_{RGO})^2 - 0.343(I_{KP} - Z_{RGO})^3 \quad (7.1)$$

This relationship is based on a rather limited dataset. It has been included here for the purpose of transforming the Kitt Peak I magnitudes into Cousins to allow candidate selection using isochrones published in the Cousins system. To determine a more accurate relationship between the above filter sets one should identify a number of very late, very red targets and standards, and observe them using both I_C and I_{KP}. I have compared this relationship to the one derived in Bessell (1986) between I_C–I_{KP} and $(R–I)_C$ by using the published (Leggett 1992) $(R–I)_C$ colours for the late M dwarfs rather than the I–Z colours. There is very good agreement between the two transforms.

The same selection criteria have been applied to this survey as with the ITP survey above. Table 7.2 presents all the photometry and flags possible cluster members as yes or no (y/n). A question mark in the flag column indicates that follow-up infrared photometry has yet to be obtained. The separation between probable cluster members and non-members is a little clearer in the I, I–K diagram than seen in the ITP data. This is mainly due to the fact that there is a sharp cut-off below approximately I=21 where the errors in the I–Z colour from the original survey become increasingly large. This is emphasized further in Chapter 5. It is clear from Figure 7.2 that not all the I, Z candidates have been followed up. Poor weather conditions meant that there were a number of candidates that still require infrared photometry. The success rate at the faintest I magnitudes is not surprising when one considers that the optical I, Z survey is only complete to $I_{KP} \sim 19.0$, corresponding to $I_C \sim 19.5$.

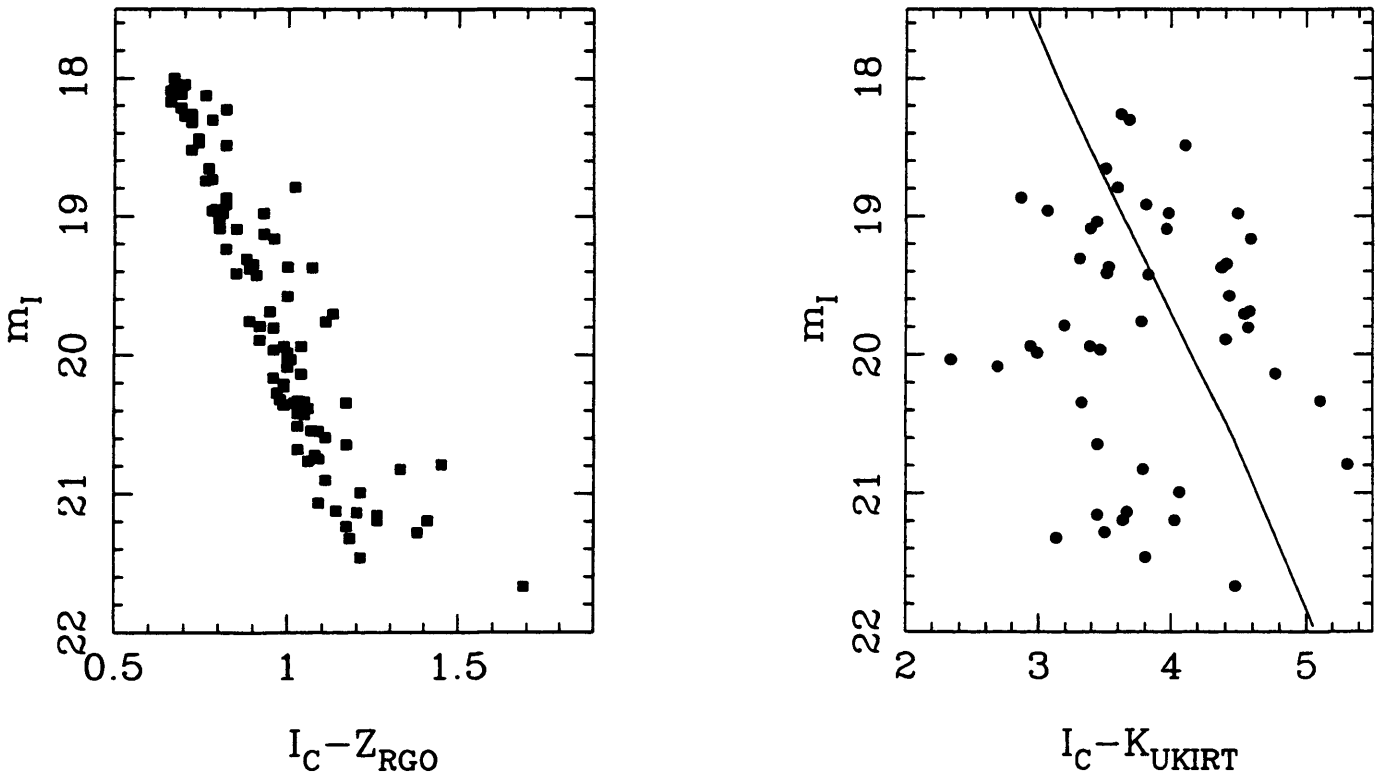

Figure 7.2: The I, I–Z and I, I–K diagrams for the Kitt Peak survey in The Pleiades. The 5 Gyr isochrone from the models of Chabrier & Baraffe (1997) is plotted on the I, I–K diagram.

Table 7.2: The I, Z and K photometry for the Kitt Peak Pleiades survey.

Name	Other Name(s)	R.A. J2000	DEC J2000	I_{KP}	$I_{KP}-Z_{RGO}$	K_{UKIRT}	Flag
1		3 39 16.83	+24 14 23.9	19.89	1.08		?
2		3 40 5.61	+24 36 43.8	17.79	0.72		?
3		3 40 6.21	+23 45 33.3	19.83	1.33	17.04±0.04	n
4		3 41 8.20	+24 17 36.8	17.99	0.72		?
5		3 42 48.10	+24 4 1.2	18.37	0.81	15.0±0.3	y
6	Roque 7	3 43 40.20	+24 30 11.3	19.19	0.92	15.49±0.02	y
7		3 43 45.63	+24 40 41.6	19.26	1.01	17.7±0.3	n
8	Roque 4	3 43 53.46	+24 31 11.3	19.53	1.05	15.23±0.1	y
9		3 45 5.99	+22 36 4.5	19.47	0.99		?
10		3 45 19.50	+22 3 26.0	19.22	1.00	17.0±0.3	n
11		3 45 45.11	+22 58 44.8	17.61	0.69		?
12		3 45 50.30	+22 36 6.3	18.73	0.91	15.6±0.3	y
13		3 45 50.43	+24 13 43.4	18.91	1.11	15.99±0.03	n
14	Roque 13	3 45 50.58	+24 9 3.5	18.43	0.96	14.58±0.03	y
15		3 45 53.18	+25 12 55.9	18.55	1.07	15.00±0.02	y
16		3 46 8.69	+22 4 48.0	19.54	1.03		?
17		3 46 16.00	+24 27 34.9	20.07	1.21	16.93±0.03	n
18		3 46 23.05	+24 20 36.1	19.07	0.96	15.24±0.02	y
19		3 46 23.62	+22 50 16.5	18.18	0.76	18.2±0.3	n
20		3 46 38.77	+24 14 14.6	18.60	1.00	15.84±0.03	n
21	Roque 14	3 46 42.90	+24 24 50.4	18.27	0.93	14.49±0.03	y
22		3 46 57.33	+24 37 45.4	18.42	0.93		?
23		3 47 5.66	+24 40 3.5	17.56	0.76		?
24		3 47 9.31	+25 13 40.9	18.01	1.02	15.20±0.02	y
25		3 47 10.88	+24 11 30.6	18.77	0.85	15.9±0.3	n
26	Roque 11	3 47 12.02	+24 28 31.5	18.81	1.00	15.15±0.04	y
27	Teide 1	3 47 17.83	+24 22 31.5	18.96	0.95	15.11	y
28		3 47 19.67	+22 55 35.3	18.15	0.78		?
29	Roque 17	3 47 23.90	+22 42 37.0	17.87	0.82	14.38±0.05	y
30		3 47 34.95	+22 51 4.8	19.32	1.00	17.4±0.3	n
31		3 47 37.82	+24 38 49.0	17.92	0.74		?
32	Roque 16	3 47 38.97	+24 36 22.1	17.73	0.72	14.64±0.03	y
33		3 47 41.93	+22 50 36.4	19.60	0.99		?
34		3 47 53.73	+23 1 40.6	18.70	0.89	17.7±0.3	n
35		3 47 54.74	+24 45 29.1	19.53	0.97		?
36		3 47 57.96	+22 6 51.3	17.61	0.66		?
37		3 48 13.45	+24 15 18.6	19.28	1.00		?
38		3 48 13.88	+24 38 30.1	17.51	0.67		?
39		3 48 18.96	+24 25 12.9	18.30	0.82	15.11±0.03	y
40		3 48 38.22	+22 33 52.5	18.25	0.82	16.0 0.2	n

Name	Other Name(s)	R.A. J2000	DEC J2000	I_{KP}	$I_{KP} - Z_{RGO}$	K_{UKIRT}	Flag
41		3 48 40.82	+24 15 26.5	17.76	0.70		?
42		3 49 12.43	+24 11 12.8	19.34	1.04	15.37±0.04	y
43		3 49 15.06	+24 36 22.3	17.53	0.70		?
44		3 49 27.08	+22 51 16.1	18.62	0.82		?
45		3 49 35.05	+24 39 16.4	18.64	0.88	16.0±0.3	n
46		3 49 37.57	+23 0 35.4	19.09	0.92	16.6±0.3	n
47		3 49 48.97	+23 1 7.5	17.69	0.66		?
48		3 49 50.82	+22 10 32.1	19.23	0.96	16.5±0.3	n
49		3 50 6.99	+25 9 56.1	19.89	1.03		?
50		3 51 18.47	+23 46 11.5	19.56	1.02		?
51		3 51 24.52	+23 50 38.8	19.57	1.06		?
52	Calar 3	3 51 25.52	+23 45 20.8	18.66	0.90	14.94	y
53		3 51 36.12	+24 18 44.0	19.08	0.89		?
54		3 51 37.62	+23 48 3.1	19.75	1.17	17.20±0.04	n
55		3 51 44.85	+23 26 38.7	18.45	0.85	15.13±0.03	y
56		3 51 49.71	+23 53 15.3	19.14	1.04	16.55±0.04	n
57		3 52 1.70	+24 49 48.9	19.63	1.03		?
58		3 52 2.00	+23 15 45.9	19.74	1.45	15.48±0.03	y
59		3 52 6.67	+24 16 0.4	17.59	0.67		?
60		3 52 6.95	+24 20 41.9	18.36	0.79		?
61		3 52 11.15	+24 22 41.8	20.23	1.09		?
62		3 52 27.83	+25 24 51.4	20.20	1.26	17.71±0.07	n
63		3 52 37.74	+25 11 17.8	19.91	1.09		?
64		3 52 52.24	+24 20 20.4	20.16	1.41	17.17±0.05	n
65		3 52 52.52	+24 11 14.3	17.89	0.74		?
66		3 52 56.69	+24 45 54.5	18.49	0.80	15.7±0.3	n
67		3 53 6.90	+25 2 11.6	19.72	1.07		?
68		3 53 10.82	+24 18 48.0	18.38	0.78	15.9±0.3	n
69		3 53 29.53	+25 13 45.5	20.25	1.14		?
70		3 53 34.39	+25 11 30.5	19.47	0.99		?
71		3 53 44.13	+25 21 4.7	20.24	1.26	17.56±0.05	n
72		3 53 47.98	+24 25 12.7	19.45	1.17	17.02±0.04	n
73		3 53 48.92	+25 25 48.2	20.26	1.38	17.78±0.06	n
74		3 53 55.04	+23 23 36.3	17.61	0.82		?
75		3 54 1.07	+24 40 36.6	19.45	0.99		?
76		3 54 3.54	+25 26 1.9	19.72	1.03		?
77		3 54 5.26	+23 33 59.5	19.43	0.96		?
78		3 54 11.06	+24 20 30.3	20.05	1.11		?
79		3 54 15.22	+25 9 51.4	18.84	1.13	15.17±0.02	y
80		3 54 44.16	+25 15 10.6	18.08	0.77	15.15±0.3	y

Name	Other Name(s)	R.A. J2000	DEC J2000	I_{KP}	$I_{KP}-Z_{RGO}$	K_{UKIRT}	Flag
81		3 54 45.78	+25 22 59.2	19.18	0.99	17.0±0.3	n
82		3 54 52.36	+24 41 50.3	20.57	1.69	17.20±0.04	n
83		3 55 0.86	+25 14 54.1	19.74	1.11		?
84		3 55 6.96	+24 51 11.2	20.22	1.20	17.47±0.06	n
85		3 55 22.99	+24 49 4.8	17.72	0.78	14.62±0.02	y
86		3 55 30.20	+23 51 48.8	19.95	1.06		?
87		3 55 34.82	+23 49 21.2	19.62	1.05		?
88		3 55 44.66	+23 26 33.2	18.44	0.80	15.6±0.3	n
89		3 55 47.06	+25 14 38.6	17.71	0.69		?
90		3 55 48.25	+25 19 45.6	20.34	1.17		?
91		3 55 49.30	+24 56 44.8	20.54	1.21	17.66±0.06	n
92		3 56 3.21	+24 34 40.6	19.62	1.03		?
93		3 56 7.15	+25 5 46.7	20.97	1.73	17.92±0.07	n
94		3 56 12.19	+24 55 18.5	20.42	1.18	18.19±0.08	n
95		3 56 14.76	+24 33 19.7	19.57	0.98		?
96		3 56 22.48	+25 7 50.7	19.71	1.09		?

The cluster Praesepe is significantly older than The Pleiades and so any brown dwarfs will have cooled over longer time periods and will therefore be fainter and harder to detect. The sub-stellar limit will in theory reside at a fainter I magnitude. The Kitt Peak survey results for Praesepe are presented in Figure 7.3. I_{KP} magnitudes have been transformed to the Cousins system as outlined above and a 5 Gyr isochrone plotted on the I, I–K diagram.

There are still many candidates from the optical survey that require follow-up infrared photometry. A second observing run is scheduled for November 1998 at UKIRT, where any remaining I, Z candidates from the Kitt Peak Pleiades and Praesepe surveys will be followed up, weather conditions permitting. For the candidates that have been followed up at K, Table 7.3 presents all the I, Z and K photometry with a flag to discriminate between possible members and non-members. For a complete list of all the optical candidates see Pinfield (1997).

The infrared follow-up survey of The Hyades cluster was unsuccessful in its attempt to identify cluster members. 33 candidates were identified from the original I, Z optical survey. The reddest objects from this survey were targeted first, moving from the faint end of the sequence to the brighter candidates later, i.e. the most promising candidates. None of these objects remained red in I–K and as a result of time constraints, the remaining candidates were not followed up during this UKIRT observing run. In the interests of completeness they should be followed up at the

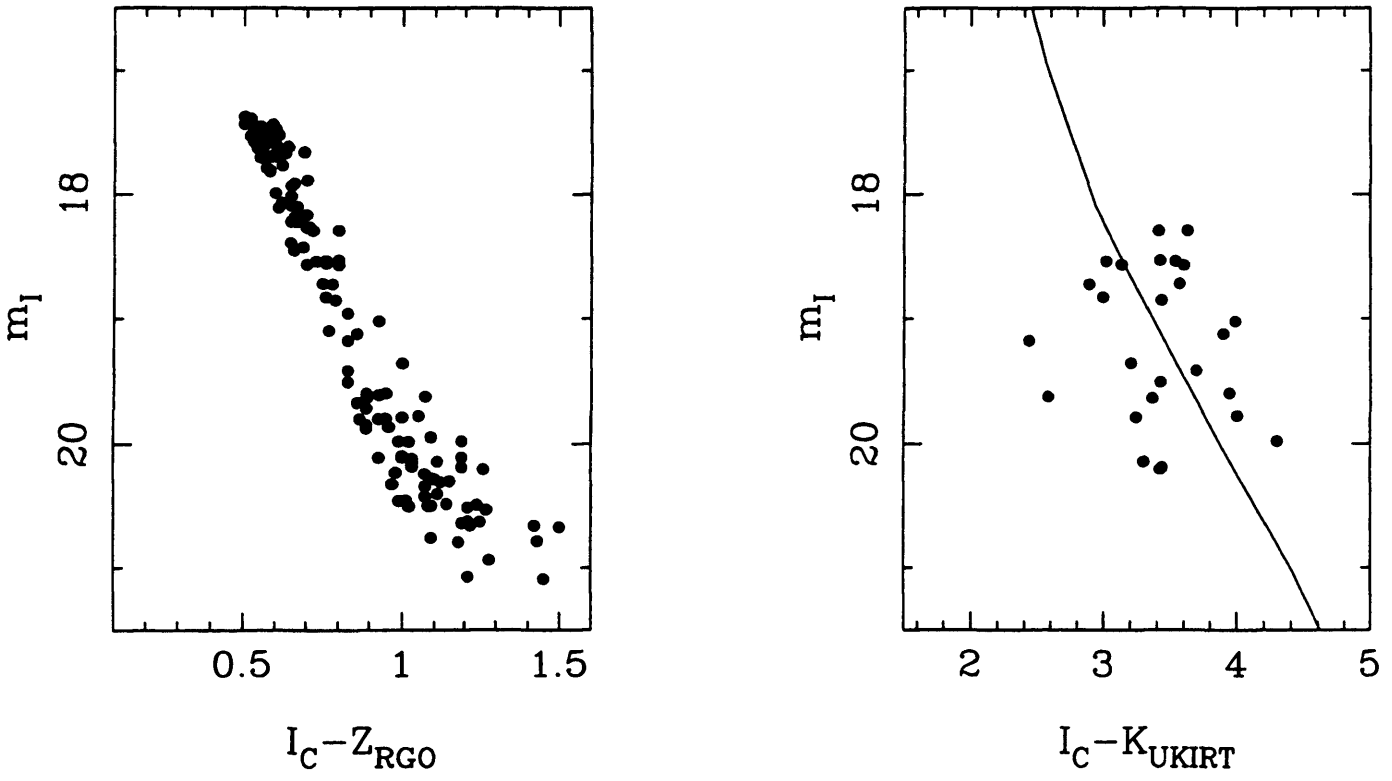

Figure 7.3: The I, I–Z and I, I–K diagrams for the Kitt Peak survey in Praesepe. The 5 Gyr isochrone from the models of Chabrier & Baraffe (1997) is plotted on the I, I–K diagram.

Name	R.A. J2000	DEC J2000	I_{KP}	$I_{KP}-Z_{RGO}$	K_{UKIRT}	Flag
izpr3	8 33 40.84	+21 12 54.3	17.93±0.05	0.80±0.07	15.11±0.02	y
izpr5	8 34 3.85	+20 34 8.1	18.14±0.08	0.78±0.09	15.83±0.03	n
izpr10	8 34 44.99	+19 29 49.5	17.97±0.06	0.80±0.07	14.97±0.02	y
izpr13	8 34 54.65	+19 52 29.3	18.88±0.10	0.83±0.12	16.08±0.04	n
izpr18	8 35 11.01	+20 06 36.6	18.26±0.07	0.79±0.09	15.42±0.04	y
izpr23	8 35 28.40	+19 12 21.8	18.87±0.13	0.95±0.15	15.65±0.04	y
izpr25	8 35 36.42	+21 25 3.9	17.69±0.04	0.80±0.05	14.66±0.02	y
izpr36	8 36 32.14	+21 18 45.8	19.07±0.15	1.19±0.17	15.68±0.02	y
izpr38	8 36 50.79	+21 4 15.2	18.00±0.05	0.73±0.07	15.52±0.03	n
izpr40	8 37 2.11	+19 52 6.4	17.76±0.06	0.72±0.07	14.88±0.02	y
izpr50	8 38 8.08	+18 3 32.0	18.05±0.05	0.70±0.07	15.43±0.03	n
izpr52	8 38 18.42	+18 35 7.8	18.96±0.12	0.89±0.14	16.27±0.04	n
izpr59	8 38 50.99	+18 5 47.1	18.26±0.06	0.76±0.08	15.83±0.04	n
izpr82	8 42 0.23	+19 50 8.2	19.02±0.13	1.00±0.17	16.54±0.04	n
izpr85	8 42 8.03	+18 16 40.3	18.80±0.19	1.07±0.21	17.04±0.06	n
izpr86	8 42 11.43	+19 52 49.4	18.31±0.10	0.93±0.14	15.03±0.03	y
izpr93	8 43 14.88	+19 44 9.3	18.97±0.10	1.05±0.14	15.77±0.03	y
izpr94	8 43 17.25	+19 32 22.6	17.97±0.05	0.76±0.08	15.00±0.03	y
izpr95	8 43 20.33	+19 5 40.4	19.25±0.16	1.26±0.19	16.78±0.03	n
izpr97	8 43 43.12	+19 51 38.5	19.28±0.22	1.19±0.27	16.75±0.04	n
izpr104	8 44 20.44	+19 52 33.3	19.29±0.21	1.11±0.26	16.84±0.06	n
izpr105	8 44 23.89	+19 43 45.9	18.59±0.08	1.00±0.12	16.15±0.03	n
izpr110	8 44 42.81	+18 54 39.3	18.55±0.08	0.83±0.11	16.74±0.05	n
izpr113	8 45 22.16	+18 13 51.0	18.16±0.04	0.75±0.06	15.15±0.03	y
izpr117	8 45 31.71	+18 34 7.5	18.79±0.05	0.83±0.08	15.72±0.03	y
izpr126	8 46 16.79	+19 52 28.8	18.47±0.07	0.86±0.11	15.22±0.02	y

Table 7.3: I, I–Z and K photometry for the Kitt Peak Praesepe sample.

Name IPMBD	RA J2000 Ep. 1995	DEC J2000 Ep. 1995	I_{IVN} ± 0.2	R_{59F} ± 0.2	I_C ± 0.04	K_{UKIRT} ± 0.03	Other ID
11	3 55 23.04	24 49 05.5	18.1		18.07	14.73	IZpl85[1]
20	3 49 04.84	23 33 39.6	18.1		18.05	14.75	
21	3 49 16.15	26 49 03.6	17.9	2.8	17.85	14.65	
22	3 49 33.03	26 50 43.0	18.0		17.90	14.92	
23	3 48 04.63	23 39 30.7	18.0	2.5		14.43	PPL 15[2]
25	2 46 26.06	24 05 09.9	18.0		17.82	14.24	
26	3 47 15.17	25 24 19.2	18.1		18.11	14.98	
29	3 45 31.33	24 52 47.8	18.2		18.35	14.48	
43	3 39 17.03	22 27 11.5	18.1			14.80	

Table 7.4: Photometry and coordinates for the Double I survey.

[1] Pinfield *et al.* (1998)

[2] Stauffer, Hamilton & Probst (1994)

next observing run at UKIRT in November 1998. A complete list of all the optical candidates can be found in Pinfield (1997).

7.4.3 The Double I Survey Results

From a target list of 45 brown dwarf / VLMS candidates 9 were found to have I–K colours consistent with cluster membership, which included the object PPL 15 (Stauffer, Hamilton & Probst 1994). These 9 brown dwarfs have been used by Hambly *et al.* (1998) to define the Pleiades initial mass function across the stellar / sub-stellar boundary. They were initially selected from a proper motion survey using Schmidt Plates, and so have photographic I magnitudes (I_{IVN}). I–K colours were derived using these I magnitudes and the UKIRT K photometry. On a recent observing trip to La Palma during December and January 1997, some of these 45 candidates were observed using the I_H filter. It was therefore possible to derive I_C magnitudes for some of the brown dwarfs by using the transforms presented in Chapter 5. I present the results from this survey in Table 7.4. The 9 brown dwarf candidates have proper motions consistent with the cluster motion at the level of 1 sigma. Optical and infrared photometry suggests that they are cluster members also, and so they are excellent brown dwarf candidates.

7.4.4 The RIZ Survey Results

Of the 26 candidate cluster members, 6 were observed at UKIRT in November 1997. Prior to this 11 of the RIZpr stars were observed using WHIRCAM on the WHT in October 1996. 8 of these candidates appear to be members on the basis of their position on an I, I–K colour-magnitude diagram (see Figure 7.4, the I, I–Z colour-magnitude diagram can be found in Pinfield *et al.* 1997.) There remain 9 candidates from the optical survey that require infrared photometry. These are close to the survey limit, and have large error bars in the I–Z colour. Table 7.5 presents the optical and infrared photometry for this survey and includes those objects that were followed up at the WHT rather than UKIRT. Non-members have been flagged as 'n' and candidates that show signs of binarity, flagged as 'b'. Signs of possible binarity are seen in the position of candidates on the I versus I–K diagram. Binary systems of equal mass should in theory (see Steele & Jameson 1995), lie on a sequence that sits 0.75 magnitudes above the cluster sequence. Plotting the binary sequence on Figure 7.4 picks out 4 binary system candidates. Any binary system where the mass ratio was not equal would lie in the intervening region between the single and binary sequences. Higher order multiple systems would sit above the binary sequence. Observations in The Pleiades cluster by Steele & Jameson (1995) suggest that the binary fraction is of the order of 50 %. The preliminary results from this infrared survey in Praesepe are in excellent agreement with this figure (of the order of 44 %).

7.5 Conclusions

In this chapter I have presented the infrared follow-up photometry for a number of different surveys that the Leicester Brown Dwarf group have been involved in. There are still a number of optical brown dwarf candidates that need to be followed up. I have used the I, I–K colour-magnitude diagram with an appropriately aged isochrone to establish membership of each respective cluster. This is not a conclusive test of course, but serves to select members for analysis of each cluster's luminosity and mass functions. In Table 7.6 I have summarised the results of this chapter in presenting the number of brown dwarf candidates that have I–K colours consistent with cluster membership, and the number of optical candidates that still require follow-up infrared photometry from each survey.

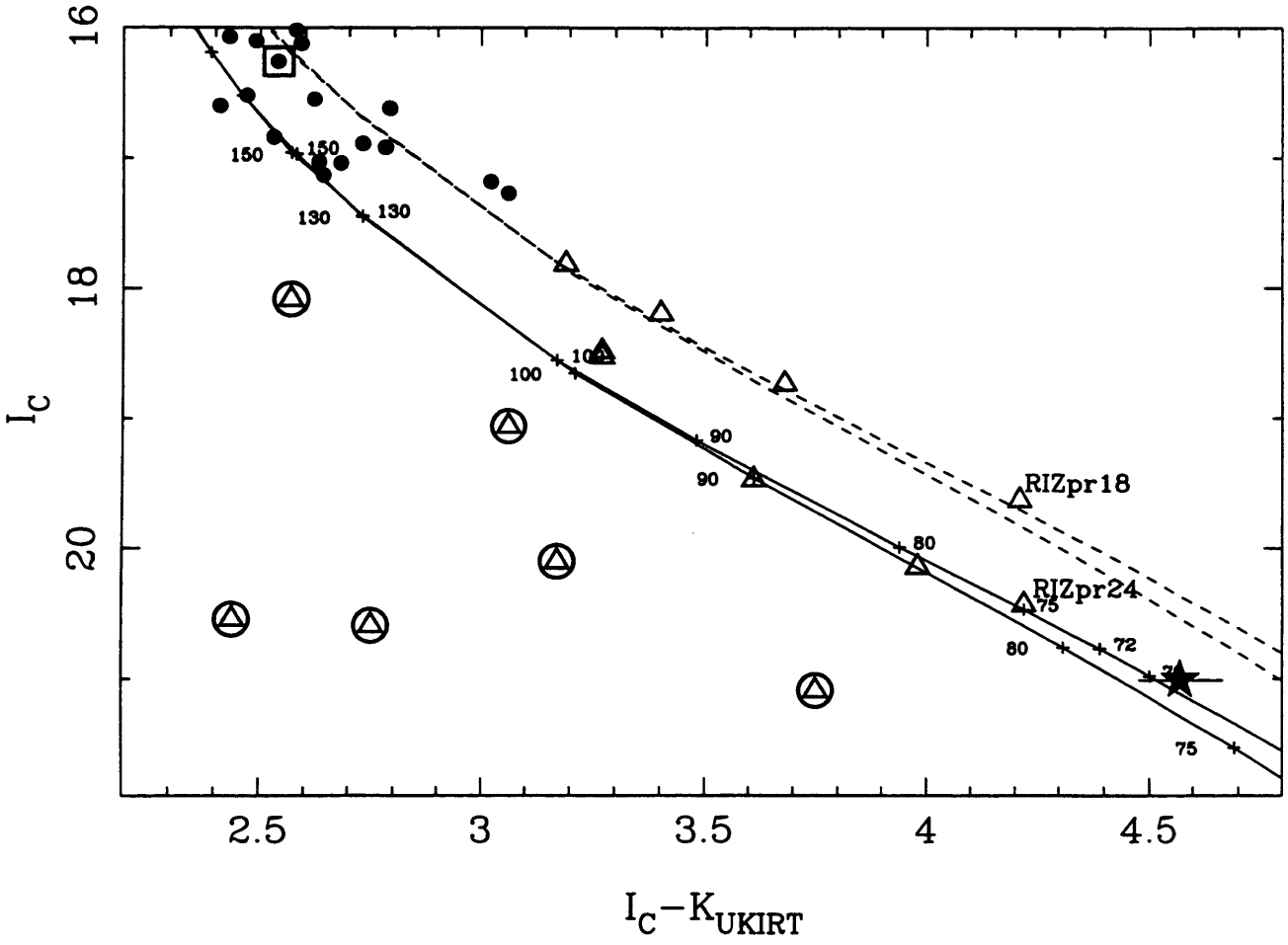

Figure 7.4: The I, I–K diagram for the lower main sequence in Praesepe. The isochrones (solid lines) are from Baraffe *et al.* (1998) for ages of 1 Gyr (lower) and 500 Myr (upper). The dashed lines are the equal mass binary sequences for each isochrone. The mass points on the isochrones are denoted by '+' signs, in Jupiter masses. The object marked as a star is RPr1 from Magazzu *et al.* (1998).

Name	R.A. (J2000)	Dec (J2000)	I_C	K	Telescope	Flag
RIZpr 1	8 36 54.6	+19 54 15	20.14±0.12	16.16±0.08	W	y
RIZpr 2	8 37 02.1	+19 52 07	18.19±0.04	14.79±0.04	W	b
RIZpr 4	8 38 11.7	+19 59 44	18.52±0.03	15.25±0.04	W	y
RIZpr 6	8 38 33.2	+19 49 13	21.09±0.16	17.34±0.05	U	n
RIZpr 7	8 39 20.0	+19 42 41	21.24±0.16	19.17±0.17	U	n
RIZpr 8	8 39 20.4	+20 01 37	17.81±0.02	14.62±0.04	W	b
RIZpr 10	8 39 20.0	+20 00 54	20.54±0.10	18.10±0.07	U	n
RIZpr 11	8 39 47.7	+19 28 04	19.47±0.06	15.86±0.14	W	y
RIZpr 12	8 39 48.8	+19 26 07	20.10±0.12	16.93±0.21	W	n
RIZpr 13	8 40 27.5	+19 28 49	20.24±0.07	18.51±0.11	U	n
RIZpr 14	8 40 46.1	+20 03 25	20.59±0.08	17.84±0.06	U	n
RIZpr 18	8 41 08.5	+19 54 01	19.63±0.08	15.42±0.04	W	b
RIZpr 20	8 41 24.8	+19 57 26	18.48±0.04	15.21±0.04	W	y
RIZpr 21	8 42 11.5	+19 52 50	18.73±0.05	15.05±0.02	W	b
RIZpr 23	8 42 54.6	+20 03 36	19.06±0.03	16.00±0.16	W	n
RIZpr 24	8 43 01.3	+19 50 00	20.43±0.16	16.21±0.03	U	y
RIZpr 26	8 43 59.5	+20 07 10	18.08±0.04	15.51±0.06	W	n

Table 7.5: I and K photometry for the RIZ Praesepe survey.

In column 6, W = WHT and U = UKIRT. In column 7, binary systems are flagged as 'b', cluster members as 'y' and non-members as 'n'.

Survey Name	Cluster	No. Brown Dwarfs after K follow-up	No. Optical candiates remaining for K follow-up	% Hit Rate
ITP	Pleiades	16	4	42
INT	Pleiades	1 (PIZ 1)	0	10
Double I	Pleiades	9	0	20
Kitt Peak	Pleiades	19	47	39
Survey Name	Cluster	No. VLMS and BDs after K follow-up	No. Optical candiates remaining for K follow-up	% Hit Rate
RIZ	Praesepe	9	0	35
Kitt Peak	Praesepe	13	115	50
Kitt Peak	Hyades	0	24	0

Table 7.6: A summary of the survey results from this chapter.

Chapter 8

The Pleiades Luminosity and Mass Functions

8.1 Introduction

In this chapter I present the luminosity and mass functions for the Pleiades cluster. Many surveys have been carried out in this cluster over the past 3 years resulting in the identification of a number of good brown dwarf candidates. I will use the latest infrared results from chapter 7 to extend the mass function well into the brown dwarf regime. I will discuss previous surveys along with their derived mass and luminosity functions, but will first outline the basic theory behind these two important quantities.

8.1.1 Review

The luminosity function (LF) of a stellar population is defined as the number of stars per unit magnitude interval. It is common to see this expressed as the number of stars per unit M_V per cubic parsec, but for cooler objects and brown dwarfs it is more fitting to use M_I rather than M_V. The use of a cubic parsec is common to studies of the field luminosity function (see below) rather than in the study of open clusters. It is more appropriate to use the entire cluster as the volume, thus calculating a cluster luminosity function instead. Most of the surveys conducted within The Pleiades concentrate on looking for brown dwarfs in the cluster centre where the population of such objects is believed to be higher. When deriving a LF for the whole cluster using data from such surveys, one must consider a correction term which will be discussed later.

The mass function (MF) of a stellar population is defined as the number of stars per unit mass interval. The relationship between the LF and the MF is shown in Equation 8.1, where $\frac{dM_\lambda}{dm}$ is the derivative of the mass-luminosity relationship.

$$\mathrm{MF} = \frac{\mathrm{dN}}{\mathrm{dm}} = \mathrm{LF}_\lambda[\frac{\mathrm{dM}_\lambda}{\mathrm{dm}}] = \frac{\mathrm{dN}}{\mathrm{dM}_\lambda}\frac{\mathrm{dM}_\lambda}{\mathrm{dm}} \tag{8.1}$$

When discussing the mass function in a cluster or the field, one refers to a power law. For the purposes of this thesis, this power law can be represented by Equation 8.2.

$$\mathrm{MF} = \mathrm{constant} \times \mathrm{m}^{-\alpha} \tag{8.2}$$

When α=2 the lower and higher mass stars contribute equally to the overall mass. For α>2 the lower mass stars begin to dominate. When one plots log N versus log mass, the mass function is represented as a line with slope -α.

8.1.2 In the field

When determining the field LFs there are three important considerations to be made. These are outlined below :

- The incompleteness of a magnitude limited sample as a result of intrinsically faint stars. This is more commonly referred to as the Malmquist bias.

- As the distance increases the number of un-resolved binaries also increases and some correction has to be made for this effect.

- There is a vertical density gradient from the Galactic disk that has to be taken into account.

For stars more massive than 0.4 $M_\odot$, Salpeter (1955) determined a power law relation for the MF of α = 2.35. More recent surveys have extended this mass limit close to the sub-stellar limit. Work by Reid (1987) concluded that the observed mass density locally is $\sim 0.09 M_\odot pc^{-3}$ and the Oort missing mass remains unfound. This local and disk missing mass was inferred from dynamical considerations, and it is possible that it may be due to an old population of dim, red stars, (see Oort (1960)). Hawkins & Bessell (1988) describe a photometric survey for late M-dwarfs

using R- and I- band Schmidt plates. Covering an approximate area of 85 square degrees the survey includes some 500 M-stars within 100 parsecs and concludes that the mass function is steadily increasing towards the survey limit of $M_R \sim 17$. Using the theoretical mass-luminosity relationship derived in Chabrier, Baraffe & Plez (1996), Mera, Chabrier & Baraffe (1996) determine the lower end of the stellar mass function in the Galactic disk from observed luminosity functions. They conclude that the MF rises with decreasing mass with $\alpha = 2 \pm 0.5$ for $0.08 < M_\odot < 0.6$. Such a result suggests a substantial number of brown dwarfs in the Galactic disk.

8.1.3 The Pleiades

Combining a deep proper motion survey using R and I Schmidt plates and subsequent follow-up infrared photometry, Hambly, Hawkins & Jameson (1991) present deep luminosity and mass functions for the cluster. Their results indicate the presence of a large number of VLMS in the cluster, and depending on the theoretical model used, a number of brown dwarf candidates also. Stauffer *et al.* (1991) determine the cluster LF down to m_v=18. By obtaining I and K photometry, Simons & Becklin (1992) derive α=2.8 for the mass function in the brown dwarf regime. Williams *et al.* (1996) obtained optical and infrared images close to the cluster centre. They followed up candidates with infrared spectroscopy and conclude that the MF is flat in the VLMS and brown dwarf regime with no significant contribution being made to the missing mass or dark matter in the cluster. The mass range for their survey is between 0.25 and 0.04 $M_\odot$. Festin (1998) finds the MF rising with α between 0 and 1 after imaging 850 square arcminutes of the cluster at R,I,J and K. Despite this rise, he concludes that the MF is still not steep enough to leave more than a few % of the cluster's overall mass in brown dwarfs. A larger area survey at R and I by Bouvier *et al.* (1998) presents a LF down to $M_I \sim 15$. They find that the MF can be described by a log-normal distribution except below the hydrogen burning mass limit where there are more objects than predicted. Hambly *et al.* (1998) used I band photographic Schmidt plates to survey the central 6 x 6 square degrees of the cluster. Using SuperCOSMOS to identify proper motion members, near infrared and infrared photometry was then obtained for a numbers of candidates as faint as PPL 15 and up to 0.3 magnitudes fainter. The MF presented from this survey is flat across the stellar/substellar boundary. In his thesis, Pinfield (1997) desribes a survey undertaken at the Kitt Peak Burrell Schmidt telescope. He presents a MF

into the brown dwarf regime with α=1.3, consistent with the findings of Hambly, Hawkins & Jameson (1991).

8.2 The Luminosity Function

To determine the LF of the cluster I have used the results of the following surveys; the Kitt Peak and ITP surveys (described in chapter 7), and the Canada France Hawaii Telescope (CFHT) survey of Bouvier *et al.* (1998). I am interested in the magnitude range I_C=17.6 to 19.5, for which all these surveys are complete. There are many brown dwarf candidates fainter than this, but to cover the largest area most completely, this brighter cut-off has to be made. This corresponds to an approximate mass range of 0.075 to 0.05 $M_\odot$. The central density of stars is not of course constant throughout the cluster. Using the profiles presented in King (1962) one can model the distribution of the higher mass stars in the cluster, (see Pinfield, Hodgkin & Jameson (1998)).

To further describe the King profiles it is necessary to define 2 important equations, 8.3 and 8.4.

$$f_s = k\left\{\frac{1}{\sqrt{1+(r/r_c)^2}} - \frac{1}{\sqrt{1+(r_t/r_c)^2}}\right\}^2 \tag{8.3}$$

$$n = \pi r_c^2 k\left\{ln(1+x) - 4\frac{(1+x)^{\frac{1}{2}}-1}{(1+x_t)^{\frac{1}{2}}} + \frac{x}{1+x_t}\right\}$$
$$where \;\; x_t = (r_t/r_c)^2 \tag{8.4}$$
$$and \;\; x = (r/r_c)^2$$

Within these 2 equations, r_c is the core radius, (the radius at which the surface density falls to half its central value, if r_t=∞), r_t is the tidal radius, (the radius where the Galactic tidal force balances the cluster's own gravity), f_s is the surface density distribution of the stars, n is the total number of cluster stars, and k is a normalisation constant. The tidal radius, r_t is 13.1 parsecs from Pinfield, Hodgkin & Jameson (1998). Defining the core radius, r_c, for the brown dwarf regime is difficult to do. In the original paper Pinfield, Hodgkin & Jameson (1998) found $r_c \sim mass^{-0.5}$ as theory predicts for a relaxed cluster for the high mass stars, but a possible turn down in the lowest mass bin. Pinfield (private communication) has split the lowest mass into several sub-bins, see Figure 8.1. This figure shows that r_c may be levelling off for the lowest masses, i.e. the cluster is not entirely relaxed. The relaxation time of a cluster is the time taken for complete equipartition of energy to occur. The

stars in a cluster interact gravitationally so that kinetic energy from the higher mass stars is transferred to the lower mass stars until equipartition of energy is reached. To derive the correct LF it is important to measure r_c for the brown dwarfs. For example, assuming r_c (brown dwarfs) = 6pc from a fully relaxed cluster and the observed central density would seriously overestimate the number of brown dwarfs. One would expect to find a higher number of brown dwarfs towards the cluster centre due to the dynamical arguments presented above. This is why most of the surveys carried out to date have concentrated on the cluster centre to improve the chances of detection.

By dividing Equation 8.4 by 8.3 one can remove the dependency on k and determine a value of r_c. To do this one must use the observational results to define the central surface density, f_s, within a specified radius. From this analysis, r_c is 2±1 parsecs, which is consistent with the findings of Pinfield, Hodgkin & Jameson (1998). Unfortunately, due to the poor statistics in this region, the error is inevitably large. Bouvier *et al.* (1998) assume that the distribution of the brown dwarfs in the cluster can be modelled using the distribution of the VLMS in the cluster. According to the calculations of Pinfield, Hodgkin & Jameson (1998) this would again result in a core radius of 3 parsecs. I have therefore decided to adopt r_c=3 pc as the least controversial conclusion. It will however be interesting to see if future data confirm or otherwise the core radius turning down in the brown dwarf regime.

The distribution of the brown dwarfs in the magnitude range 17.6 to 19.5 (I_C, is shown in 8.2. The outer circle defines a radius of 2.2 degrees, encompassing an area of 15.2 square degrees. The brown dwarf surveys cover 7.16 square degrees, corresponding to approximately 47% of this total area. The position of the fields from each survey are also shown as rectangles in this figure.

One needs to determine the number of brown dwarfs out to the tidal radius, r_t=13.1 pc, for each magnitude bin. Table 8.1 shows the number of brown dwarfs in each bin, out to a radius of 5.19 pc, which is 2.2 degrees at a distance of 135 pc. From Equation 8.4, one can now write Equation 8.5 shown below. All the above assumes r_c=3 pc for brown dwarfs of all masses. Clearly with the limited statistics available, a more sophisticated analysis would not be appropriate.

$$\frac{n(r_t)}{n(r)} = \frac{\left\{ ln(1+x_t) - 4\frac{(1+x_t)^{0.5}-1}{(1+x_t)^{0.5}} + \frac{x_t}{1+x_t} \right\}}{\left\{ ln(1+y) - 4\frac{(1+y)^{0.5}-1}{(1+x_t)^{0.5}} + \frac{y}{1+x_t} \right\}} \qquad (8.5)$$

$$where \quad y = (r/r_c)^2$$

$$and \quad x_t = (r_t/r_c)^2$$

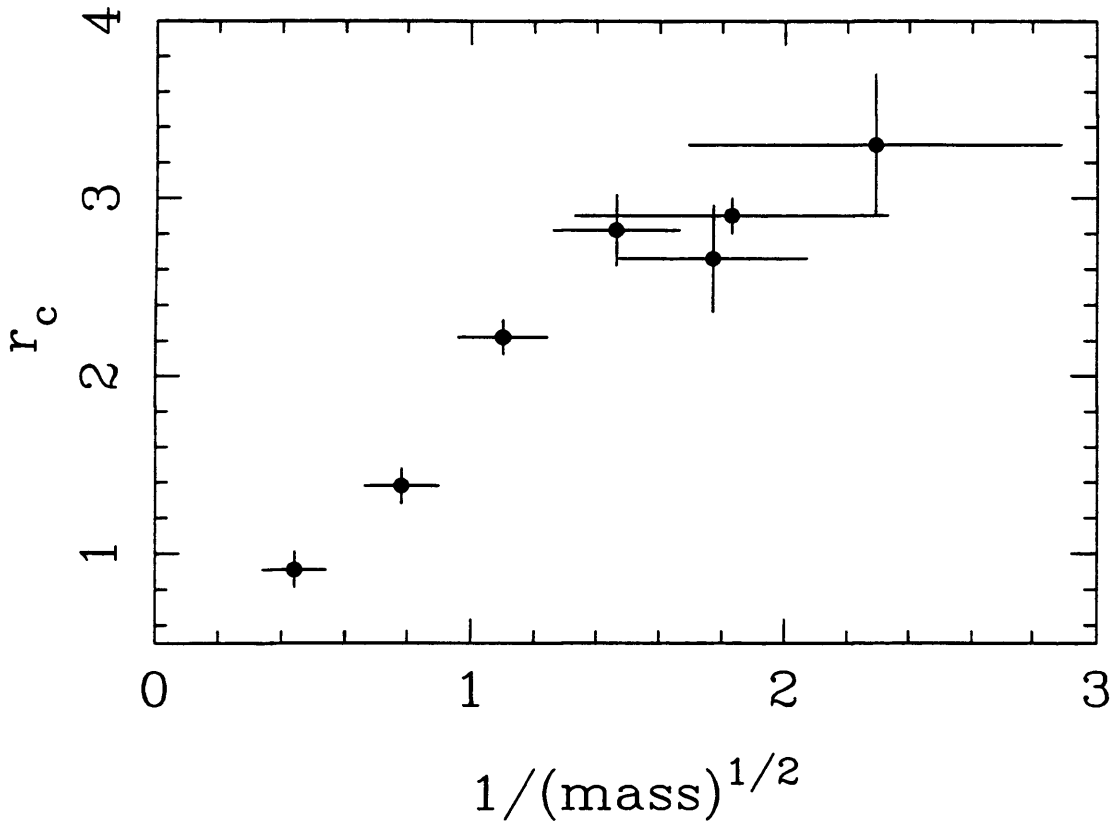

Figure 8.1: The core radius mass relationship for the Pleiades. r_c may be levelling off, or even beginning to decrease at the lowest masses. Further observational data points are essential to properly understand this effect.

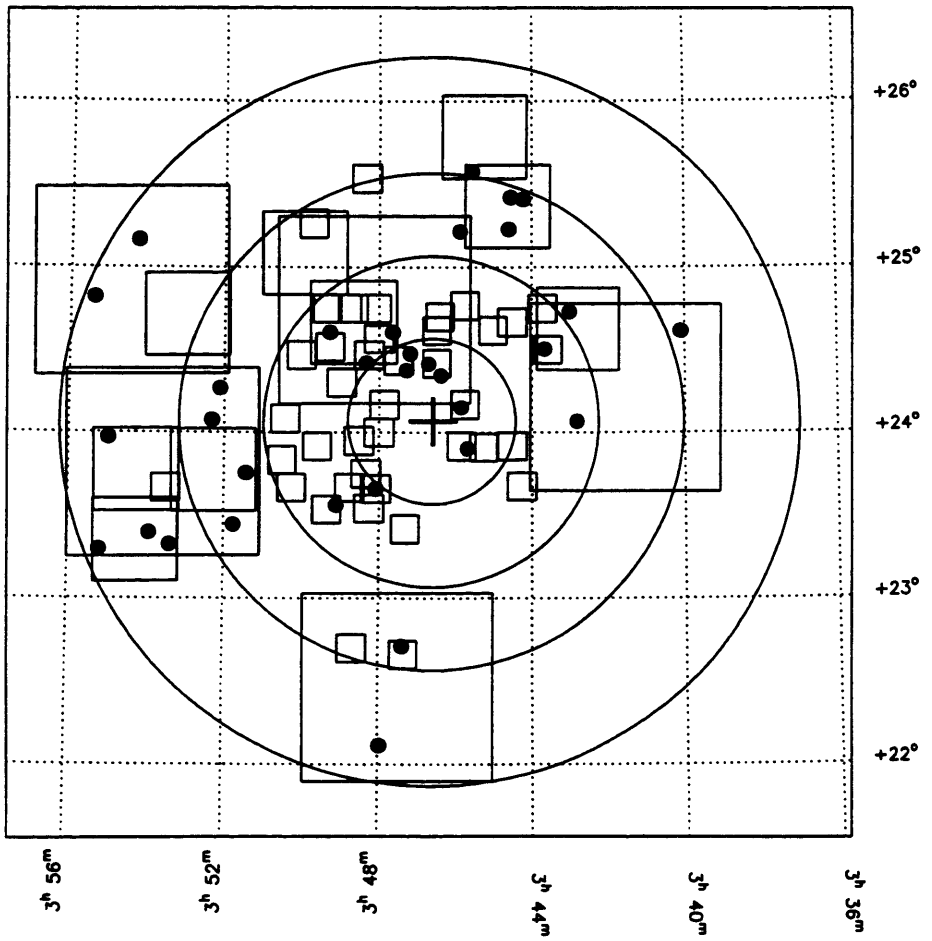

Figure 8.2: The distribution of brown dwarfs (solid circles), in the central region of the Pleiades. The concentric circles of radius (moving outwards), 0.5, 1.0, 1.5 and 2.2 degrees are also plotted on this figure. The rectangles show the actual fields covered in the original surveys.

Magnitude Bin (I_C)	Number of Brown Dwarfs
17.5-18.0	19
18.0-18.5	11
18.5-19.0	25
19.0-19.5	17

Table 8.1: The Luminosity Function of the Pleiades out to 5.19 parsecs

Magnitude Bin (I_C)	Number of Brown Dwarfs per unit magnitude	$\pm$
17.5-18.0	50	19
18.0-18.5	28	13
18.5-19.0	66	19
19.0-19.5	44	16

Table 8.2: The Cluster Luminosity Function of the Pleiades out to the tidal radius.

By putting r=5.19 pc, r_t=13.1 pc and knowing n(r) for each magnitude bin, given in Table 8.1, Equation 8.5 then reduces to Equation 8.6 below :

$$n(r_t) = n(r) \times 1.29 \tag{8.6}$$

The cluster luminosity function out to the tidal radius of 13.1 pc then follows and is given in Table 8.2. The overall luminosity function for the cluster is shown in Figure 8.3. The stellar data is taken from Hambly *et al.* (1998) and has also been corrected to the tidal radius.

8.3 Mass Function

To convert the LF given in Table 8.2 I used a mass luminosity relationship from Chabrier & Baraffe (1997) for an age of 120 Myr and applied a distance modulus of 5.65 (Steele & Jameson 1995), for the cluster. Using a mass-luminosity (ML) relationship in this way requires a note of caution. The internal structure of VLMS and brown dwarfs is essentially fully convective, with increasing molecular opacities

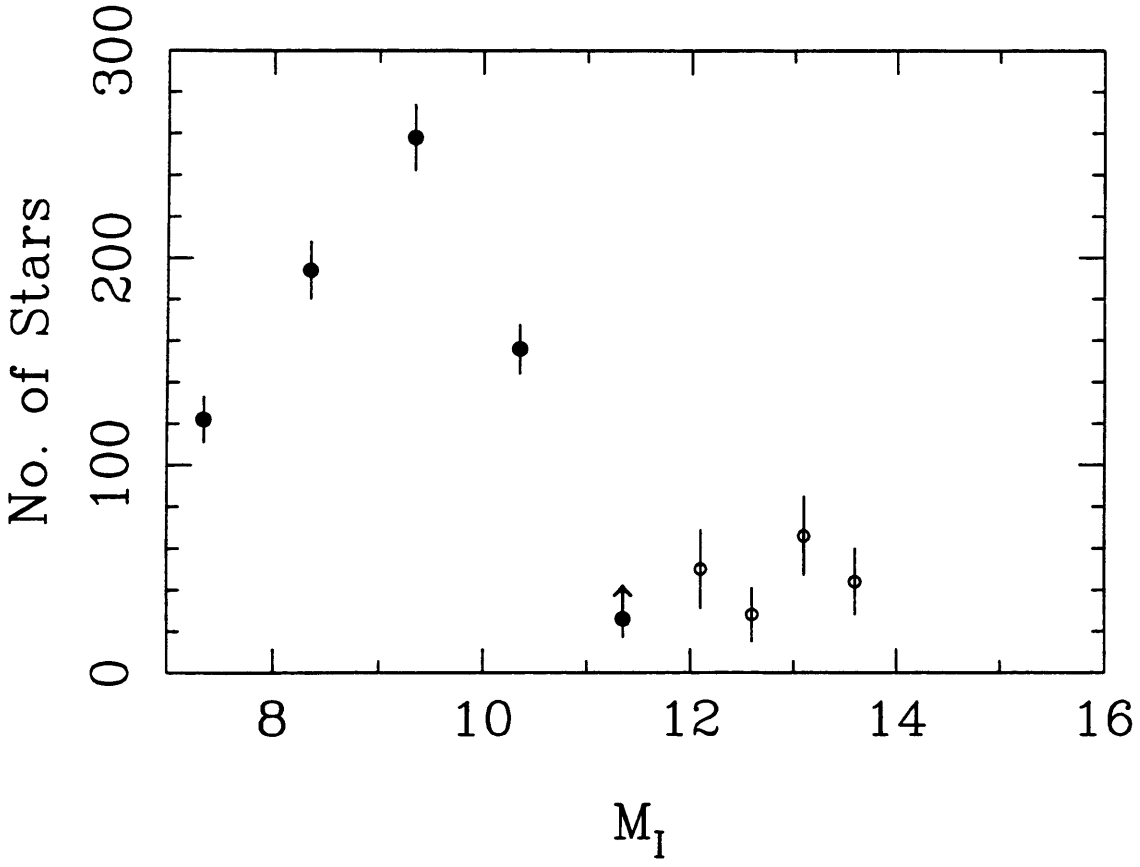

Figure 8.3: The Luminosity Function of The Pleiades. The stellar data is taken from Hambly *et al.* (1998) and is shown as solid circles. The LF derived here is presented as open circles. Square root errors are plotted.

I_C range	m($M_\odot$)	m range	log m	log N(M)
17.5-18.0	0.076	0.081-0.071	-1.119	2.90
18.0-18.5	0.067	0.071-0.062	-1.174	2.89
18.5-19.0	0.059	0.062-0.055	-1.229	3.37
19.0-19.5	0.053	0.055-0.050	-1.276	3.34

Table 8.3: The Mass Function of The Pleiades.

as one moves to lower masses. The increased opacities have a direct impact on the ML relationship so it is important that they are treated as accurately as possible. The derived mass function is given in Table 8.3. This is plotted in Figure 8.4. Also plotted in the figure is the mass function from the HHJ survey, (Hambly, Hawkins & Jameson 1991).

The MF presented in Figure 8.4 shows strong evidence that it continues with the same slope on reaching the sub-stellar boundary and shows no sign of a turn-down beyond it. One could in fact interpret the two lowest mass bins as showing evidence of a steepening of the slope, but with the small number statistics available here, this conclusion would need further observational data. The star symbol plotted on Figure 8.4 is from Hambly *et al.* (1998). In their paper, they claim that the MF can be represented by a log normal distribution in the dN/dm - log m plane, consistent with the arguments presented in Adams & Fatuzzo (1996). Indeed, they fit such a model to the data between masses of approximately 5 $M_\odot$ and 0.07 $M_\odot$. Before one can confirm or otherwise the validity of using such a model distribution, further data is needed to reduce the error bars on the points in the brown dwarf regime. Hambly *et al.* (1998) do stress the dangers of extrapolating this model into the brown dwarf mass bins as there may be some evidence, as seen here, of a possible turn-up in the mass function. This MF reaches masses as low as 50 $M_{Jupiter}$ and presents evidence that brown dwarfs are not as rare as predicted by Adams & Fatuzzo (1996). Although this MF is still not steep enough in the sub-stellar regime for brown dwarfs to account for all the missing mass or dark matter within clusters, it is a very encouraging result for the future study of such very low-mass objects.

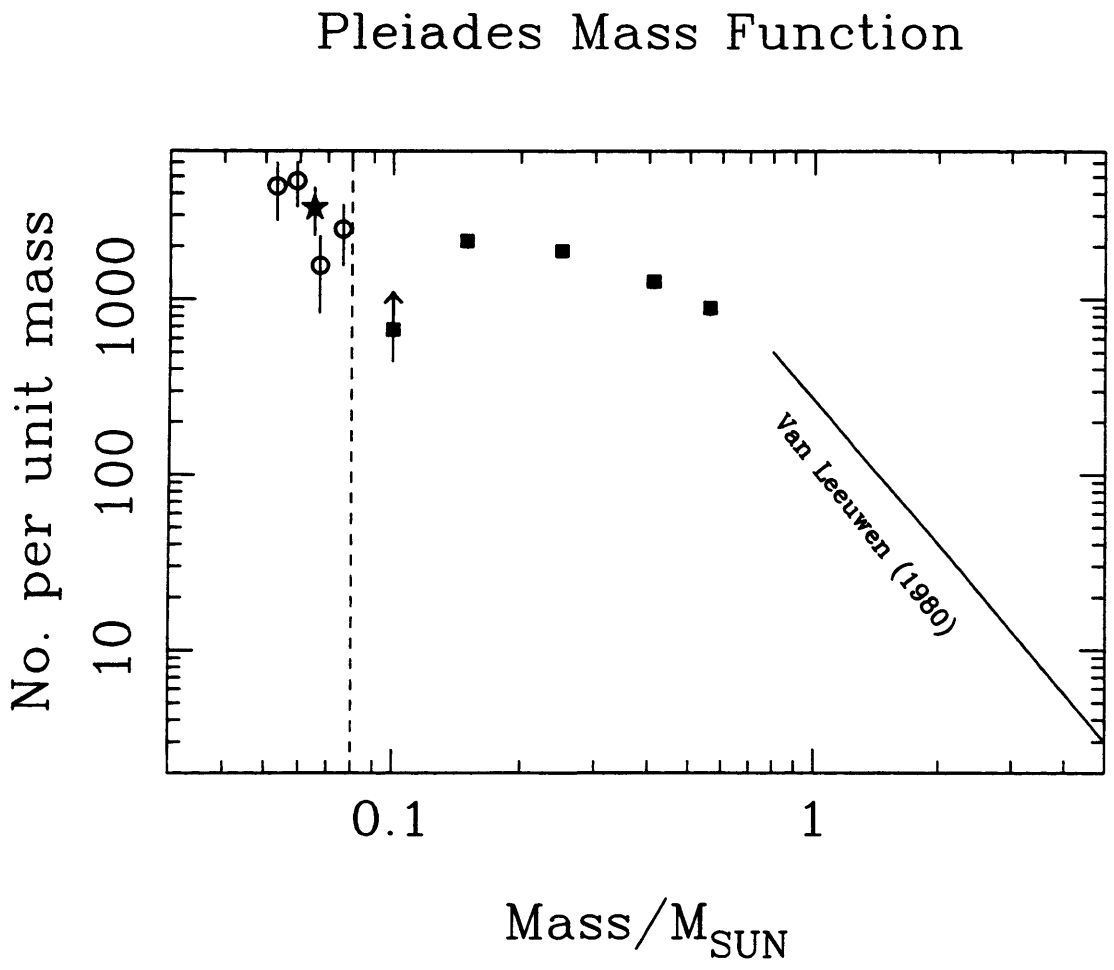

Figure 8.4: The Mass Function of The Pleiades. The stellar data is taken from Hambly, Hawkins & Jameson (1991) and is shown as solid squares. The revised mass function derived from the analysis in this chapter is presented as open circles. The arrow on the datapoint close to 0.1 $M_{\odot}$ indicates the incompleteness in this mass bin from the HHJ survey of Hambly, Hawkins & Jameson (1991). The star symbol represents the mass function derived from Hambly *et al.* (1998).

8.4 Conclusions

In this chapter I have used the infrared and optical observational data from a number of surveys in the Pleiades cluster, including the CFHT, ITP and Kitt Peak surveys. By modelling the distribution of brown dwarfs in the central region of the cluster, where the observational data is more complete, using the models and theory of King (1962), I have derived mass and luminosity functions for the whole cluster, out to the tidal radius of 13.1 pc. I have used a core radius, r_c, of 3 pc and have justified the use of this value. r_c can be at best constrained to 2 ± 1 pc using the King models and the available observational data. It is therefore essential that further observations are made to reduce the error in this important quantity. A core radius of 3 pc for the brown dwarfs has implications for the dynamical state of the cluster, in that this value suggests that the cluster is not relaxed for this mass regime.

The luminosity function is presented for the central region of the cluster out to $\sim$6 pc and then extrapolated out to the tidal radius. The resultant mass function continues with the same slope across the stellar sub-stellar boundary, and may even be rising slightly at the very lowest masses presented here, 0.055 down to 0.050 $M_{\odot}$. To confirm this increase in slope, one requires further observational data. The problem of the missing mass or dark matter still remains but this MF is very encouraging for future observational and theoretical studies.

All objects have been treated as single, that is I have ignored binarity. The effects of binarity are considered in the next chapter on Praesepe but would equally well apply to the Pleiades.

Chapter 9

The Mass Function of Praesepe

9.1 Introduction

In this chapter I present the mass function for the Praesepe cluster using the latest infrared results from the surveys outlined in chapter 7. Previous surveys and their derived mass and luminosity functions are discussed in the next section. Chapter 8 discusses the field luminosity and mass functions, and so will not be discussed any further here.

9.1.1 Review

Obtaining deep proper motion measurements of the cluster to $m_v \sim 17$, Jones & Cudworth (1983) calculated the luminosity function assuming an exponential cluster distribution. Mermilliod *et al.* (1990) determined a luminosity function for the central square degree of the cluster but did not correct this for the cluster as a whole. Their work followed up the proper motion members presented in Artjukhina (1966). Jones & Stauffer (1991) obtained proper motion measurements of the cluster down to $m_v \sim 18$ and assumed an exponential cluster distribution to calculate the luminosity function. Using the same cluster distribution analysis, Hambly *et al.* (1995a) measured proper motions covering a cluster area of approximately 19 square degrees. This survey went significantly deeper than previous surveys in the use of R and I band Schmidt plates. In a second paper, Hambly *et al.* (1995b) derived the cluster mass function. This was seen to be rising with a slope of 1.3 down to masses of $0.1 M_{\odot}$. Williams, Rieke & Stauffer (1995) imaged 290 square arcminutes of the cluster at V, I and K. From their photometry they estimate that they reach masses as low as 0.08 $M_{\odot}$, finding 6 cluster members in the range $0.40 < M < 0.08 M_{\odot}$. Their

resultant mass function is similar to the field star initial mass function (IMF). In Pinfield (1997) the mass function of the cluster has been determined down to the brown dwarf limit using results from two independent surveys. The RIZ and Kitt Peak surveys discovered candidate members using the I and Z filter combination. Pinfield (1997) uses an exponential surface cluster distribution along with surface density profiles from King (1962) to determine the luminosity function for the whole cluster. Combining this with a mass luminosity relationship from D'Antona & Mazzitelli (1994), a mass function is presented. Where the mass bins overlap with the Hambly *et al.* (1995b) survey there is excellent agreement. The slope of the mass function towards the brown dwarf limit is consistent with the α=1.5 determined from Hambly *et al.* (1995b). Pinfield (1997) presents evidence of a turn-up in the slope to α=3.8 in the lowest mass bins, which would suggest that brown dwarfs could dominate the mass of the cluster. It is these lowest mass bins that are examined in this chapter based on the follow-up infrared photometry.

9.2 Mass Function

The mass function for Praesepe from the results of the optical surveys at R, I and Z has been determined by Pinfield (1997), see above, and so the following sections will use the infrared photometry presented in Chapter 7 to redetermine the mass function in the lowest mass bins. To do this the poor weather photometry (discussed in Chapter 7) will also be used where optical candidates can be identified as definite non-members.

9.2.1 The RIZ Survey

The mass function for the RIZ survey, taken from Pinfield (1997) is presented in Table 9.1 below. Of the 6 magnitude bins in the optical survey, only the bin for I=16.0 to 17.0 has not been followed up at K. For the I=17.0 to 18.0 bin, one optical candidate was imaged at K and had infrared colours consistent with cluster membership. The remaining 7 have yet to be observed. 4 of the 5 optical candidates between I=18.0 to 19.0 had I–K colours consistent with membership and so the weighting for this bin increases from 50% to 80%. For the I=19.0 to 20.0 magnitude bin, I find a weighting of 67% and for the 20.0 to 21.0 bin a weighting of 33%, based on the I and K photometry. The two optical candidates in the faintest magnitude bin did not show infrared colours consistent with membership.

I_{RGO}	$logM/M_{\odot}$	log N(m)	Weight
16-17	-0.837	3.62	100%
17-18	-0.977	3.71	100%
18-19	-1.052	3.71	50%
19-20	-1.085	3.87	50%
20-21	-1.094	4.23	50%
21-22	-1.149	4.39	50%

Table 9.1: Praesepe Mass Function from Pinfield (1997) for the RIZ survey.

I_{KP}	log m	log N(m)	Weight
17-18	-0.987	3.77	50%
18-19	-1.061	3.78	50%
19-20	-1.092	4.10	50%

Table 9.2: Praesepe Mass Function from Pinfield (1997) for the Kitt Peak survey.

9.2.2 The Kitt Peak Survey

The optical survey (Pinfield 1997) presented 141 candidates for $17.0<I_{KP}<21.0$. Not all these candidates were followed up at UKIRT, due to poor weather and lack of time, and so one has to be careful when calculating the effect that the new photometry has on the previously determined mass function. In Pinfield (1997) three luminosity bins were defined before the mass function was calculated. These are tabulated in Table 9.2. The I magnitudes presented in Table 9.2 are in the Kitt Peak system.

There are 67 optical candidates in the I=17.0 to 18.0 magnitude bin. From the K photometry this bin is poorly sampled for I<17.8 but well sampled between I=17.8 to 18.0. In this magnitude range there are 3 candidates that were observed during photometric conditions, 4 during the poorer conditions and 1 that has not been imaged at K. There are 3 photometric members, 1 unknown and 4 definite non-members. The success rate from this analysis is 38±5%. This is in rough agreement with the 50% contamination estimated from the I, Z survey

For the I=18.0 to 19.0 the sampling is significantly better. There are a total of 19

objects in this magnitude range, of which 15 have been observed during photometric conditions and 4 during the poorer conditions. There are 7 photometric members and 12 definite non-members, resulting in a success rate of 37%. This is in rough agreement with the optical survey's contamination estimates.

The faintest bin from I=19.0 to 20.0 is better sampled between I=19.0 to 19.4. In this magnitude range 13 objects were imaged at K, 5 during photometric conditions and 10 during the poorer conditions. 10 candidates remain that were not observed at K in this magnitude range. Of the 13 candidates imaged at K only 1 retained its membership identity. The error on the success rate is large as a direct result of the 10 candidates that were not followed up. The resultant success rate is 25±21%, which is significantly lower than the 50% estimation from the optical survey. This is not entirely surprising as the errors in the I–Z colour at the faint end of the Praesepe sequence become increasingly large.

9.3 The New Mass Function

The above results have been summarised in Table 9.3 and are presented in Figure 9.1. Plotted on this figure is a line of slope 1.5, consistent with the findings of Hambly *et al.* (1995b). The modification to the lowest mass bins from the RIZ and Kitt Peak surveys of Pinfield (1997) suggest that the slope of 3.8 is not consistent with the new infrared results. The success rate of candidate selection for the faintest objects in the I versus I–Z colour-magnitude diagram is reduced as a direct result of the increased errors in the optical photometry. One can say that this revised mass function shows no sign of turning up, and is best interpreted as continuing with the same slope. Square root error bars are plotted. A larger area, deeper survey of the cluster is required to push this MF into the brown dwarf regime. To this end, the Leicester group has obtained I and Z photometry of the cluster covering an approximate area of 3 square degrees, with good signal to noise down to I=22.0. These observations, carried out in December 1997 using the wide field camera on the Isaac Newton Telescope in La Palma, have yet to be analysed, and as a result, could not be included in this chapter. They will help to constrain the mass function at and below the brown dwarf limit in Praesepe.

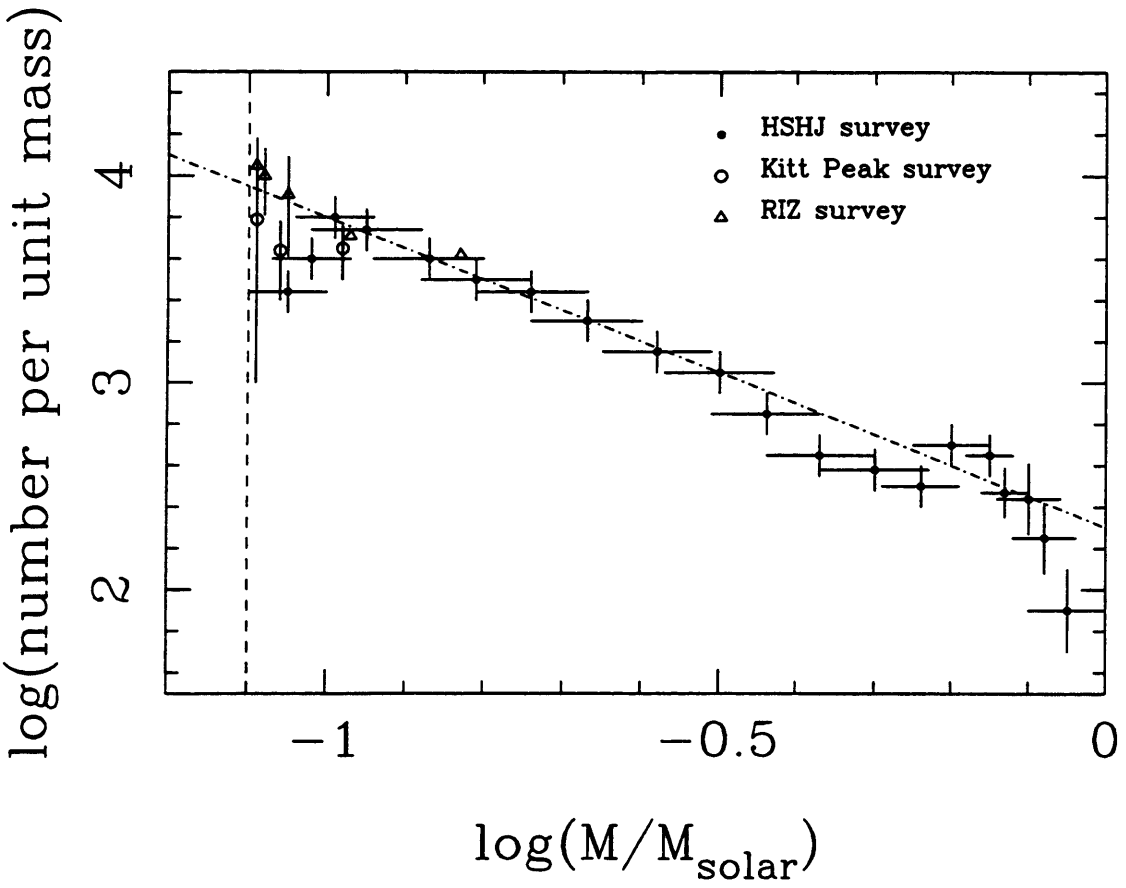

Figure 9.1: The revised mass function of Praesepe. The mass function from the HSHJ survey of Hambly *et al.* (1995b) is plotted as solid circles, with the RIZ and Kitt Peak surveys shown as open triangles and open circles respectively. The 3 lowest mass bins in the HSHJ suffer from incompleteness and so these points represent lower limits. The vertical dashed line indicates the brown dwarf limit in the cluster. The dot dash line represents a slope of 1.5. Square root error bars are plotted.

The RIZ survey		
I_{RGO}	$\log M/M_{\odot}$	log N(m)
16-17	-0.837	3.62
17-18	-0.977	3.71
18-19	-1.052	3.91
19-20	-1.085	4.00
20-21	-1.094	4.05
The Kitt Peak survey		
I_{KP}	log m	log N(m)
17-18	-0.987	3.65
18-19	-1.061	3.64
19-20	-1.092	3.79

Table 9.3: The revised mass function of Praesepe

9.3.1 The effect of binarity

In chapter 7 the infrared follow-up photometry from the RIZ survey indicated that a number of stars lay on the binary sequence in Praesepe. It is important to calculate the effect that this has on the revised mass function, presented above. Using a model isochrone for an age of 1 Gyr from Chabrier & Baraffe (1997), for the mass range 0.075 to 0.2 $M_{\odot}$, one can derive an I–band mass luminosity relationship of the form given in Equation 9.1, shown below,

$$\text{Luminosity}_{\text{I}} \propto \text{Mass}^{\alpha} \tag{9.1}$$

where $\alpha \sim 3$. If one considers the case of an equal mass binary, then it is appropriate to assume that each component contributes equally to the total luminosity of the system, i.e. the luminosity of one component is 0.5 L_{total}. From Equation 9.1 above, the mass of such a component is proportional to $L^{\frac{1}{3}}$. The total mass of the system, assuming α=3 from above, relative to the mass inferred from no consideration of binarity is $(\frac{1}{2})^{\frac{1}{3}} + (\frac{1}{2})^{\frac{1}{3}} = 1.59$. Therefore, if all the stars were in equal mass binaries, the total mass would increase by the order of 59%. However not all binaries will be equal mass. Clearly for an unequal mass binary, say 3 to 1, this effect is reduced, $(\frac{27}{28})^{\frac{1}{3}} + (\frac{1}{28})^{\frac{1}{3}} = 1.32$. Furthermore, the binary fraction is of the order

of 47% (Steele & Jameson (1995) and Pinfield (1997)) and so this factor reduces to $\lesssim$28%. This effect is within the error bars of the revised mass function derived above. Also there is no information on binary mass ratios. Binarity should ideally be reconsidered when better data is available.

9.4 Conclusions

In this chapter I have reviewed the previous luminosity and mass functions derived for the Praesepe cluster. I have concentrated on the optical RIZ and Kitt Peak surveys of the cluster from Pinfield (1997) as it is these surveys that were followed up in the infrared at K. Using the new infrared photometry I have recalculated the mass function of the cluster to show that it is consistent with previous surveys having a slope of 1.5 and shows no evidence of turning over. The upward trend described in Pinfield (1997) is less obvious after this analysis, and a slope of 3.8 is not seen. I have also discussed the possible effect of binarity on the revised mass function, in the context of the small number statistics presented here. The revised mass function reaches the brown dwarf limit in the cluster, and with the soon to be reduced data from a recent large area, deep survey of Praesepe using the INT's wide field camera, one would hope to reduce the large error bars at the lowest masses and determine the shape of the MF well into the brown dwarf regime.

Chapter 10

Conclusions

In this chapter I review the main conclusions of this thesis. There are 6 important chapters to review here. They constitute the main part of my research over the last 3 years and include chapters 4 through to 9. Chapters 2 and 3 describe a review of the field and description of data acquisition and analysis respectively, and will not be discussed here.

10.1 Chapter (4) - The HST Survey

This was my introductory project when I first joined the Leicester group. Using the HST to survey a cluster such as the Pleiades has more disadvantages than advantages. It may be able to obtain the deepest images using the shortest exposure times, compared to any ground based telescope, but its very small field of view is useless for large area surveys. Searching for brown dwarfs in the HST data was a secondary priority, as the initial proposal attempted to image suspected companions to HHJ stars. The analysis of the data for this exercise had been completed before my arrival in the department. The wide field camera data that I subsequently analysed turned up 3 candidates and possible evidence of 2 companions to the stars HHJ6 and HHJ10. Using H and K photometry from UKIRT, none of these five candidates were found to be real. Considering the small survey area this result is not surprising. The lack of evidence of any possible binary companions to the HHJ stars does not categorically disprove their existence. It must be that the binaries have companions where the separations are less than $\sim$ 12 AU.

10.2 Chapter (5) - Calibration of I-Z

In this chapter I present some key results regarding the successful use of the Z filter and I–Z colour in survey work in the field and within open clusters. I show that the I–Z colour continues to increase for very late type objects and present a relationship between I–Z colour and effective temperature. Until a more accurate method of deriving temperatures for these VLMS, i.e. improved model atmospheres and spectral fitting, this relationship will remain somewhat limited. I have also presented a transformation between the Harris and Cousins photometric systems. For very red objects, as presented in this thesis, the difference between these photometric systems is large, up to 0.4 of a magnitude. It is vital that observers using the Harris filter sets incorporate these offsets before comparing their results to any theoretical models. To further promote the use of the Z filter, I have presented a preliminary table of non A0 Z standards. The errors are large at this stage and require repeat observations to reduce them, but do allow a rough calibration at the telescope for future survey work.

10.3 Chapter (6) - PIZ 1 Discovery

This chapter outlines the first observing trip of my Ph.D. Using the I and Z filters at the INT in La Palma, a small area survey of the Pleiades was carried out. Nine fields, each of approximately 100 square arcminutes were imaged in both filters and 10 brown dwarf candidates identified. From follow-up infrared observations at K, one of these candidates, now called PIZ 1, remained red in I–K. Optical spectroscopy confirmed the presence of TiO and VO molecular bands indicative of a very low-mass object. Using the pseudo-continuum ratios of Martin, Rebolo & Zapatero-Osorio (1996) I assigned a spectral type of M9 for PIZ 1. Using the latest models of Chabrier & Baraffe (1997) I estimate a mass of 48 $M_{Jupiter}$ for PIZ 1 and an effective temperature of approximately 2400K. There is some chance that PIZ 1 may not be a cluster member. From statistical arguments I show that this probability is of the order of 2%.

The remaining 9 candidates discovered in this survey have been followed up at K and do not remain red in I–K, which is not surprising when one considers the appalling weather conditions during the initial I, Z observing run.

The discovery of PIZ 1, the first sub-stellar object identified using the I–Z colour, was extremely important. Surveys conducted in The Pleiades since, using the same

filter combination, but during far superior weather conditions have been very successful.

10.4 Chapter (7) - The Infrared Photometry

In this chapter I have presented the infrared photometry for a number of follow-up surveys in the Pleiades and Praesepe. The optical surveys that were followed up include the ITP, INT, Double I survey and Kitt Peak survey of the Pleiades, and the RIZ and Kitt Peak surveys in Praesepe. The follow-up is not complete for a number of these surveys, but does allow a determination of the mass function within the brown dwarf regime in the Pleiades, and down to the sub-stellar limit within Praesepe. The selection of cluster members was achieved using an I versus I–K colour magnitude diagram and an appropriately aged isochrone from the latest models of Chabrier & Baraffe (1997). This selection of possible cluster members is not exhaustive as the need for optical and infrared spectroscopy and proper motion measurements is required to fully confirm cluster membership.

10.5 Chapter (8) - The Pleiades Luminosity and Mass Functions

The Pleiades luminosity function is derived by modelling the distribution of stars in the central region of the cluster where most recent surveys have concentrated, and applying the models of King (1962) to the observational data. This involves determining a value for the core radius, r_c for the sub-stellar mass bin. Due to the constraints imposed by a limited observational dataset, $r_c=2\pm1$ and implies that for this mass range the cluster is not yet relaxed. It is stressed however that this is in no way a firm conclusion and further observational points are necessary to confirm or otherwise this result. Using a core radius of 3 pc the luminosity function and then mass function of the cluster are presented. The mass function appears to continue with the same slope across the stellar-substellar boundary with perhaps some evidence of a turn-up in the lowest mass bins.

10.6 Chapter (9) - The Mass Function of Praesepe

Using the infrared follow-up photometry for the Praesepe cluster from chapter 7, I have recalculated the mass function for the cluster. This is based on revising the results and conclusions from Pinfield (1997) who used the RIZ and Kitt Peak optical surveys of the cluster to determine a mass function down to the sub-stellar limit. The previously determined slope of 3.8 towards the brown dwarf regime, presented in Pinfield (1997), is shown to be incorrect with a more likely result being the continuation of the slope of 1.5 in this mass range. It is important to note however that there is no sign of the mass function turning down as the sub-stellar limit is approached.

10.7 Future Work

The field of brown dwarf research has been transformed over the past three years, and so I have been very fortunate to have been involved in this project over that time. At the start of my studies few good brown dwarf candidates existed, either in open clusters or in the field. The use of the lithium test to examine the possibility of substellar status for a candidate confirmed the identity of PPL 15 as a brown dwarf in the Pleiades that essentially determined the position of the stellar-substellar boundary in the cluster. Teide 1 and Calar 3 soon followed, as fainter cluster members. Ongoing searches in clusters and the field had produced very few candidate brown dwarfs until the emphasis shifted from using the V–I and R–I colours to I–Z colour as a detection discriminant.

I have been involved in the application of this colour to large area surveys of the Pleiades. The first results led to the discovery of PIZ 1, the first brown dwarf discovered by the Leicester Group. To confirm the sub-stellar nature of PIZ 1 requires further work which means the acquisition of a better (higher signal to noise) optical spectrum, allowing one to determine a radial velocity. A high resolution optical spectrum to resolve the lithium feature at 670.8 nm is needed, but this would be difficult to achieve even with a 10 metre telescope such as the Keck Telescope in Hawaii. A better quality optical spectrum has been obtained by Simon Hodgkin, using the William Herschel Telescope in La Palma, and should be of a sufficiently high enough resolution to determine a radial velocity. Time constraints have prevented me from including it in this thesis. To confirm cluster membership proper motion

measurements are needed. Using the original I and Z CCD images taken in 1995, one could measure this by obtaining second epoch images within the next 3 years.

The calibration of the I–Z colour in chapter 5 can now be greatly extended by observing a new classification of objects tentatively termed L type dwarfs. These objects discovered by the DENIS and 2MASS surveys would provide an excellent test of the I–Z colour for lower and lower effective temperatures, and an observing run to extend the work in chapter 5 would be a worthwhile project.

Further infrared photometry is needed to follow-up the many Pleiades and Praesepe candidates not selected for the UKIRT programme of 1997. The results of which would help to improve the statistics used for the corresponding mass and luminosity functions presented in chapters 8 and 9 for both clusters. Extending the areal coverage of the Pleiades optical surveys at I and Z is essential so that one can improve the statistics used to determine the core radius for the cluster. At present, results indicate the possibility of the cluster not being relaxed for the brown dwarfs, a somewhat controversial result.

Deep surveys at J will ultimately determine the shape of the luminosity and mass functions down to masses of $\sim 0.01 M_{\odot}$ but are difficult to do efficiently at present because of the relatively small field of view of current detectors. As the theoreticians constantly improve their models and provide better agreement with observational data, the move to detecting methane and water features in the lowest mass sub-stellar objects could lead observers to using custom built filter systems to cover these spectral regions.

Appendix A

Published Papers

This appendix includes copies of the publications that have resulted from the work in this thesis.

SPECIAL NOTE

This item is tightly bound and while every effort has been made to reproduce the centres force would result in damage.

. Not. R. Astron. Soc. 288, L23–L27 (1997)

iscovery of the lowest mass brown dwarf in the Pleiades

. R. Cossburn, S. T. Hodgkin, R. F. Jameson and D. J. Pinfield

rtment of Physics and Astronomy, Leicester University, University Road, Leicester LE1 7RH

epted 1997 April 14. Received 1997 April 9; in original form 1997 February 6

ABSTRACT

We have imaged the Pleiades open cluster at I and Z in a search for low-mass stars and brown dwarfs. One very red object, which we have called PIZ 1, at $I = 19.64$, $I - Z = 1.33$ has been detected within an area of 100 arcmin^2. Follow-up infrared photometry verifies that this object is extremely red with a K magnitude of 15.5. We have also obtained a spectrum which exhibits the spectral features indicative of an extremely cool M dwarf. We estimate the effective temperature and mass of PIZ 1 to be 2300 K and 0.048 $M_\odot$, respectively.

Key words: stars: low mass, brown dwarfs – open clusters and associations: individual: Pleiades.

INTRODUCTION

lowest mass brown dwarf discovered to date is GL229B kajima et al. 1995). This object has an effective tempera- of less than 1200 K and a mass in the range 20 to 50 iter masses. GL229B was discovered as a companion to earby star (approximately 5.7 parsec away) using both ical coronagraphic and direct infrared imaging thods.

o directly detect single brown dwarfs of known age, tance and metallicity, the ideal place to search is within ng open clusters. Many brown dwarf surveys have been ducted in the Pleiades open cluster (age 70 to 120 Myr). is is because the Pleiades cluster is near enough so that lower main sequence is not beyond the limits of detec- , but far enough away so that the area of sky covered proximately 20 deg^2) is not too large. The cluster is ng enough so that any brown dwarfs will be relatively ht. A 0.07-$M_\odot$ brown dwarf will have $\log(L/L_\odot) \sim -2.7$ $\log(T_{\rm eff}) \sim 3.495$ (D'Antona & Mazzitelli 1994).

o date, three brown dwarfs have been found in the ades: PPL 15 (Stauffer, Hamilton & Probst 1994), de 1 (Rebolo, Zapatero Osorio & Martin 1995), and ar 3 (Zapatero Osorio, Rebolo & Martin 1997). To con- the identity of PPL 15 as a brown dwarf, Basri, Marcy & ham (1996) detected the presence of lithium at 670.8 . The thick convective atmosphere of a brown dwarf ds to efficient mixing of lithium within the interior so that ection of lithium at 670.8 nm helps to constrain the tral temperature. Teide 1 is a proper-motion member of cluster and, from spectroscopic measurements, contains ium. It has a mass of approximately 55 Jupiter masses (Rebolo et al. 1996). The identity of Calar 3 as a brown dwarf member of the Pleiades has been well documented in Martin, Rebolo & Zapatero Osorio (1996). We have obtained a deep CCD image of the Pleiades in the I and Z filters, detecting an extremely faint red object (PIZ 1). In this paper we present follow-up K-band photometry and optical spectroscopy.

2 OBSERVATIONS

2.1 Observing strategy

Searches for brown dwarfs at V and I, or R and I, rely on the need to observe during dark time. Long exposures are necessary to compensate for the predicted lack of flux from brown dwarf sources at V and R. To be more flexible in the approach to this particular problem, the idea of using the Gunn Z filter (Schneider, Hoessel & Gunn 1983) was proposed. Brown dwarfs should be relatively bright at this wavelength. The I, Z combination suffers little penalty in bright time because the sky background at these wavelengths is dominated by OH emission and not by the lunar continuum. The spectrum of a very low-mass star is very steep in the wavelength region around I and Z and so the $I - Z$ colour should in theory be a good discriminant for low-mass M dwarfs, even though there is a large degree of overlap between the filters (see Pinfield et al. 1997). We also avoid the problems associated with long-baseline colour surveys such as $I - K$, where a large number of red galaxies are found because of the effects of redshifting the Balmer discontinuity (see Jameson, Hodgkin & Pinfield 1996).

Table 1. The coordinates and exposure times for each field.

Name	R.A. (2000)	dec (2000)	I Exposure Time (seconds)	Z Exposure Time (seconds)
PL 1	3 49 50.2	24 31 07	240	800
PL 2	3 49 10.2	24 30 40	500	940
PL 3 (PIZ 1 field)	3 48 31.9	24 30 40	500	640
PL 4	3 47 53.0	24 30 39	180	300
PL 27	3 48 38.0	24 00 39	400	600
PL 28	3 47 59.0	24 00 39	240	300
PL 29	3 48 15.0	23 51 00	480	540
PL 53	3 50 30.0	24 03 59	120	520
PL 63	3 49 51.0	24 03 59	120	120

Observations

servations in I and Z were made in 1995 December using TEK3 CCD at the prime focus of the Isaac Newton lescope at the Observatorio del Roque Muchachos on island of La Palma. The survey covered some nine fields 100 arcmin^2 each and yielded 10 candidates. The five arest candidates have been followed up by obtaining rared photometry at K. PIZ 1 was the only candidate that ained red in $I-K$. The remaining five candidates have yet been followed up. The nine field centres and expoe times are listed in Table 1. The images were bias subcted, flat-fielded and trimmed using IRAF routines ning on STARLINK. DAOFIND was used to search for point rces and magnitudes derived using the DAOPHOT aperphotometry routines. To differentiate between stellar rces and faint red galaxies, a star–galaxy separation proure was performed, in which all the sources were plotted a $\log_{10}$(peak counts) versus $\log_{10}$(total counts) diagram. form of shape analysis allowed the rejection of cosmic and galaxies from the data. The cleaned data for the Z 1 field have been presented in a colour–magnitude diam (Fig. 1).

The infrared photometry was obtained in UKIRT service e on 1996 October 22 using IRCAM3. The weather was otometric. The infrared photometry was reduced using STARLINK package IRCAMDR. The infrared data has been d to put PIZ 1 on an I versus $I-K$ diagram (Fig. 2) to pare our object with confirmed Pleiades members. Fig. ows the finder charts for PIZ 1 at I and K. Coordinates photometry are given in Table 2.

The spectroscopy was carried out in service time on the -m William Herschel Telescope (WHT) on 1996 Novem- 30. The ISIS double arm spectrograph and R158R grat- were used together with the TEK 1124 × 1124 chip. Five min integrations were carried out. The spectral coverage rom 6500 to 9500 Å. The spectrum was reduced using F software. This included bias subtraction, flat-fielding, imal extraction and wavelength calibration. The star rest to PIZ 1 has been identified as spectral type G5 n its photometry, and was used to remove the instruntal response from the spectrum of PIZ 1. The extracted ctrum of PIZ 1 is presented in Fig. 4. We have also tted the spectra of Teide 1 (Rebolo et al. 1995), BRI 21 − 0214 (Kirkpatrick, Henry & Simons 1995), and ASP-J0345 (Kirkpatrick, Beichman & Skrutskie 1997) in figure.

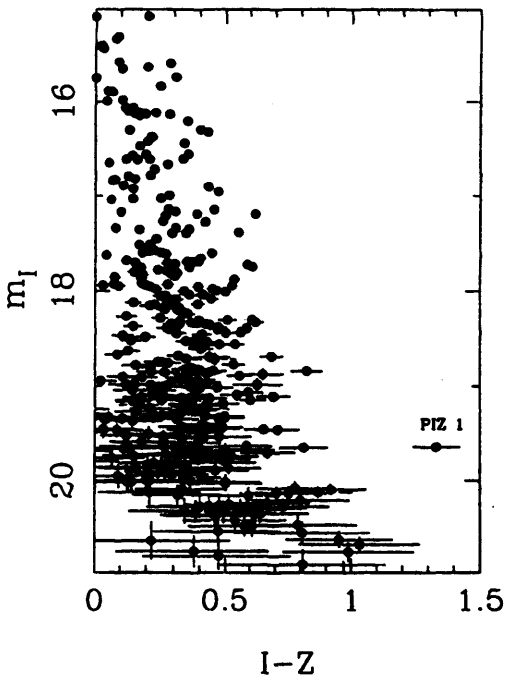

Figure 1. The I versus $(I-Z)$ colour–magnitude diagram for 100 arcmin^2, showing the position of PIZ 1. Error bars are 1σ.

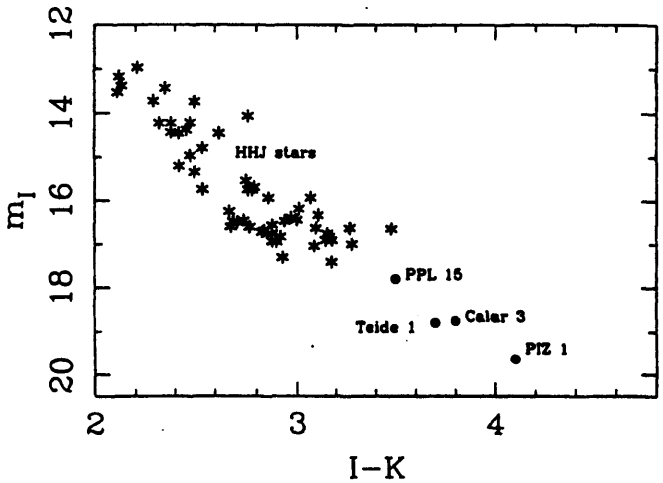

Figure 2. The I versus $(I-K)$ colour–magnitude diagram for the Pleiades showing the low-mass HHJ stars (Hambly et al. 1993), the brown dwarfs, PPL 15, Teide 1 and Calar 3, and our object PIZ 1.

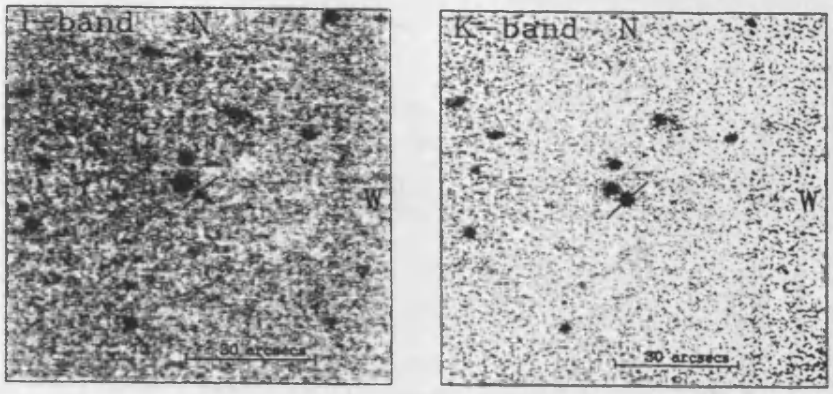

Figure 3. Finder charts for PIZ 1 at *I* and *K*. Coordinates and photometry are given in Table 1.

Table 2. A summary of the photometry for PIZ 1. Coordinates have been measured to sub-arcsec accuracy.

PIZ 1 distance modulus = 5.65

R.A. (J2000)	Dec (J2000)	m_I	m_Z	m_K	I–Z	I–K
3 48 31.4	+24 34 37.7	19.64	18.31	15.5	1.33	4.1

DISCUSSION

From an experimental point of view the $I-Z$ colour works as a good discriminate for faint red objects, picking out the object PIZ 1 from the background field stars extremely well. This object extends the cluster sequence below Teide 1 well into the brown dwarf regime, having an apparent I magnitude of 19.64 and $I-Z$ colour of 1.33. Photometrically, PIZ 1 is a good candidate for membership of the cluster. Both optical and infrared point spread functions are stellar when compared to other objects in the field, indicating that PIZ 1 is not a galaxy, but the conclusive proof is the spectrum, clearly that of a late M dwarf. There is a remote possibility that PIZ 1 is a rare field star that coincides with the cluster main sequence. An old field star of the same effective temperature as PIZ 1 is, from theory, 0.4 mag fainter than PIZ 1. Thus to mimic a brown dwarf Pleiad it must be in the distance range of approximately 60 to 130 pc. A field of 100 arcmin^2 then corresponds to a volume of 5.29 pc^3. Both Tinney, Reid & Mould (1993) and Kirkpatrick et al. (1994) find $\Phi \approx 10^{-2.3}$ star pc^{-3} of $M_I = 13.25$ to 14.25. Thus the expected contamination of our sample of stars is of the order of 0.027 field stars per 100 arcmin^2. The luminosity functions from both Tinney et al. and Kirkpatrick et al. are local to the Sun. Unfortunately, there is no information on the scaleheight of the luminosity function for very faint field stars. Furthermore, the Sun may be 10 to 40 pc above the plane (Kirkpatrick et al. 1994) and the Pleiades (galactic latitude $-24°$) therefore 40 to 10 pc below the plane, so it would be difficult to use scaleheight information even if it were available. Unless the field star luminosity function dies steeply at fainter magnitudes than Teide 1, the contamination would not increase substantially. The likelihood of the field star luminosity function increasing without an increase in the cluster luminosity function is small.

It is useful to compare this object with the low-mass stars and brown dwarfs already identified in the Pleiades cluster. Fig. 2 shows the low-mass HHJ stars (Hambly, Hawkins & Jameson 1993) and the three brown dwarfs, PPL15, Teide 1 and Calar 3. Object PIZ 1 has been plotted and its position indicates that it is significantly redder than Teide 1. PIZ 1 has a K magnitude of 15.5, giving an $I-K$ colour of 4.1. Combining the data from Jones et al. (1994) and the latest models by Chabrier, Baraffe & Plez (1996) we have determined a relationship between the $I-K$ colour and effective temperature. From this we estimate that the effective temperature of PIZ 1 is approximately 2300 K.

To determine the spectral type of PIZ 1, we have used the pseudocontinuum spectral ratios, PC3 and PC4, as defined by Martin et al. (1996). Using both PC3 and PC4 we have classified PIZ 1 as M9. We also note the similarities between PIZ 1 and 2MASP-J0345 in the wavelength region 9300 to 9400 Å. The blueward edge of this feature is a result of H_2O absorption in the atmosphere of PIZ 1. The redward edge also has a contribution from terrestrial atmospheric absorption by H_2O, which we have not removed. TiO absorption at 9208, 9230 and 9248 Å in the spectrum of 2MASP-J0345 appears considerably stronger than in PIZ 1, indicating that 2MASP-J0345 is cooler. Kirkpatrick et al. (1995) argue that the heights of the pseudocontinuum points at 7500 and 8250 Å decrease, moving to objects of later spectral type as a result of increased VO opacity. The VO bands lie on the blueward side of these features, and the effect can be seen in PIZ 1 at 7550 Å. However, at 8250 Å the effect is less noticeable. Hα appears to be present but the errors are large. Hα emission is also found in Teide 1, Calar 3 and other low-mass stellar Pleiads. It is our aim to obtain a better spectrum of PIZ 1 in the near future to determine the effective temperature of the object, its Hα equivalent width and, if possible, its radial velocity. Detect-

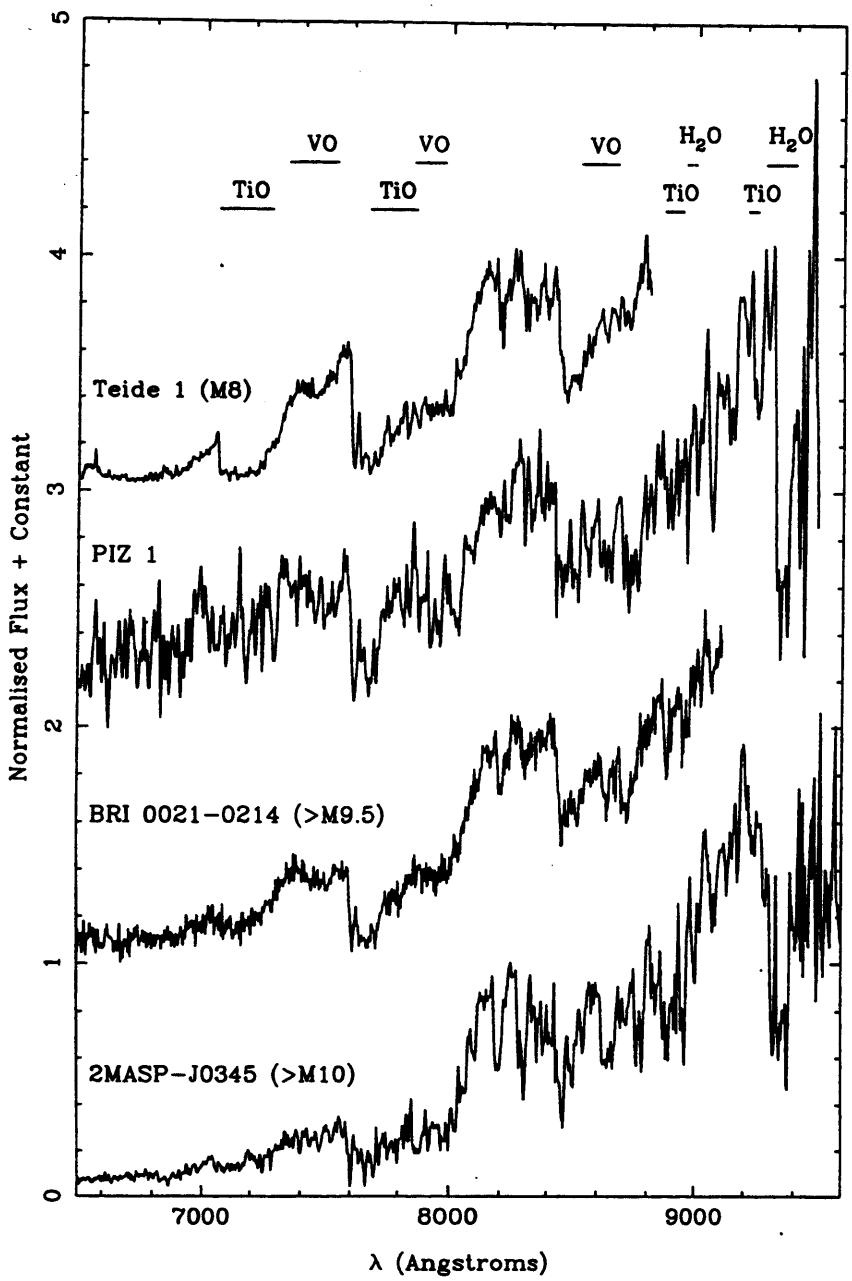

ure 4. The spectra of Teide 1, PIZ 1, BRI 0021 − 0214 and 2MASP-J0345 ordered by increasingly late spectral type from top to ttom.

lithium in an object this faint will be extremely difficult, n with the Keck Telescope. Ultimately we should asure the proper motion of this object to further check iades membership.

As a first step towards determining the mass of PIZ 1 we st find the bolometric luminosity (L_{bol}). Jones et al. 94) derived accurate measurements of M_{bol} and hence lometric corrections (BC_I, BC_K) for a sequence of cool arfs. So we can form a relation between $I-K$ and BC_I or C_K and convert the I, K photometry of PIZ 1 directly to . We adopt a distance modulus of 5.65 to the Pleiades eele et al. 1995) and take $M_{bol}=4.75$ for the Sun. We find t BC_I and BC_K gives the same results for all the Pleiades wn dwarfs. For PIZ 1 we find $\log(L/L_\odot)=-3.39$. Simily we find $\log(L/L_\odot)=-2.83$ for PPL 15 (cf. −2.80, Basri et al. 1996) and $\log(L/L_\odot)=-3.17$ for Teide 1 (cf. −3.18, Rebolo et al. 1996). Standard procedure would be to locate these objects on the Hertzsprung–Russell diagram and compare them with theoretical isochrones (see e.g. Rebolo et al. 1995). However, there is a well-known problem with current models in that they overpredict effective temperatures for the coolest objects. To avoid this, Basri et al. (1996) compared the luminosity and lithium abundance of PPL 15 with lithium depletion models from Nelson, Rappaport & Chiang (1993). They found a tight constraint on the age of the Pleiades of 115 Myr and derive a mass of $0.078\,M_\odot$ for PPL 15. The age constraint arises because PPL 15 shows partial lithium depletion (~99 per cent). The time-scale for the final stages of lithium depletion is extremely short for an object of this mass (around 5 Myr)

have found such an object is extremely fortuitous. It be stressed that this result does not depend solely on odel; a quick look at fig. 17 of D'Antona & Mazzitelli) shows that essentially the same mass and age would ived for PPL 15 given the same observed quantities. er PPL 15 is a 'transition object' or a brown dwarf is ant for calculating the masses of the remaining es brown dwarfs. We may use PPL 15 as a known ty in mass-luminosity space. For any given model, one en find that isochrone which best reproduces the mass minosity of PPL 15. Using the most recent models of ona & Mazzitelli (private communication) we simply e mass of PIZ 1 and Teide 1 from their luminosities e to PPL 15. Using this technique we obtain 056 $M_\odot$ for Teide 1 (in excellent agreement with the found by Rebolo et al. 1996), and $M = 0.048\ M_\odot$ for . It is our belief that the same masses would be found any model (and indeed we find the same values using odel of Nelson, Rapapport & Joss 1986). The only ack of this method is the heavy reliance on one object 15. We have assumed that PPL 15 is a single star; its n on the colour–magnitude diagram would actually t that it may be a binary. If this is the case all masses ed above must be reduced and the low-mass Pleiads ve an age greater than 115 Myr.

ONCLUSIONS

rown dwarf PIZ 1 has been detected within an area of cmin^2, suggesting that the use of the *Z* filter has been ful. The follow-up *K*-band photometry shows that ject is very red with an effective temperature in the of 2300 K. This is further supported by the spectrum 1. We have determined a mass for PIZ 1 of 0.048 $M_\odot$. ve also shown that the likely contamination of our by field stars should be minimal.

NOWLEDGMENTS

a PPARC-supported research associate and MRC JP are indebted to the same research council for research studentships. We would also like to thank Don Pollaco for obtaining the spectrum of PIZ 1 in 1996 November in service time at the WHT and Sandy Leggett for the *K* photometry from UKIRT service time. Our thanks also to Davy Kirkpatrick and Maria Rosa Zapatero Osorio for their digitized spectra, and to Francesca D'Antona and Italo Mazzitelli for sending us their latest models.

REFERENCES

Basri G., Marcy G. M., Graham J. R., 1996, ApJ, 458, 600
Chabrier G., Baraffe I., Plez B., 1996, ApJ, 459, L91
D'Antona F., Mazzitelli I., 1994, ApJS, 90, 467
Hambly N. C., Hawkins M. R. S., Jameson R. F., 1993, A&AS, 100, 607
Jameson R. F., Hodgkin S. T., Pinfield D. J., 1996, in Pallavicini R., Dupree A. K., eds, Proc. ASP Conf. Ser. 109, Cool Stars, Stellar Systems and the Sun. Astron. Soc. Pac., San Francisco, p. 363
Jones H. R. A., Longmore A. J., Jameson R. F., Mountain C. M., 1994, MNRAS, 267, 413
Kirkpatrick J. D., McGraw J. T., Hess T. R., Liebert J., McCarthy D. W., 1994, ApJS, 94, 749
Kirkpatrick J. D., Henry T. J., Simons D. A., 1995, ApJ, 109, 797
Kirkpatrick J. D., Beichman C. A., Skrutskie M. F., 1997, ApJ, in press
Martin E. L., Rebolo R., Zapatero Osorio M. R., 1996, ApJ, 469, 706
Nakajima T., Oppenheimer B. R., Kulkarni S. R., Golimowski D. A., Matthews K., Durrance S. T., 1995, Nat, 378, 463
Nelson L. A., Rappaport S., Joss P., 1986, ApJ, 311, 226
Nelson L. A., Rappaport S., Chiang E., 1993, ApJ, 413, 364
Pinfield D. J., Hodgkin S. T., Jameson R. F., Cossburn M. R., von Hippel T., 1997, MNRAS, in press
Rebolo R., Zapatero Osorio M. R., Martin E. L., 1995, Nat, 377, 129
Rebolo R., Martin E. L., Basri G., Marcy G. M., Zapatero Osorio M. R., 1996, 469, L53
Schneider D. P., Hoessel J. G., Gunn J. E., 1983, ApJS, 264, 337
Stauffer J. R., Hamilton D., Probst R., 1994, AJ, 108, 155
Steele I. A., Jameson R. F., Hodgkin S. T., Hambly N. C., 1995, MNRAS, 275, 841
Tinney C. G., Reid I. N., Mould J. R., 1993, ApJ, 414, 245
Zapatero Osorio M. R., Rebolo R., Martin E. L., 1997, A&AS, 317, 164

E ASTROPHYSICAL JOURNAL, 491:L81–L84, 1997 December 20

NEW BROWN DWARFS IN THE PLEIADES CLUSTER

M. R. ZAPATERO OSORIO, R. REBOLO, AND E. L. MARTÍN[1]
Instituto de Astrofísica de Canarias, E-38200 La Laguna, Tenerife, Spain; mosorio@iac.es, rrl@iac.es, ege@iac.es
G. BASRI
Department of Astronomy, University of California, Berkeley, Berkeley, CA 94720; basri@soleil.berkeley.edu
A. MAGAZZÙ
Osservatorio Astrofisico di Catania, Città Universitaria, I-95125 Catania, Italy; antonio@ct.astro.it
AND
S. T. HODGKIN, R. F. JAMESON, AND M. R. COSSBURN
Department of Astronomy, Leicester University, Leicester LE1 7RH, England, UK; sth@star.le.ac.uk, rfj@star.le.ac.uk, mrc@star.le.ac.uk
Received 1997 September 10; accepted 1997 October 21; published 1997 November 6

ABSTRACT

We present intermediate- and low-resolution optical spectroscopy (650–915 nm) of seven faint, very red objects ($20 > I \geq 17.8$, $I - Z \geq 0.5$) discovered in a CCD-based *IZ* survey covering an area of 1 deg^2 in the central region of the Pleiades open cluster. The observed spectra show that these objects are very cool dwarfs having spectral types in the range M6–M9. Five out of the seven objects can be considered Pleiades members on the basis of their radial velocities, Hα emissions, and other gravity-sensitive atomic features like the Na I doublet at 818.3 and 819.5 nm. According to current evolutionary models, the masses of these new objects range from roughly 80 M_{Jup} for the hottest in the sample down to 45 M_{Jup} for Roque 4, the coolest and faintest confirmed member. These observations prove that the cloud fragmentation process extends well into the brown dwarf realm, suggesting a rise in the initial mass function below the substellar limit.

Subject headings: open clusters and associations: individual (Pleiades) — stars: low-mass, brown dwarfs — stars: evolution — stars: fundamental parameters

1. INTRODUCTION

In the last 2 years, with the discoveries of the first bona fide own dwarfs (BDs; Rebolo, Zapatero Osorio, & Martín 1995; kajima et al. 1995), it has been proved that objects with sses between those of stars and planets can be formed in ture. Because of its youth and proximity, the Pleiades star ster is an ideal hunting ground for substellar objects (see mbly 1997 for a review). The discovery of BDs like Teide nd Calar 3 in a small survey of the Pleiades (Zapatero Osorio al. 1997b) suggests that a large number of very low mass jects may populate this cluster. If this is the case, astronomers ve a unique opportunity to establish the observational prop- ies of these rather elusive objects and to characterize the tial mass function beyond the star-BD boundary.

With the aim of searching for new Pleiades BDs, Zapatero orio et al. (1997c) have performed a deep CCD *IZ* survey vering 1 deg^2 within the central region of the cluster. More n 40 faint ($I \geq 17.5$), very red ($I - Z \geq 0.5$) objects have en detected down to $I \sim 22$. Their location in the *I*-*Z* color gram suggests cluster membership. According to the extGen" theoretical evolutionary models of Chabrier, Bar- e, & Plez (1996), they should have masses in the interval -30 M_{Jup} (1 $M_{Jup} \sim 10^{-3}$ $M_\odot$). In this Letter, we present spec- scopic observations for seven of the candidates with mag- udes in the interval $I = 17.8$–20 mag. We have determined ctral types, radial velocities, and Hα emissions that allow to assess their membership and, therefore, their substellar ure.

2. OBSERVATIONS AND RESULTS

We have collected intermediate- and low-resolution spectra in optical wavelengths for the objects listed in Table 1 (the full name of the objects is Roque Pleiades, hereafter "Roque") using the William Herschel Telescope (WHT; Observatorio del Roque de los Muchachos, La Palma) and the Keck II telescope (Mauna Kea Observatory, Hawaii). Table 1 summarizes the log of the observations. Finding charts for these objects are provided in Zapatero Osorio et al. (1997c). Figure 1 depicts the color-magnitude diagram of our 1 deg^2 survey in which the locations of the new BD candidates are indicated. Our targets were chosen to be fainter than HHJ 3 (Hambly, Hawkins, & Jameson 1993) and with ($I - Z$) colors redder than those given by an extrapolation of the borderline denoting the separation between cluster members and field objects.

The instrumentation used was the ISIS double-arm spectrograph at the WHT (we used only the red arm) with the grating R158R and a TEK (1024 × 1024 pixel^2) CCD detector and the LRIS spectrograph with the 830 and 1200 line mm^{-1} gratings and the TEK (2048 × 2048 pixel^2) CCD detector at the Keck II telescope. The nominal dispersions and the wavelength coverage provided by each instrumental setup are listed in Table 1. Slit width projections were typically 3 pixels, except for the observations of Roque 14 and 15, for which the seeing conditions forced us to have a slit width projecting onto 5 pixels. Exposure times ranged from 30 minutes to 1 hr for the faintest objects. Spectra were reduced by a standard procedure using IRAF,[2] which included debiasing, flat-fielding, optimal extraction, and wavelength calibration using the sky lines appearing in each individual spectrum (Osterbrock et al. 1996). Finally,

[1] Present address: Department of Astronomy, University of California, keley, Berkeley, CA 94720. USA

[2] IRAF is distributed by National Optical Astronomy Observatories, which is operated by the Association of Universities for Research in Astronomy, Inc., under contract with the National Science Foundation.

TABLE 1
LOG OF SPECTROSCOPIC OBSERVATIONS

Object	Telescope	Dispersion (Å pixel^{-1})	Δλ (nm)	Date (1996)
Roque 4 & 11; Calar 3	Keck II	1.83	654–833	Dec 3
Roque 11	Keck II	0.63	654–775	Dec 4
Roque 13, 14, 15, 16 & 17; PPl 15	WHT	2.90	650–915	Dec 8–9

tra were flux calibrated making use of the standards 45 (WHT) and HD 84937 (Keck II), which have ab- ux data available in the IRAF environment. The final re presented in Figure 2 together with comparison f PPl 15 (M6.5) and Calar 3 (M8) obtained with the trumental configuration.

bserved spectra clearly correspond to very late M-type howing prominent VO and TiO molecular absorption d rather strong atomic lines of K I (766.5 and 769.9 Na I (818.3 and 819.5 nm). In Table 2, we give accurate types derived by measurements of the pseudocontin- 1–4 indices (Martín, Rebolo, & Zapatero Osorio 1996), the derived radial velocities and the equivalent widths tomic lines (Hα and Na I) present in the spectra. The (Kirkpatrick, Henry, & Simons 1995), also measured, d to be consistent with late spectral types (M6–M9). locities were obtained by cross-correlating the spectra gions 654–700 nm, 730–750 nm, and 840–880 nm with templates observed using the same instrumental configuration. These templates were LHS 248 (M6.5V; Basri & Marcy 1995) and Calar 3 (M8; Rebolo et al. 1996). We have not measured radial velocities for Roque 14 and 15 because the resolution of their spectra is rather low (~15 Å). We note that for Roque 11, spectra of two different resolutions (~2 and 6 Å) are available, and the radial velocities agree well with each other.

There are several spectroscopic indicators that allow us to investigate the membership of our objects in the Pleiades. Cluster members are found with radial velocities in the range 0–14 km s^{-1} (Stauffer et al. 1994). All our candidates with radial velocity measurements clearly meet this criterion within the estimated error bars. Further evidence for membership is given by the presence of Hα in emission. According to Stauffer et al. (1994) and to Hodgkin, Jameson, & Steele (1995), Hα equivalent widths among very cool cluster members seem to be greater than 3 Å. We find that all of our targets, except Roque 4, share this characteristic, which supports their membership. The lack of Hα in emission in Roque 4 (M9) should not be interpreted as inconsistency with membership because

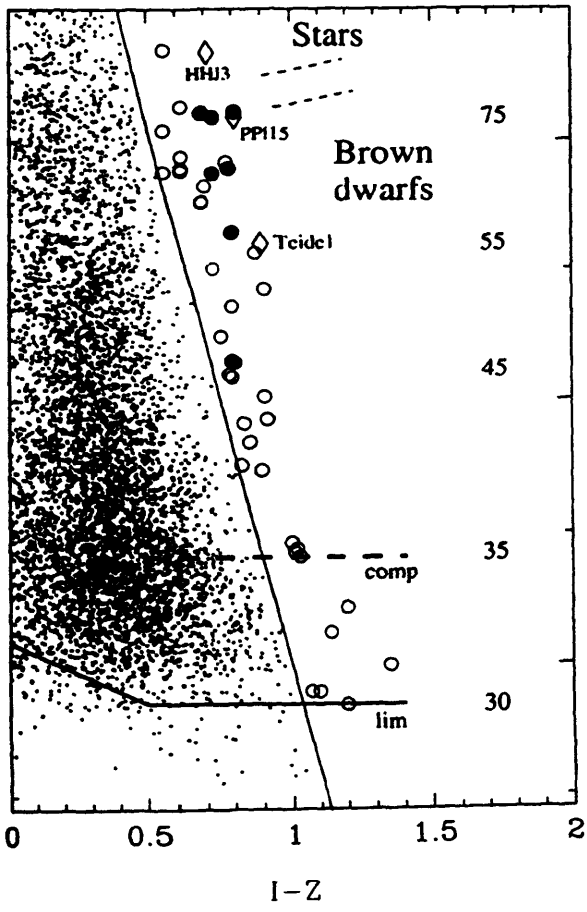

I vs. (I − Z) diagram resulting from our survey covering 1 deg^2 in region of the Pleiades cluster. Filled symbols represent the BD whose spectra we present in this Letter. Masses (*right-hand side*, M_{sun}) correspond to 120 Myr (Chabrier, Baraffe, & Plez 1996) at distance of 127 pc.

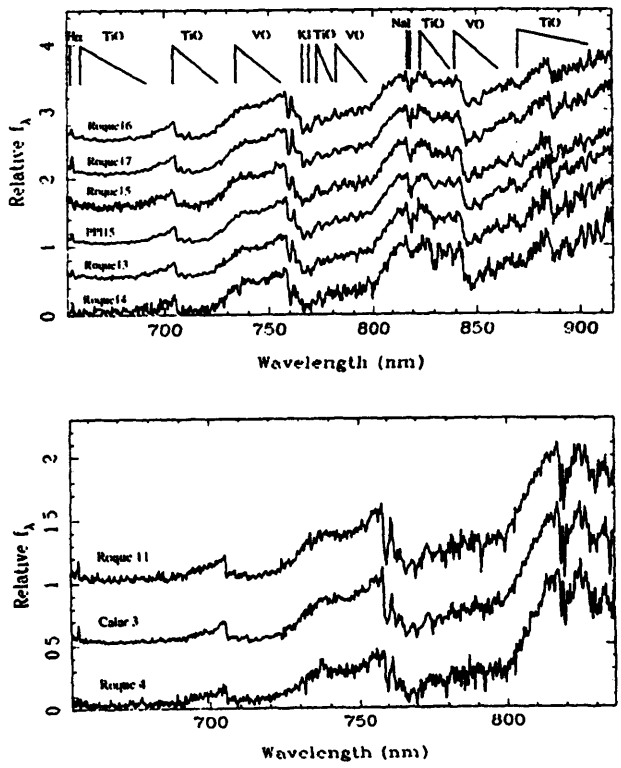

FIG. 2.—Low-resolution (4–15 Å) spectra obtained for our Pleiades BD candidates and for the BDs PPl 15 and Calar 3 (*top panel*: WHT spectra; *bottom panel*: Keck II spectra). Spectral types range from M6 to M9. Some atomic and molecular features are indicated. The normalization point has been taken at 813 nm. A constant step of 0.5 units has been added to each spectrum for clarity.

TABLE 2

DATA FOR OUR PLEIADES BDs

Name	R.A. (J2000)	Decl. (J2000)	I	$I-K$	SpT	Na I (Å)	Hα (Å)	v_{rad} (km s^{-1})	log $L/L_{\odot}$
Roque 16	3 47 39.0	24 36 22	17.79	3.18	M6	4.7	5.0	-20 ± 15	−2.89
Roque 15	3 45 41.2	23 54 11	17.82	...	M6.5	6.0	4.0	...	−2.86
Roque 17	3 47 23.9	22 42 38	17.78	3.45	M6.5	4.5	15.0	-14 ± 15	−2.83
Roque 14	3 46 42.9	24 24 50	18.21	...	M7	5.0	17.0	...	−3.00
Roque 13	3 45 50.6	24 09 03	18.25	3.65	M7.5	5.4	10.5	-1 ± 15	−3.00
Roque 11	3 47 12.1	24 28 32	18.73	3.63	M8	4.8	5.8	-6 ± 12 -3.5 ± 7[a]	−3.15
Roque 4	3 43 53.5	24 31 11	19.75	4.52	M9	4.7	<5	$+4 \pm 12$	−3.35

NOTES.—Units of right ascension are hours, minutes, and seconds, and units of declination are degrees, arcminutes, and arcseconds. Coordinates are accurate to ±3″. The uncertainty in the spectral type determination is ±0.5 subclasses. Typical error bars for the equivalent widths of the atomic lines are ±1 Å. Luminosities are given to a relative accuracy of ±0.02 dex owing to errors in the photometry. All error bars are given at 1 σ.

[a] Radial velocity measured from the high-resolution spectrum obtained at the Keck II telescope.

behavior of this line for Pleiades later than M8 is unknown. could be that beyond a certain temperature, activity decreases nsiderably in the atmospheres of such cool objects, and Hα y be no longer seen in emission. The sensitivity of the I doublet to gravity makes it, too, useful as a membership erion (Steele & Jameson 1995; Martín et al. 1996). We find t the equivalent width of this doublet is lower in our objects n in field stars with similar spectral type and temperature, licating lower gravity and hence, younger age. Finally, as pected for true Pleiades, our objects nicely fit and extend the quence delineated by very low mass cluster members in the magnitude versus spectral type diagram of Martín et al. 996).

We conclude on the basis of all the above spectroscopic mbership criteria that five of our objects (Roque 4, 11, 13, , and 17) are very likely members of the cluster. Additional pport is provided by our K-band measurements that locate m in the Pleiades IR photometric sequence (Zapatero Osorio, artín, & Rebolo 1997a). We remark that Roque 11 is a photometric and spectroscopic "twin" of Teide 1 and of Calar 3 d that Roque 4 could be the least luminous and coolest cluster mber yet found, being very similar in appearance to PIZ 1 ossburn et al. 1997). These two Roque objects together with oque 13 can be classified as genuine BDs, while Roque 16 d 17 might be transition objects lying in the region between rs and BDs. To reach a definitive conclusion on the membership status of Roque 14 and 15, we shall await radial velocity asurements and IR photometry.

We find higher VO indices and more intense TiO molecular nds in the M8 and M9 Pleiades than in the field dwarfs with e same spectral types. This might be associated with the rmation of dust in the atmospheres (Tsuji, Ohnaka, & Aoki 96) and its dependence on gravity. The larger the gravity is, e larger the pressure, which favors the formation of grains cool temperatures. Young BDs have lower gravities than ld objects and, therefore, dust molecules (silicates and grains) y condense less efficiently. The effect of grain formation is decrease the number of vanadium, titanium, and oxygen oms in the gas phase and therefore the abundance of the olecular species of VO and TiO, resulting in a more transrent atmosphere in field dwarfs than in young BDs at optical avelengths.

3. DISCUSSION AND FINAL REMARKS

In order to estimate the mass of our objects, we must first rive their luminosities. One can convert IK photometry and spectral type to bolometric luminosity by employing relationships derived for cool field dwarfs (Jones et al. 1994, and references therein) and averaging the results. Good agreement (±0.15 dex) has been found between luminosities derived from different calibrations. We have adopted a distance modulus of 5.53 to the Pleiades, an extinction of $A_I = 0.07$ mag, and $M_{bol} = 4.76$ mag for the Sun. The resulting luminosities are given in Table 2. Masses have been inferred by comparing these luminosities with the theoretical evolutionary tracks for an isochrone of 120 Myr provided by Chabrier et al. (1996). We find that Roque 16 and 17 have masses in the range 80–60 M_{Jup}, similar to PPl 15 (Basri, Marcy, & Graham 1996), and thus may help to define the star-BD boundary in the Pleiades cluster. Roque 13 has a mass between those of PPl 15 and Teide 1. Roque 11 resembles Teide 1 and Calar 3, and hence we infer the same mass (55 ± 15 M_{Jup}; Rebolo et al. 1996). Since Roque 4 is 0.2 dex less luminous than Roque 11, its mass is 10 M_{Jup} smaller according to the same models, and thus it is the least massive BD in our sample. An object with similar photometric and spectroscopic characteristics, PIZ 1, has been found by Cossburn et al. (1997), although it still lacks a radial velocity measurement. Recently, the *Hipparcos* satellite has provided new parallax measurements, deriving a Pleiades distance modulus of 5.32 mag (van Leeuwen & Hansen-Ruiz 1997). This would impose a reduction in our luminosities by 0.08 dex. Lower luminosities should lead to an older cluster age (up to about 130–150 Myr). However, a closer distance and an older age roughly compensate without introducing significant changes in the masses determined above.

We recall that lithium is preserved in BDs less massive than 65 M_{Jup} during their whole lifetime, in marked contrast with low mass stars ($M \leq 0.3\ M_{\odot}$), which significantly destroy this element at very young ages. The reappearance of lithium, although dependent on age and mass, should take place in a quite short luminosity range (see, e.g., D'Antona & Mazzitelli 1994). At the age of the Pleiades, the lithium- and hydrogen-burning mass limits coincide, which makes this cluster ideal for characterization of the substellar borderline. According to theoretical predictions, Roque 11 and 4 have fully preserved their initial lithium content and will never deplete it, while our remaining higher mass BDs are destroying or are about to destroy their lithium. Until now, only PPl 15 was considered to be on the borderline between BDs and stars in the Pleiades. Additional measurements of lithium in objects with similar characteristics are needed in order to provide a better location of this boundary as well as an improved age determination for

uster (Basri et al. 1996). The observation of lithium in e 4, which is cooler than Teide 1, is also important as it give key information on the formation of lithium lines atmospheres of very cool dwarfs. This is a subject of sing importance given the detections of lithium in re- discovered extremely cool field dwarfs (Ruiz, Leggett, rd 1997; Martín et al. 1997a; Tinney, Delfosse, & Forv- 997; Rebolo et al. 1997).

y a small fraction (~17%) of the BD candidates found *IZ* survey (see Fig. 1) have been investigated in this We have collected follow-up low-resolution optical spec- py for seven of the brighter candidates ($I < 20$). These vations confirm cluster membership for five of them and te that the other two are likely members, although radial ty measurements are still required. The number of re- g candidates in the explored area is large enough to that follow-up spectroscopic and infrared observations nfirm many more BDs. Among the faintest ones, there be BDs with masses as low as 30 M_{Jup}.

spectroscopic results show that a high percentage of the found in the Zapatero Osorio et al. (1997c) photometric in the Pleiades may indeed be true cluster members. mber of BD candidates identified indicates a continuing the initial mass function (IMF; $dN(m)/dM \sim M^{-\alpha}$) across llar-substellar boundary. A preliminary estimate of the ndex can be found in Martín et al. (1997b), which gives ± 0.5. A similar IMF slope was found by Meusinger, ach, & Souchay (1996) for Pleiades members with in the range 1.0–0.4 $M_\odot$ and by Hambly & Jameson (1991) for the range 0.5–0.1 $M_\odot$. Even though the IMF appears to rise up to about 45 M_{Jup}, it is not steep enough for BDs in the mass range 75–45 M_{Jup} to make a significant contribution to the total mass of the cluster. However, their population is probably quite numerous, 200–300 in the whole cluster area. If the IMF is extrapolated toward very low masses, say 10 M_{Jup} (roughly the deuterium-burning limit), the total number of BDs in the cluster would be increased to the order of 1000 objects, and thus BDs may even double the number of known members in the Pleiades. Nevertheless, they would not contribute significantly to the mass of the cluster (providing less than 5% the mass contained in stars). Assuming that the substellar Pleiades IMF is representative of field objects and normalizing to the local volume density of M0–M8 dwarfs identified within $d = 5$ pc (0.0726 stars pc^{-3}; Lang 1992), we find that, in the solar neighborhood, BDs with masses 80–40 M_{Jup} could be as numerous as M-type dwarfs.

This work is based on observations obtained at the W. M. Keck Observatory, which is operated jointly by the University of California and Caltech, and at the WHT telescope operated by the Isaac Newton Group of Telescopes funded by PPARC at the ORM. This work has been supported by the European Commission through the Activity "Access to Large-Scale Facilities" within the Programme TMR, awarded to the Instituto de Astrofísica de Canarias to fund European Astronomers access to the Canary Islands Observatories (European Northern Observatory). Partial support has been provided by the Spanish DGES project number PB95-1132-C02-01.

REFERENCES

., & Marcy, G. W. 1995, AJ, 109, 762
., Marcy, G., & Graham, J. R. 1996, ApJ, 458, 600
, G., Baraffe, I., & Plez, B. 1996, ApJ, 459, L91
n, M. R., Hodgkin, S. T., Jameson, R. F., & Pinfield, D. J. 1997, AS, 288, L23
a, F., & Mazzitelli, I. 1994, ApJS, 90, 467
, N. C. 1997, in ASP Conf. Proc., Brown Dwarfs and Extrasolar Planets, Rebolo, E. L. Martín, & M. R. Zapatero Osorio (San Francisco: ASP), ss
, N. C., Hawkins, M. R. S., & Jameson, R. F. 1993, A&AS, 100, 607
, N. C., & Jameson, R. F. 1991, MNRAS, 249, 137
, S. T., Jameson, R. F., & Steele, I. A. 1995, MNRAS, 274, 869
. R. A., Longmore, A. J., Jameson, R. F., & Mountain, C. M. 1994, AS, 267, 413
ick, J. D., Henry, T. J., & Simons, D. A. 1995, AJ, 109, 797
R. 1992, Astrophysical Data: Planets and Stars (New York: Springer)
E. L., Basri, G., Delfosse, X., & Forveille, T. 1997a, A&A, submitted
E. L., Rebolo, R., & Zapatero Osorio, M. R. 1996, ApJ, 469, 706
E. L., Zapatero Osorio, M. R., & Rebolo, R. 1997b, in ASP Conf. Brown Dwarfs and Extrasolar Planets, ed. R. Rebolo, E. L. Martín, R. Zapatero Osorio (San Francisco: ASP), in press
Meusinger, H., Schilbach, E., & Souchay, J. 1996, A&A, 312, 833
Nakajima, T., Oppenheimer, B. R., Kulkarni, S. R., Golimowski, D. A., Matthews, K., & Durrance, S. T. 1995, Nature, 378, 463
Osterbrock, D. E., et al. 1996, PASP, 108, 277
Rebolo, R., Martín, E. L., Basri, G., Marcy, G. W., & Zapatero Osorio, M. R. 1996, ApJ, 469, L53
Rebolo, R., Zapatero Osorio, M. R., & Martín, E. L. 1995, Nature, 377, 129
Rebolo, R., et al. 1997, in preparation
Ruiz, M. T., Leggett, S., & Allard, F. 1997, in 10th Workshop on Cool Stars, Stellar Systems and the Sun, ed. B. Donohue & J. Bookbinder (Cambridge: Cambridge Univ. Press), in press
Stauffer, J. R., Liebert, J.R., Giampapa, M., Macintosh, B., Reid, N., & Hamilton, D. 1994, AJ, 108, 160
Steele, I. A., & Jameson, R. F. 1995, MNRAS, 272, 630
Tinney, C. G., Delfosse, X., & Forveille, T. 1997, ApJ, 490, L95
Tsuji, T., Ohnaka, K., & Aoki, W. 1996, ApJ, 305, L1
van Leeuwen, F., & Hansen-Ruiz, C. S. 1997, Proc. *hipparcos* Symp., ESA-SP 402 (Garching: ESA), in press
Zapatero Osorio, M. R., Martín, E. L., & Rebolo, R. 1997a, A&A, 323, 105
Zapatero Osorio, M. R., Rebolo, R., & Martín, E. L. 1997b, A&A, 317, 164
Zapatero Osorio, M. R., et al. 1997c, in preparation

Mon. Not. R. Astron. Soc. 000, 000–000 (0000) Printed 28 October 1998 (MN LaTeX style file v1.4)

RIZ Photometry of Low Mass Stars

M.R. Cossburn, S.T. Hodgkin and R.F. Jameson
Department of Physics and Astronomy, Leicester University, University Road, Leicester LE1 7RH

ABSTRACT

We have observed a complete spectral sequence of M dwarfs from type M0 to M10 in the R, I Harris filters and the Z RGO filter, using the Jacobus Kapteyn Telescope. We show that the I–Z colour is a good indicator of late spectral type. Published effective temperatures (T_e) for some of the target stars have allowed us to derive a relationship between I–Z and T_e. We present transformations between the I Harris and Cousins filter systems for very red objects and identify targets that show signs of photometric variability. The motivation for this work is that the I and Z filters have a deep imaging capability for cool stars and are not very dependent on dark time.

Key words: stars: low-mass, brown dwarfs.

1 INTRODUCTION

The photometric identification of very low-mass stars (VLMS) and brown dwarfs is based on the assumption that objects of late spectral type have large V–I and R–I colours. The early survey work of Jameson and Skillen (1989) and Stauffer et al (1989) within the Pleiades open cluster used the I, R–I or V–I colour-magnitude diagrams to define the lower main sequence towards the sub-stellar boundary. Many similar surveys followed, with varying degrees of success in the hunt for brown dwarfs. When carrying out a deep search within an open cluster, the longer the baseline of the colour being used, the greater the separation between likely cluster members and field stars on the colour-magnitude diagram. The work of Williams et al. (1996) demonstrates this effect particularly well in the use of the V–K colour. There are certain disadvantages to using such long baseline colours in this kind of large area survey work. The primary concern is the number of galaxies that appear red as a result of a redshifted Balmer discontinuity. This contamination can often be removed by careful analysis of the object's point spread function, but in some cases can only be removed after follow-up infrared imaging and optical spectroscopy.

Furthermore, the lack of flux at R and V for VLMS and brown dwarfs results in increased exposure times and a need for dark time. This places enormous overheads on telescope time and reduces the competitiveness of the project proposal. In 1995 in an attempt to remedy the above drawbacks, we proposed to use the I and Z filter combination. The Z filter is an extension to the Gunn system (Schneider et al. 1983) with a bandpass that is defined by Schott RG850 glass and the quantum efficiency of the CCD detector (see Figure 1). The I–Z colour is a relatively short baseline colour, but has the advantage that it covers a particularly steep region of the VLMS / brown dwarf spectrum. Exposure times are therefore reduced and there is little dependence on dark time as the sky background is dominated by airglow at I and Z. This allows more flexibility for scheduling of observational programmes.

Our first small area survey of the Pleiades (see Cossburn et al. 1997) led to the discovery

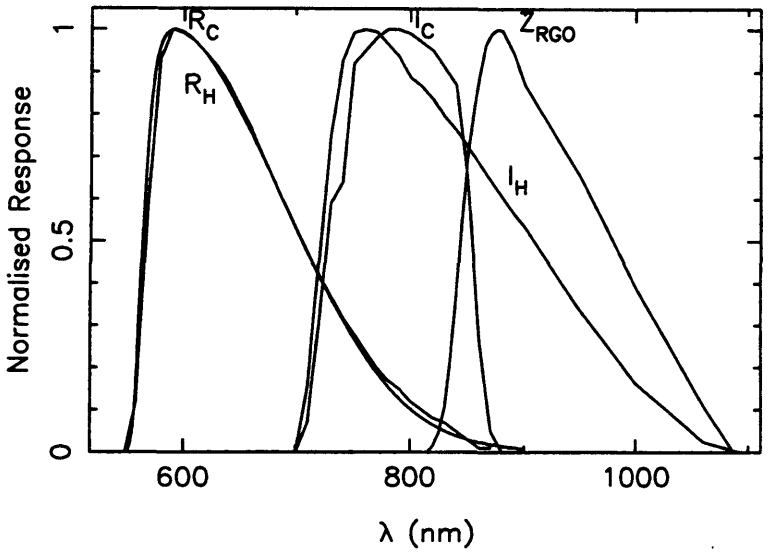

Figure 1. The filter profiles convolved with the TEK 4 CCD response. The filters used in this programme were R_H, I_H and Z_{RGO}. Also shown are the Cousins R and I standard passbands.

of PIZ 1, a brown dwarf of approximately 48 Jupiter masses. The success of this discovery has initiated a number of programmes: an I, Z survey in Praesepe (Pinfield et al. 1997 with follow-up infrared photometry in Hodgkin et al. 1998) and the International Time Project (ITP) survey in the Pleiades cluster (Zapatero-Osorio et al. 1997b, followed up in the infrared by Jameson et al 1998). These surveys have been extremely successful in discovering a number of VLMS in Praesepe and many brown dwarfs in the Pleiades. The success rate, (defined as the ratio of likely cluster members to initial candidates), from the ITP survey is of the order of 50% in the magnitude range I=18 to 20, but falls off as the survey limit is approached where the errors in I–Z increase.

It became apparent that we needed to calibrate the I–Z colour as a function of spectral type. The main objectives of the programme were to attempt an effective temperature (T_e) calibration and to obtain a number of Z observations of standards for future survey work. It was therefore necessary to include some target objects with reasonably well defined T_es. Defining T_es for VLMS is a particularly difficult task. Jones et al. (1994) used the water vapour features in the infrared spectra of a number of known VLMS, including GD165B (> M10), to estimate T_e. Targets for this observational programme were selected from this list, as well as from Leggett (1992), Veeder (1974) and Berriman et al. (1992). In this paper we examine the relationship between R–I and I–Z. The relationship between the I–Z colour and T_e is derived from the data and we present a transformation between the more commonly used Harris filter system and the Cousins standard system.

2 OBSERVATIONS AND DATA REDUCTION

All observations were carried out using the TEK4 CCD at the Cassegrain focus of the Jacobus Kapteyn Telescope (JKT) at the Observatorio del Roque de los Muchachos on the island of La Palma. Our filters were the Harris R and I (R_H, I_H) and RGO Z (Z_{RGO}), (see Figure 1. for the filter profiles). The observing run took place between the 15th and 18th of February 1997. The weather was generally stable, but the extinction was unusually high due to dust in the atmosphere. All images were de-biased, trimmed and flat-fielded using the CCDPROC routines in IRAF. Flat-fields were taken in twilight at the beginning and end of each night in each filter. Individual flats in each respective filter were co-added to obtain the best resultant flat, which was then normalised to unity. All target images were then flat-fielded using the corresponding normalised flat. Instrumental magnitudes were obtained using the PHOT software routines in IRAF.

To calibrate the target stars the following procedure was adopted. We assumed, see Figure 1, that $R_H = R_C$ (R Cousins). We further assumed that I_C (I Cousins) = $I_H = Z_{RGO}$ for unreddened A0 stars since these by definition have zero colours. Unreddened B9 to A1 Cousins standards were taken from Landolt (1992). Airmass curves were then determined in the usual manner. These were well determined and we are satisfied that the effect of atmospheric dust has been removed. Thus we obtain R_H (=R_C), I_H and Z_{RGO} for the target stars. The results are summarised in Table 1.

3 DISCUSSION

We have plotted $(R\text{–}I)_H$ against I_H–Z_{RGO} for all the targets presented in Table 1, shown in Figure 2. The crosses plotted in Figure 2 are our measurements of the Landolt standard stars observed as target stars.

We now have a catalogue of Z magnitudes for a range of Landolt standards for future observations in this filter system (see Table 2), but we emphasize that repeat observations are necessary to reduce the errors. Also plotted on this figure is the brown dwarf discovered by the DENIS survey, DENIS-PJ1228.2-1547, (Delfosse et al. 1997) shown as a solid circle. The large error in the R–I colour of this object is due to our short R exposure.

Most of the objects included in Table 1 have measured spectral types. In the main, these have been obtained from Leggett (1992), but for some of the latest and reddest objects, the spectral types have been taken from Kirkpatrick et al. (1995). Figure 3 shows the relationship between I–Z and spectral type, with the colour smoothly increasing with spectral type. The discovery of a number of objects with spectral types > dM10, (see Kirkpatrick et al. 1997, Delfosse et al. 1997 and Ruiz et al. 1997) has led to the proposed L-type classification of these objects, (see Kirkpatrick at al. 1998 and Liebert et al. 1998). Obtaining I and Z photometry for a number of these targets will show whether or not the I–Z colour continues to increase with spectral type.

One of the key objectives of this observational programme was to include targets with estimated effective temperatures. There have been many attempts to derive T_e for VLMS and brown dwarfs by a number of different authors. Measuring T_e is difficult for such objects due to the complex nature of the molecular and dust opacities. LHS 2924, taken from Jones et al. (1994), has the lowest spectroscopically determined temperature of all the objects in this target sample. Temperatures for the other targets have been taken from Veeder (1974), Berriman et al (1992) and Leggett (1996). The temperatures derived by Kirkpatrick et al. (1993) are significantly higher than those taken from the above authors and have, accordingly, not been included. All the data used is presented in Table 3. Figure 4 shows the

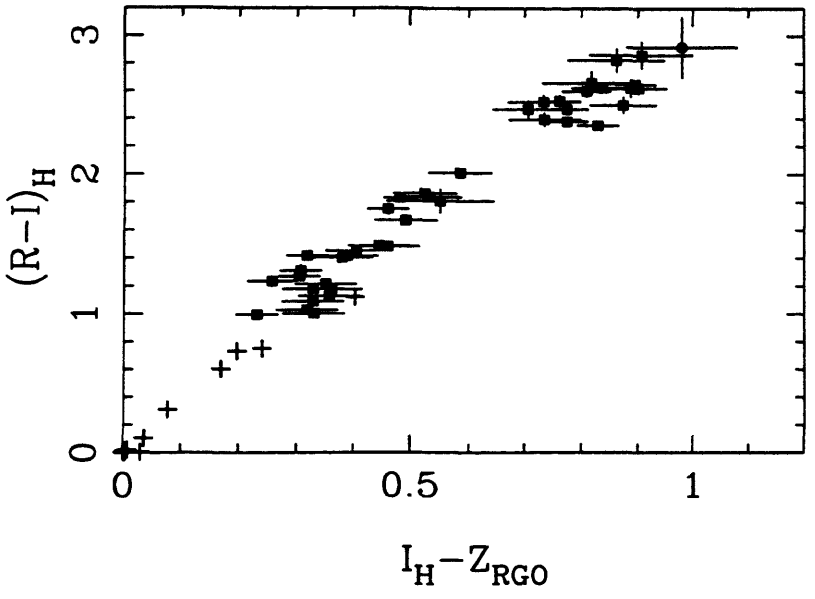

Figure 2. The R–I versus I–Z diagram showing the target objects (solid squares), the standard stars (crosses) and the DENIS brown dwarf DBD 1228 plotted as a solid circle.

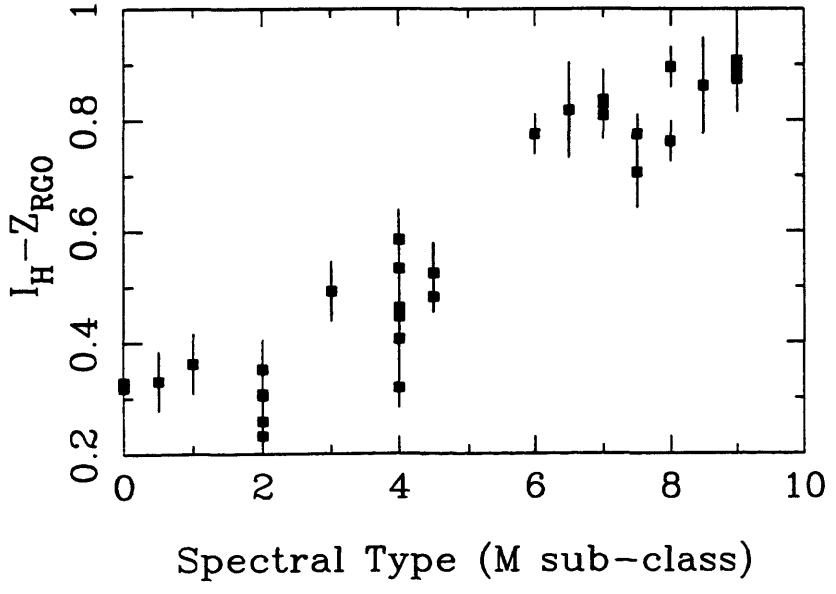

Figure 3. I–Z plotted against spectral type for the target sample.

Table 1. The photometry for all the target stars in the sample

Object Name	$(R-I)_H$	I_H	±	$I_C^{(a)}$	Z_{RGO}	±	Sp. Typ.[b]	I-K[c]
Gl 270	0.99	8.11	0.02	8.27	7.88	0.03	M2.0	1.90
Gl 328	1.00	8.08	0.02	8.22	7.75	0.05	M0.5	1.80
Gl 319A	1.02	7.70	0.02	7.79	7.39	0.05	M0.0	1.91
Gl 353	1.08	8.14	0.02	8.27	7.82	0.05	M0.0	1.93
Gl 464	1.12	8.42	0.02	8.57	8.07	0.05	K5.0	1.88
Gl 494	1.15	7.55	0.02	7.71			M2.0	2.10
Gl 424	1.17	7.25	0.02	7.42	6.89	0.05	M1.0	1.87
Gl 524	1.17	8.07	0.02		7.74	0.05		
Gl 459.3	1.21	8.61	0.02	8.75	8.26	0.05	M2.0	1.91
Gl 272	1.23	8.35	0.03	8.50	8.09	0.03	M2.0	2.01
Gl 361	1.26	8.01	0.02	8.18	7.71	0.03	M2.0	2.01
Gl 393	1.30	7.27	0.03	7.41	6.96	0.02	M2.0	2.07
Gl 452	1.40	9.42	0.02	9.55	9.04	0.05		2.10
GJ 347ab	1.41	9.59	0.02	9.72	9.20	0.05		2.09
Gl 476	1.41	8.99	0.02	9.19	8.67	0.03	M4.0	2.04
GJ 333-2a	1.45	9.77	0.02	9.94	9.37	0.05	M4.0	2.17
GJ 333-2b	1.48	10.05	0.02	10.20	9.61	0.05	M4.0	2.20
Gl 463	1.48	9.05	0.02	9.24	8.59	0.05	M4.0	2.11
Gl 436	1.67	8.09	0.02	8.28	7.60	0.05	M3.0	2.18
Gl 299	1.75	9.79	0.03	9.91	9.33	0.02	M4.0	2.27
GJ 1103A	1.80	10.00	0.07		9.45	0.06		
Gl 268	1.83	8.29	0.02	8.44	7.81	0.02	M4.5	2.57
Gl 402	1.83	8.64	0.02	8.86	8.11	0.05	M4.0	2.44
Gl 285	1.86	8.08	0.02	8.20	7.56	0.05	M4.5	2.47
Gl 447	2.01	7.90	0.02	8.14	7.32	0.05	M4.0	2.51
LHS 3003	2.35	12.18	0.02	12.53	11.35	0.03	M7.0	3.60
LHS 2026	2.39	14.00	0.04	14.27	13.27	0.05		3.12
LHS 2632	2.46	14.36	0.03		13.58	0.02	M7.5	
LHS 2645	2.46	14.20	0.05		13.49	0.04	M7.5	
GL 406	2.48	9.18	0.02	9.50	8.41	0.03	M6.0	3.31
BRI 1222-1222	2.49	15.12	0.05		14.25	0.03	M9.0	
LHS 2243	2.52	14.27	0.03		13.51	0.02	M8.0	
LHS 2471	2.52	13.35	0.04	13.69	12.62	0.05		3.39
CTI115638.4+280000	2.60	16.42	0.03		15.61	0.03	M7.0	
LHS 2924	2.62	14.59	0.05	15.21	13.70	0.04	M9.0	4.54
LHS2065	2.62	14.05	0.03	14.44	13.15	0.03	M9.0	4.46
VB8	2.62	11.89	0.02	12.24	11.06	0.05	M7.0	3.42
LHS2397A	2.64	14.51	0.02	14.95	13.61	0.03	M8.0	4.11
Gl316.1	2.65	13.11	0.07	13.45	12.30	0.05	M6.5	3.42
TVLM 513-46546	2.82	14.56	0.07	15.09	13.70	0.05	M8.5	4.32
TVLM 868-110639	2.86	15.37	0.07	15.79	14.47	0.06	M9.0	4.35
DENIS-PJ1228.2-1547	2.92	17.58	0.04	18.19[d]	16.60	0.10	>M10	5.46[d]

[a] The I_C magnitudes were taken mostly from Leggett (1992). Other sources included Tinney (1993) and Kirkpatrick (1995).
[b] Spectral Types are from Leggett (1992) and Kirkpatrick (1995).
[c] K photometry taken from Leggett (1992) and Tinney (1993).
[d] I,K photometry taken from Delfosse et al. (1997).

$(R-I)_C = (R-I)_H + I_H - I_C$

I–Z versus T_e diagram. The errors arise from the differences in individual measurements. A cubic fit has been determined for this data and is given in Equation 1. A cubic fit is required to pass through I–Z=0 for an A0 star at $T_e \sim 9700$, although a linear fit is adequate for $0.5<(I-Z)<0.9$.

$$T_e = 9700 - 30200(I-Z) + 45800(I-Z)^2 - 24100(I-Z)^3 \quad (0.5 < (I-Z) < 0.9) \tag{1}$$

As a result of the difficulty in deriving the T_e for such cool objects, the inherent errors are

Table 2. The Catalogue of Landolt Standards with calibrated Z magnitudes

Object Name	R_C	I_C	Z_{RGO}	±
LAN95-96	9.931	9.836	9.72	0.04
LAN95-97	14.296	13.750	13.48	0.04
LAN95-98	13.725	13.106	12.86	0.04
LAN95-100	15.095	14.672	14.46	0.04
LAN95-101	12.241	11.814	11.66	0.04
LAN98-670	11.207	10.555	10.27	0.04
LAN98-671	12.810	12.314	12.06	0.04
LAN98-675	12.316	11.313	10.79	0.04
LAN98-676	12.385	11.716	11.39	0.04
LAN98-682	13.383	13.032	13.05	0.04
LAN98-685	11.664	11.384	11.27	0.04
RU-149B	12.268	11.914	11.79	0.04
RU-149D	11.459	11.451	11.42	0.04
RU-149E	13.397	13.081	12.69	0.04
RU-149F	12.877	12.339	12.13	0.04
RU-149G	12.507	12.184	12.08	0.04
PG0918+029	13.456	13.615	13.68	0.05
PG0918+029A	14.165	13.829	13.66	0.05
PG0918+029B	13.546	13.176	12.96	0.05
PG0918+029C	13.170	12.815	12.72	0.05
PG0918+029D	11.697	11.164	10.92	0.05
101-262	13.855	13.468	13.28	0.04
PG1323-086	13.529	13.608	13.60	0.04
PG1323-086A	13.339	13.085	12.87	0.04
PG1323-086B	12.980	12.573	12.37	0.04
PG1323-086C	13.608	13.244	13.06	0.04

Table 3. The targets used with estimated T_{eff} to calibrate the I–Z colour.

Object Name	I–Z	±	Sp. Typ.	T_{upper} (K)	T_{lower} (K)
GL299	0.46	0.04	M 4.0	3250	2950
GL268	0.48	0.03	M 4.5	3250	2950
GL285	0.53	0.05	M 4.5	3250	2950
GL406	0.78	0.04	M 6.0	2500	2670
LHS2924	0.89	0.06	M 9.0	2100	2300

large. The relationship derived above therefore merely demonstrates the effectiveness of the I–Z colour as a discriminant for objects with effective temperatures down to approximately 2000K.

In Figure 5 we show the relationship between I–K and I–Z. For objects with large I–K colours, the I–Z colour appears to be tending towards saturation. This implies that R–I may also be saturating (see Figure 2), as there is no change in slope in this diagram. This conclusion is reinforced by the data of Bouvier et al. (1998) for Pleiades brown dwarfs (see their Figure 5), where the I, R–I sequence appears to turn down at R–I$\sim$ 2.5.

Most of the objects we have measured have published Cousins I photometry, (Leggett 1992), which we have also listed in Table 1. We can therefore derive the conversion between I_C and I_H. We plot I_C–I_H against $(R–I)_H$ and I_H–Z_{RGO} in Figures 6(a) and 6(b) respectively. These plots can be described by Equations 2 and 3 below.

$$I_C - I_H = 0.0788(R-I)_H + 0.0219(R-I)_H^2 \quad (0 < (R-I)_H < 2.9) \tag{2}$$

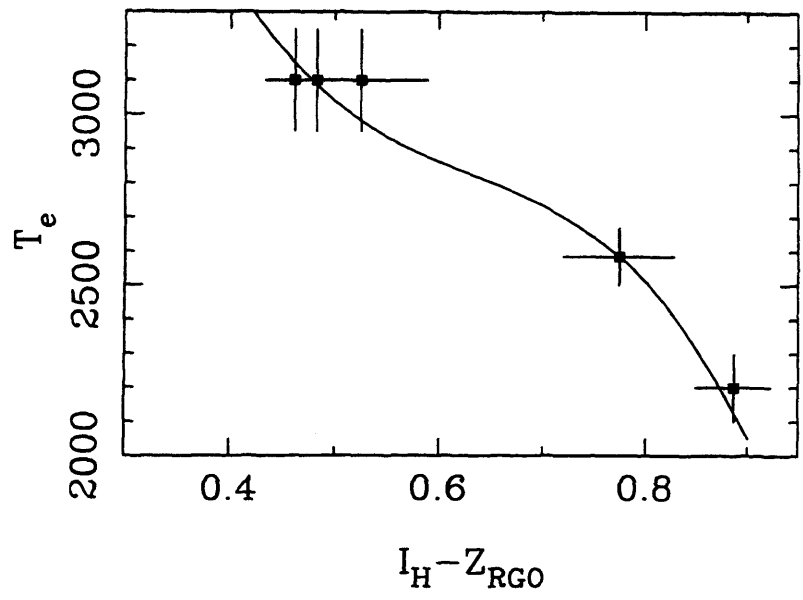

Figure 4. The relationship between effective temperature and the I–Z colour. The fit, shown as a solid line, is given in Equation 1.

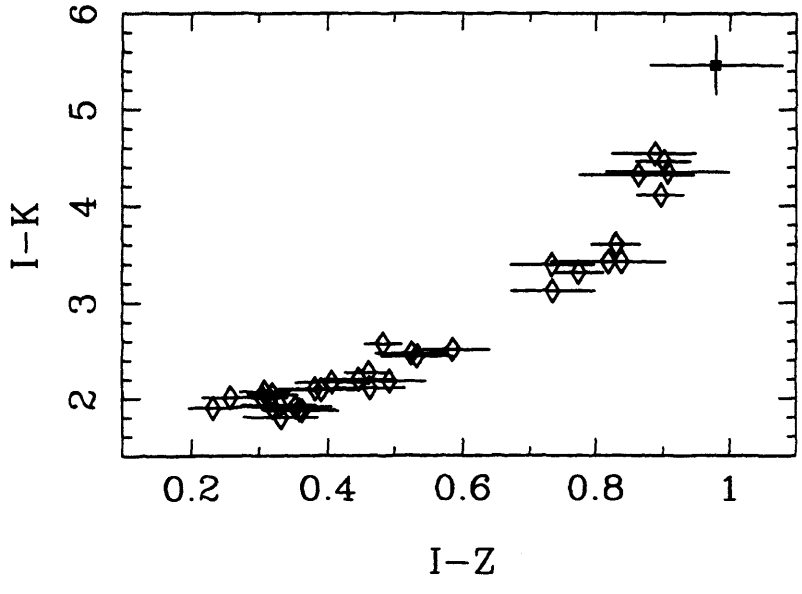

Figure 5. The I–K versus I–Z diagram for all the target objects (shown as open diamonds) including the DENIS brown dwarf, DENIS-PJ1228.2-1547, (shown as a solid symbol).

$$I_C - I_H = 0.298(I_H - Z_{RGO}) + 0.1401(I_H - Z_{RGO})^2 \quad (0 < (I_H - Z_{RGO}) < 0.95) \tag{3}$$

The objects plotted as solid squares in Figures 6(a) and 6(b) are TVLM 513-46546 and LHS 2924. They show a larger deviation in I_C - I_H than expected which could be attributed to variability. As a result, these 2 objects were not used to determine the above fits. The suggestion that TVLM 513-46546 shows signs of variability has already been proposed in Tinney (1993). Further observations of both objects are essential to confirm this hypothesis.

4 CONCLUSIONS

We show the validity of our initial proposal to use the Z filter in the search for brown dwarfs in open clusters and the field. The continued increase of the I–Z colour for very late type objects is seen. We have also shown the relationship between the I–Z colour and effective temperature and spectral type. Evidence of the saturation of the I–Z colour is seen in the I–K, I–Z diagram. The transformations between the Harris and Cousins filter systems are derived and a catalog of Z standards has been created for future survey work using the Harris and RGO filter systems. Follow up observations of these standards at Z are required to reduce the photometric errors.

5 ACKNOWLEDGEMENTS

STH is a PPARC-supported research associate and MRC is indebted to the same research council for a research studentship. We would also like to thank Matt Burleigh and Nigel Bannister for obtaining the DENIS brown dwarf photometry on a recent JKT run. This research has made use of the Simbad database operated at CDS, Strasbourg, France.

REFERENCES

Berriman G., Reid N., Leggett S.K., 1992, ApJL, 392, L31
Bouvier, J., Stauffer, J.R., Martin, E.L., Barrado y Navascues, D., Wallace, B., Bejar, V.J.S., 1998, A&A, in press.
Cossburn M.R., Hodgkin S.T., Jameson R.F., Pinfield D.J., 1997, MNRAS, 288, L23
Delfosse, X., Tinney, C.G., Forveille, T., Epchtein, N., Bertin, E., Borsenberger, J., Copet, E., de Batz, B., Fouque, P., Kimeswenger, S., Le Bertre, T., Lacombe, F., Rouan, D., Tiphene, D., 1997, A&AS, 327, L25-28
Hodgkin, S.T., Pinfield, D.J., Jameson, R.F., Steele, I.A., Hambly, N.C., Cossburn, M.R., 1998, MNRAS, submitted.
Jones, H.R.A., Longmore, A.J, Jameson, R.F., Mountain, C.M., 1994, MNRAS, 267, 413
Jameson, R.F., Skillen, I., 1989, MNRAS, 239, 247
Jameson, R.F., Pinfield, D.J., Hodgkin, S.T., Cossburn, M.R., 1998, in prep.
Kirkpatrick, J.D., Kelly, D.M., Rieke, G.H., Liebert, J., Allard, F., Wehrse, R., 1993, ApJ, 402, 643-654
Kirkpatrick, J.D., Henry, T.J., Simons, D.A., 1995, AJ, 109, 797
Kirkpatrick, J.D., Beichman, C.A., Skrutskie, M.F., 1997, ApJ, 476, 311
Kirkpatrick J.D., 1998, in Rebolo, R., Martin, E.L., Zapatero Osorio, M.R., eds, Proc. ASP Conf. Ser. 134, Brown Dwarfs and Extrasolar Planets, Astron. Soc. Pac., San Francisco, p.405
Landolt, A. U., 1992, AJ, 104, 340
Leggett, S.K., 1992, ApJS, 82, 351
Leggett S.K., Allard F., Berriman G., Dahn C.C., Hauschildt P.H., 1996, ApJS, 104, 117
Liebert, J., 1998, in Very Low-Mass Stars and Brown Dwarfs in Stellar Clusters and Associations (La Palma), in prep.
Pinfield, D.J., Hodgkin, S.T., Jameson, R.F., Cossburn, M.R., von Hippel, T., 1997, MNRAS, 287, 180
Ruiz, M.T., Leggett, S.K., Allard, F., 1997, ApJ, 491, L107
Schneider, D.P., Hoessel, J.G., Gunn, J.E., 1983, ApJ, 264, 337
Stauffer, J., Hamilton, D., Probst, R., Rieke, G., Mateo, M., 1989, ApJ, 344, L21-24
Tinney, C.G., 1993, 414, 279
Veeder, G.J., 1974, AJ, 79, 1056
Williams, D.M., Boyle, R.P., Morgan, W.T., Rieke, G.H., Stauffer, J.R., Rieke, M.J., 1996, ApJ, 464, 238
Zapatero-Osorio, M. R., Rebolo, R., Martin, E.L., 1997a, A&A, 317, 164
Zapatero-Osorio, M. R., Rebolo, R., Martin, E.L., Basri, G., Magazzu, A., Hodgkin, S.T., Jameson, R.F., Cossburn, M.R., 1997b, ApJL, 491, 81

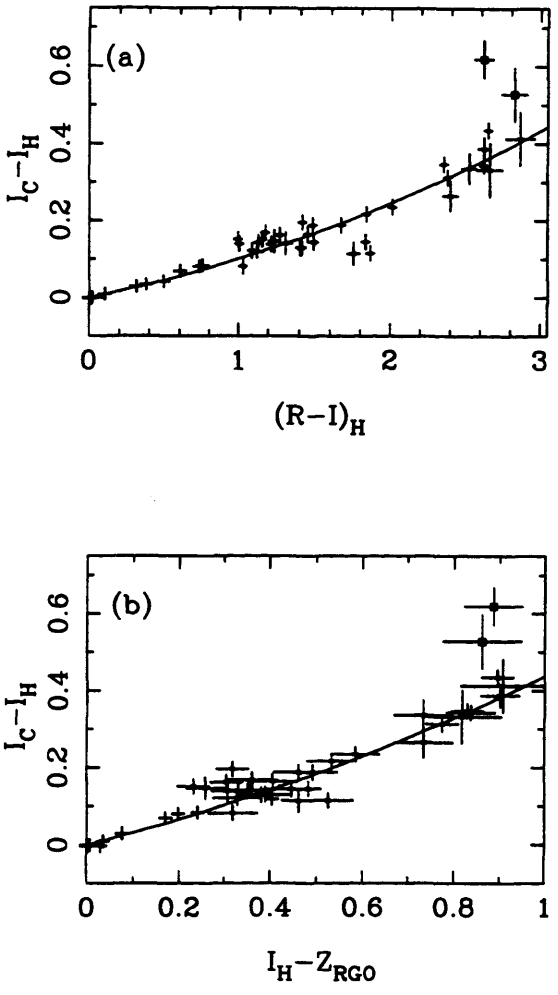

Figure 6. The relationship between I_C and I_H as a function of (a) $(R-I)_H$ and (b) I_H-Z_{RGO}. The objects plotted as solid squares were rejected from the data set used to derive the fits given in Equations 2 and 3, (solid lines), because we believe they show signs of photometric variability, (see text for more details).

Mon. Not. R. Astron. Soc. 000, 000–000 (0000) Printed 6 March 1998 (MN LATEX style file v1.4)

Brown Dwarfs in the Pleiades and the Initial Mass Function across the stellar/substellar boundary

N.C. Hambly[1], S.T. Hodgkin[2], M.R. Cossburn[2] and R.F. Jameson[2]

[1] *Royal Observatory, Blackford Hill, Edinburgh, EH9 3HJ*

[2] *Astronomy Group, Department of Physics and Astronomy, Leicester University, University Road, Leicester, LE1 7RH*

Accepted —. Received —; in original form —

ABSTRACT

We present a new sample of brown dwarf (BD) candidates from a survey covering $6° \times 6°$ centred on the Pleiades. The survey was constructed using I and R band photographic plates, from the United Kingdom Schmidt Telescope, measured using the new high precision microdensitometer SuperCOSMOS at the Royal Observatory, Edinburgh. Objects as faint, or up to ~ 0.3 magnitudes fainter than the confirmed BD member PPL 15 were selected on the basis of having extremely red photographic colours and proper motions consistent with cluster membership; follow–up near–infrared and infrared photoelectric photometry yielded 9 candidate BD Pleiads (including PPL 15). Co-ordinates, magnitudes and finders are presented for these objects. We use these data and information on higher mass stars to construct a mass function that indicates a flat initial mass function across the stellar/substellar boundary, and we discuss the implications of these results for future surveys.

Key words: stars: low mass, brown dwarfs, mass function – open clusters and associations: individual: Pleiades

1 INTRODUCTION

The amount of unseen mass, or dark matter, in stellar systems has been the subject of much discussion for some time (e.g. Kormendy & Knapp 1987 and references therein). For example, since the original work of Oort (1960), it has been assumed that some fraction of any disk missing mass (inferred from dynamical considerations) may be in the form of substellar

objects, or brown dwarfs (BDs) – i.e. those stars having insufficient mass to achieve the core pressures and temperatures necessary for hydrogen fusion. In fact, there is some dispute over the local mass density and fraction of missing mass (e.g. Bienaymé et al. 1987; Kuijken & Gilmore 1989,1991; Bahcall et al. 1992), and the subject has recently received an upsurge in interest due to the discovery of a brown dwarf orbiting the star Gliese 229 (Nakajima et al. 1995) along with the detection of populations of dark microlensing bodies in the Galactic disk ('OGLE', Udalski et al. 1993) and halo ('EROS', Aubourg et al. 1993; 'MACHO', Alcock et al. 1997). It is therefore important to measure the contribution that substellar objects make to the membership and total mass in stellar systems in order to help to resolve a number of problems concerning Galactic structure. Moreover, the spectrum of masses resulting from star formation processes is currently unknown at the lowest masses and the form of this initial mass function (IMF) is open to question, although there are compelling theoretical arguments for the IMF having a log–normal form to a good approximation (Adams & Fatuzzo 1996).

A theoretical exposition concerning the existence of BDs seems to have been given originally by Kumar (1963). He calculated analytically that for a Population I chemical composition, objects having masses $m \lesssim 0.07 M_{\odot}$ would be unable to fuse hydrogen in the manner of a stable main sequence star. Kumar called such objects 'black dwarfs' – the term 'brown dwarf' is due to Tarter (1975). Important reviews concerning both the observation and theory of BDs can be found in Kafatos, Harrington & Maran (1986), Liebert & Probst (1987) and Greenstein (1989). It was not until the identification of a unique spectral diagnostic (Rebolo, Martín & Magazzù 1992 and references therein) that the assignment of unequivocal BD status became a possibility for isolated candidates, yet the feature in question (the lithium resonance doublet at 6708Å) remained unobserved in all objects examined (e.g. Magazzù, Martín & Rebolo 1993; Marcy, Basri & Graham 1994; Martín, Rebolo & Magazzù 1994). So, up until relatively recently, the existence of isolated BDs continued to be the subject of some debate in the literature – see Tinney (1995) for a concise summary of the situation up to that time. Finally, however, lithium was observed in two Pleiades BD candidates: PPL 15, discovered by Stauffer, Hamilton & Probst (1994) and observed spectroscopically by Basri, Marcy & Graham (1996); followed closely by Teide 1, discovered by Rebolo, Zapatero–Osorio & Martín (1995) and observed spectroscopically by Rebolo et al. (1996). Clearly, the Pleiades is a good hunting ground for BDs and the race is now on to make a complete, magnitude limited survey to determine the mass function for BDs in this

cluster. For an up–to–date review of the extensive work being carried out in the Pleiades, see Rebolo, Martín & Zapatero–Osorio (1998).

Proper motion surveys of young Galactic clusters provide a means for identifying cluster members with a reasonably high degree of confidence. Hambly et al. (1995a;1995b) presented a deep proper motion survey of Praesepe, and applied the Sanders (1971) membership probability technique to derive a complete and accurate IMF for the cluster. It is unfortunate that membership probabilities are increasingly difficult to derive for fainter stars – the scatter in the proper motion vector–point diagram increases due to increasing astrometric errors, and the ratio of non–member field stars to cluster members also increases dramatically beyond the peak in the luminosity function. In addition, for the Pleiades the reflex solar motion can make nearby, very low luminosity M dwarfs appear as high probability proper motion members (e.g. Jones 1973). Despite these problems, proper motion surveys for very low luminosity stars in the Pleiades have been very successful in identifying members – indeed, Teide 1 was identified as a BD candidate partly because it had a measured proper motion consistent with cluster membership (Rebolo et al. 1995). Hambly, Hawkins & Jameson (1991;1993 – HHJ) presented a deep, proper motion survey of the Pleiades cluster for very low mass stars and BDs. This survey was limited to R $\sim$ 20.5 by the use of R–band Schmidt plates. The faintest confirmed member from that survey turned out to be HHJ 3, which has I $\sim$ 17.5, i.e. around 0.4 mag brighter than PPL 15. Since a near infrared spectrum of HHJ 3 does not show an absorption feature due to lithium in its atmosphere it must be at the limit of the hydrogen burning main sequence (Marcy, Basri & Graham 1994).

Several groups (e.g. Zapatero–Osorio et al. 1997b; Cossburn et al. 1997; Stauffer et al. 1998) are using deep imaging with sensitive photoelectric detectors to probe the Pleiades membership at masses m$< 0.05 M_{\odot}$, over areas of order a few square degrees. Here we take the different approach of employing less sensitive I band photographic Schmidt plates to survey the whole cluster, i.e. several tens of square degrees. By pushing these plates to their limits, we have still reached masses below the hydrogen burning threshold. In this paper we present a new list of BD candidates having magnitudes in the range 17.8 $<$ I $<$ 18.3, i.e. as faint or fainter than the confirmed lithium BD member PPL 15. These stars all have proper motions, measured from positions on seven I–band plates spread in epoch over seven years, consistent with Pleiades membership and are extremely red, either from their measured (R–I) colours or by virute of the fact that they fail to appear in the R–band at all. The BD PPL 15, which previously had no proper motion measurement, appears in this list. Since the

Plate No.	Date	LST	Emulsion	Filter	Exp. /min
I12259	30/10/87	03:08	IVN	RG715	90
OR12839	2/11/88	03:42	IIIaF	OG590	70
OR13496	17/12/89	02:18	"	"	60
I13497	17/12/89	03:36	IVN	RG715	90
I15278	30/12/92	03:08	"	"	"
I15281	31/12/92	03:45	"	"	61
I16395	9/11/94	02:40	"	"	90
I16448	7/12/94	03:20	"	"	"
I16464	26/12/94	02:54	"	"	"
I16468	27/12/94	02:59	"	"	"

Table 1. Plate material used for this survey

presence of lithium is the best indicator of substellar nature for such objects (e.g. Rebolo et al. 1996), one ideally requires spectra of sufficient resolution and signal–to–noise ratio to measure the 6708Å lithium feature in order to confirm BD status and cluster membership for the candidates presented here. However, it has been shown in the past that infrared photometry is efficient at weeding out non–member contamination from candidate lists via the (I–K) temperature index (e.g. Steele, Jameson & Hambly 1993; Zapatero–Osorio, Martín & Rebolo 1997a). Such data are presented here, and we go on to produce a mass function for the cluster that, for the first time, samples a mass bin within the substellar régime to an easily quantifiable degree of completeness. Section 2 describes the photographic plate measurement, astrometry and photometry along with the photoelectric photometry (both near infrared and infrared). Section 3 describes the methods of transformation from luminosity to mass and the membership probability analysis for higher mass bins which enables comparison with previously derived results. Section 4 discusses these data and results, while in Section 5 we present our conclusions.

2 OBSERVATIONS AND REDUCTIONS

2.1 Photographic astrometry and photometry

The photographic plate collection used for this survey is presented in Table 1. All plates were taken centred at 3^h44^m, +23°57' (B1950.0) on the United Kingdom Schmidt Telescope at Siding Springs Observatory, New South Wales, Australia and are archived in the plate library of the Royal Observatory, Edinburgh.

All plates were scanned using the new, high precision microdensitometer SuperCOSMOS at the Royal Observatory, Edinburgh (e.g. Hambly et al. 1998). This machine digitises the

6° × 6° area of the Schmidt plate in 2.5 hr, with 10μm (0.67 arcsec) pixels, producing $\sim$ 2Gbyte of data. This digitised map is then thresholded and examined for connected pixels to produce a parameterised image catalogue (Beard, MacGillivray & Thanisch 1990 and references therein). The data presented here were thresholded at 3σ above sky, and a minimum area cut of 5 connected pixels was used, resulting in typically 200,000 to 300,000 image detections on each plate. In addition to processing the individual scans, the pixel data for the 8 individual I plates and 2 R plates were 'stacked' using software described in Knox et al. (1998) to produce two deep R and I catalogues for photometry, completeness calculations and the creation of finder charts. The procedure for photometric calibration using photoelectric sequences is described in HHJ and references therein; we note here that cubic splines were used as the calibrating functions as oppose to polynomials. Only 7 of the 8 available I plates were used for the astrometry (the exposure limited plate I15281 was excluded as it has lower sensitivity). Using procedures described in HHJ and references therein but with new software, relative shifts were determined for each image on each plate with respect to the mean positions from all 7 plates. Weighted linear least–squares fits, to these shifts as a function of time, then yielded the relative proper motion for each image (for more details, see for example Hambly, Smartt & Hodgkin 1997).

2.2 Infrared photometry

K band photometry for the sample of 45 stars selected via proper motion and red photographic colours (see Section 3) was made on the nights of 1997 November ?? to ?? using IRCAM3 on the United Kingdom Infrared Telescope (UKIRT) on the island of Hawai'i ...

2.3 Near–infrared photometry

I band photoelectric photometry for the sample of 9 candidates defined as a result of the infrared photometry described in the previous Section (see Section 3) was obtained on the nights of 1997 December ?? to ?? using the Wide Field Camera on the Isaac Newton Telescope (INT) at the Observatorio del Roque de los Muchachos on the island of La Palma ...

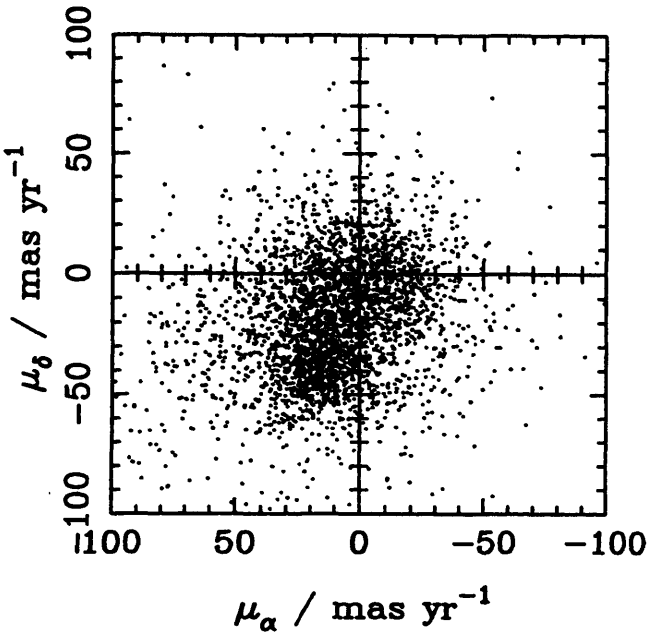

Figure 1. Proper motion vector–point diagram of a colour–selected sample of stars. The cluster members stand out clearly as a group in the SE quadrant.

3 RESULTS

In Figure 1 we show a proper motion vector–point diagram (PMVPD) for a colour–selected sample of stars. We selected all objects having I > 12.5 and I < 2.875(R–I)+11.875, i.e. a conservative cut in the I, (R–I) colour–magnitude diagram to include all possible members, while at the same time minimising the non–member contamination. All images were required to be present on at least six I plates; images not present in the R stack (which reaches R ∼ 21) were included as possible members with assumed large (R–I). Figure 2 illustrates the measured astrometric errors as a function of I magnitude for the best plate (I16448) and the worst plate (I12259). These curves show the characteristic form expected for centroiding accuracies of images in a photographic emulsion — see, for example, Hambly et al. (1998) and references therein. Because these errors increase dramatically towards the plate limit, the proper motion errors are correspondingly large in the magnitude range of most interest. We applied the Sanders (1971) membership probability technique, in an implementation described in Hambly et al. (1995a) and references therein, for three magnitude ranges: $12.5 < I_1 < 13.5 < I_2 < 14.5 < I_3 < 15.5$. The PMVPDs and membership probability histograms are ahown in Figure 3. Summing membership probabilities for all stars in these ranges

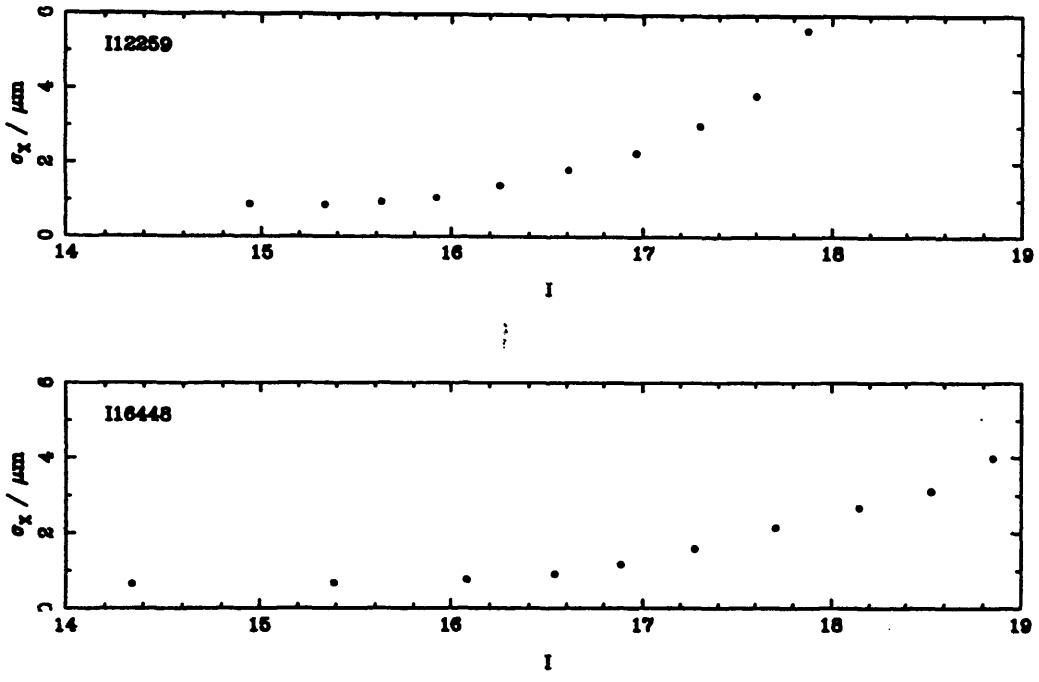

Figure 2. Astrometric errors (i.e. RMS errors in centroiding) for the best (I16448) and worst (I12259) plates in the proper motion study. Note that 1μm $\equiv$ 67 mas.

No. of stars	Range in I
122	12.5:13.5
194	13.5:14.5
258	14.5:15.5

Table 2. Total membership in the three magnitude ranges analysed.

yielded the statistically complete luminosty function in Table 2

In Figure 4(a) we show the PMVPD for a sample of stars having $17.8 < I < 18.3$ (the bright limit is ~ 0.2 mag brighter than PPL 15 while the faint limit is the sensitivity limit of this survey). Typical astrometric error bars are shown — clearly, the errors are too large and the density of members too small for the Sanders fitting technique to be stable. To make a selection of stars for photometric follow–up, we chose all objects having proper motions within 1σ of the known cluster motion $(\mu_\alpha, \mu_\delta) \equiv (+19, -43)$ mas yr^{-1} (e.g. Jones 1973). This selection of 45 possible members is plotted in the PMVPD in Figure 4(b). In order to determine which objects in this list of 45 stars were good BD candidates, K band photometry was obtained at UKIRT. This yielded nine objects as high probability members from (I–K) colour; these 9 were subsequently measured for accurate photoelectric I photometry

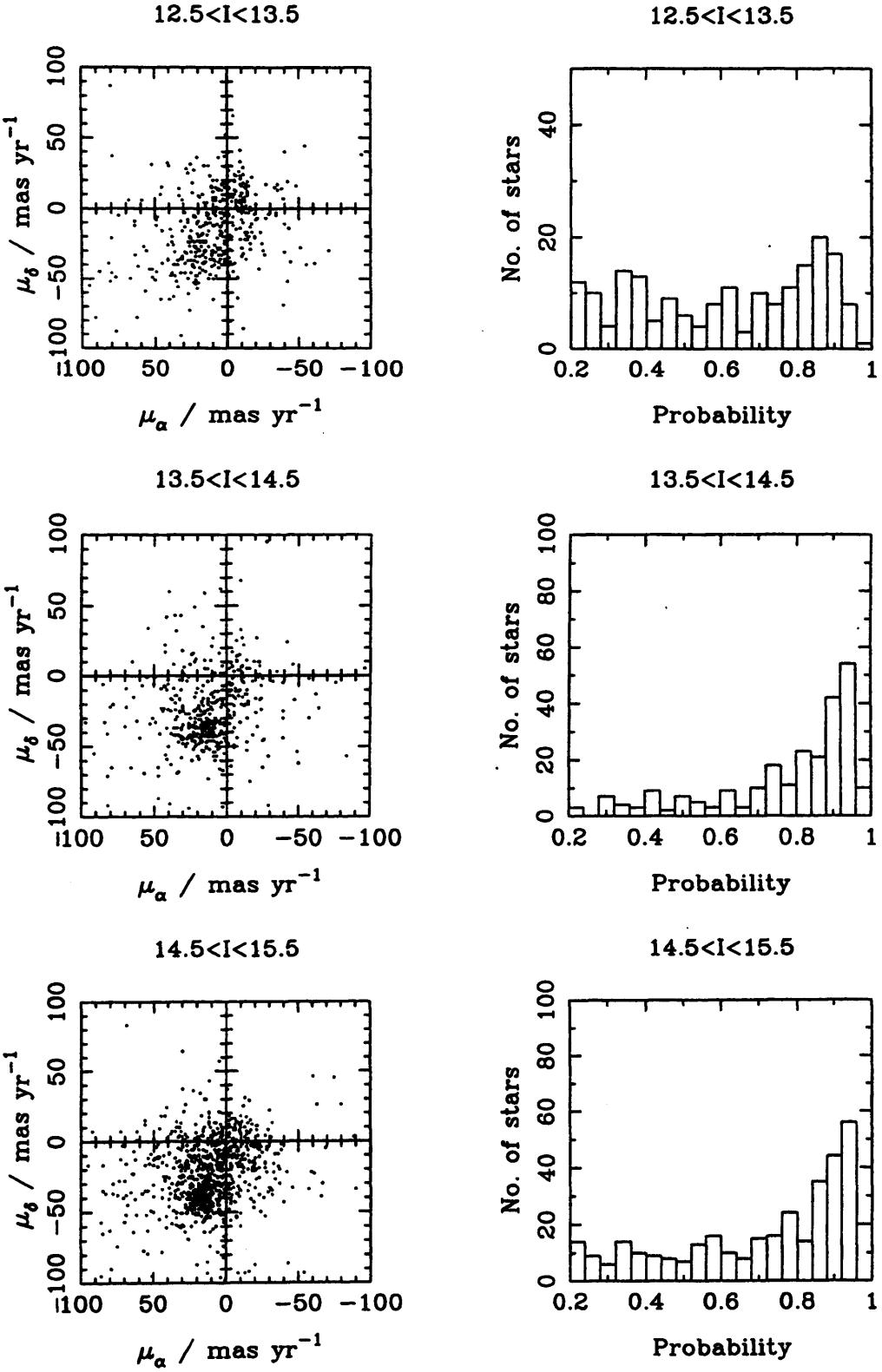

Figure 3. Proper motion vector-point diagrams and membership probability histograms for the three magnitude ranges $12.5 < I_1 < 13.5 < I_2 < 14.5 < I_3 < 15.5$. Note that the large number of field stars with probability <20% are not shown in the histograms.

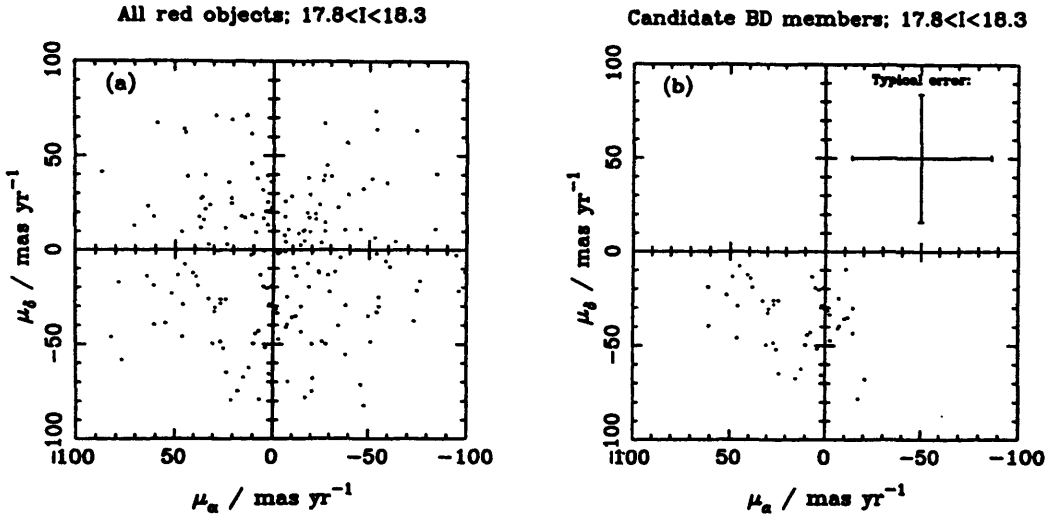

Figure 4. Proper motion vector–point diagrams, (a) for all red stars in the magnitude range $17.8 < I < 18.3$, and (b) for all stars having pms within 1σ of the known cluster motion (a typical error bar is shown).

on the INT. Figure 5 shows an I versus (I–K) colour–magnitude diagram for the objects, while Table 3 lists co–ordinates and magnitudes; in addition we have cross–checked this new list of candidates against those previously identified in the following surveys: Jameson & Skillen (1989); Stauffer et al. (1989); Simons & Becklin (1992); Hambly et al. (1993); Stauffer, Hamilton & Probst (1994); Stauffer, Liebert & Giampapa (1995); Williams et al. (1996); Zapatero–Osorio, Rebolo & Martín (1997a); Zapatero–Osorio et al. (1997b); Festin (1998) and finally Pinfield (1998). We included Jameson & Skillen (1989) and Simmons & Becklin (1992) despite the fact that these candidates are now thought to be non–members (e.g. Zapatero–Osorio et al. 1997a; Martín, Zapatero–Osorio & Rebolo 1998 and references therein) since we wished to check that our objects have not been previously eliminated as candidate members. Using a 20 arcsec search radius and checking all objects from the above surveys in the range $17 < I < 19$, we found that two objects have been identified previously (see Table 3). Finder charts for all 9 stars are given in Figure 6.

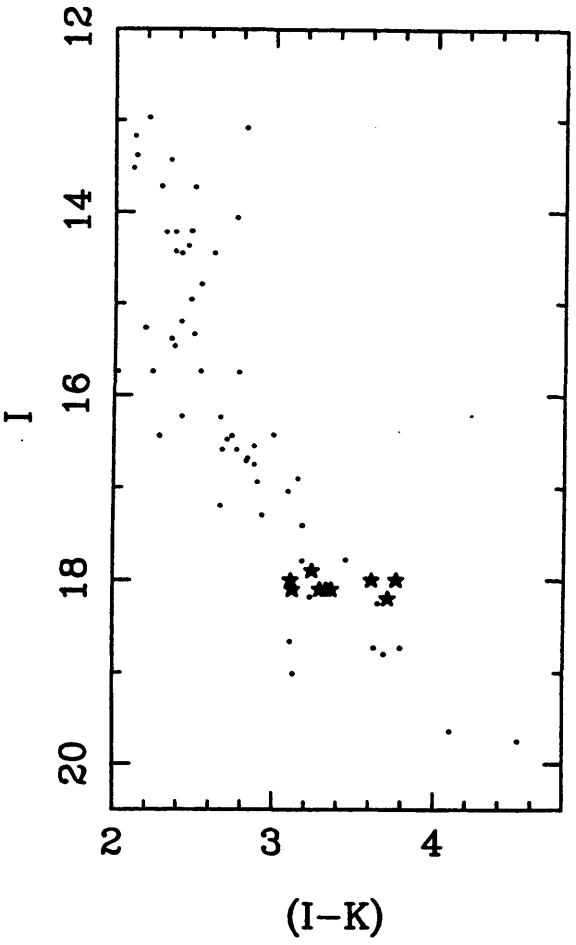

Figure 5. I versus (I–K) colour–magnitude diagram for the 9 candidates in this survey (stars) along with other known low-luminosity members of the Pleiades (small dots).

Name: IPMBD	RA (Equinox J2000.0; Epoch 1995.0)	DEC	I_{IVN}	R_{59F}	I_C	K	Other ID
11	3 55 23.05	24 49 05.41	18.1			14.77	IZpl 85[1]
20	3 49 04.82	23 33 39.65	18.1			14.74	
21	3 49 16.17	26 49 03.85	17.9	2.8		14.66	
22	3 49 33.06	26 50 43.17	18.0			14.89	
23	3 48 04.62	23 39 30.72	18.0	2.5		14.39	PPL 15[2]
25	3 46 26.05	24 05 09.91	18.0			14.24	
26	3 47 15.17	25 24 19.23	18.1			14.98	
29	3 45 31.32	24 52 47.79	18.2			14.49	
43	3 39 17.02	22 27 11.53	18.1			14.81	

[1]Pinfield (1998)
[2]Stauffer, Hamilton & Probst (1994).

Table 3. Observational parameters of the 9 candidate brown dwarfs

To provide a conversion of luminosity into mass, we used the data presented in Hambly et al. (1995b) to construct a relationship between BC_I and $\log(T_{\rm eff})$. This is shown in Figure 7, and a cubic least-squares polynomial fit yields the following:

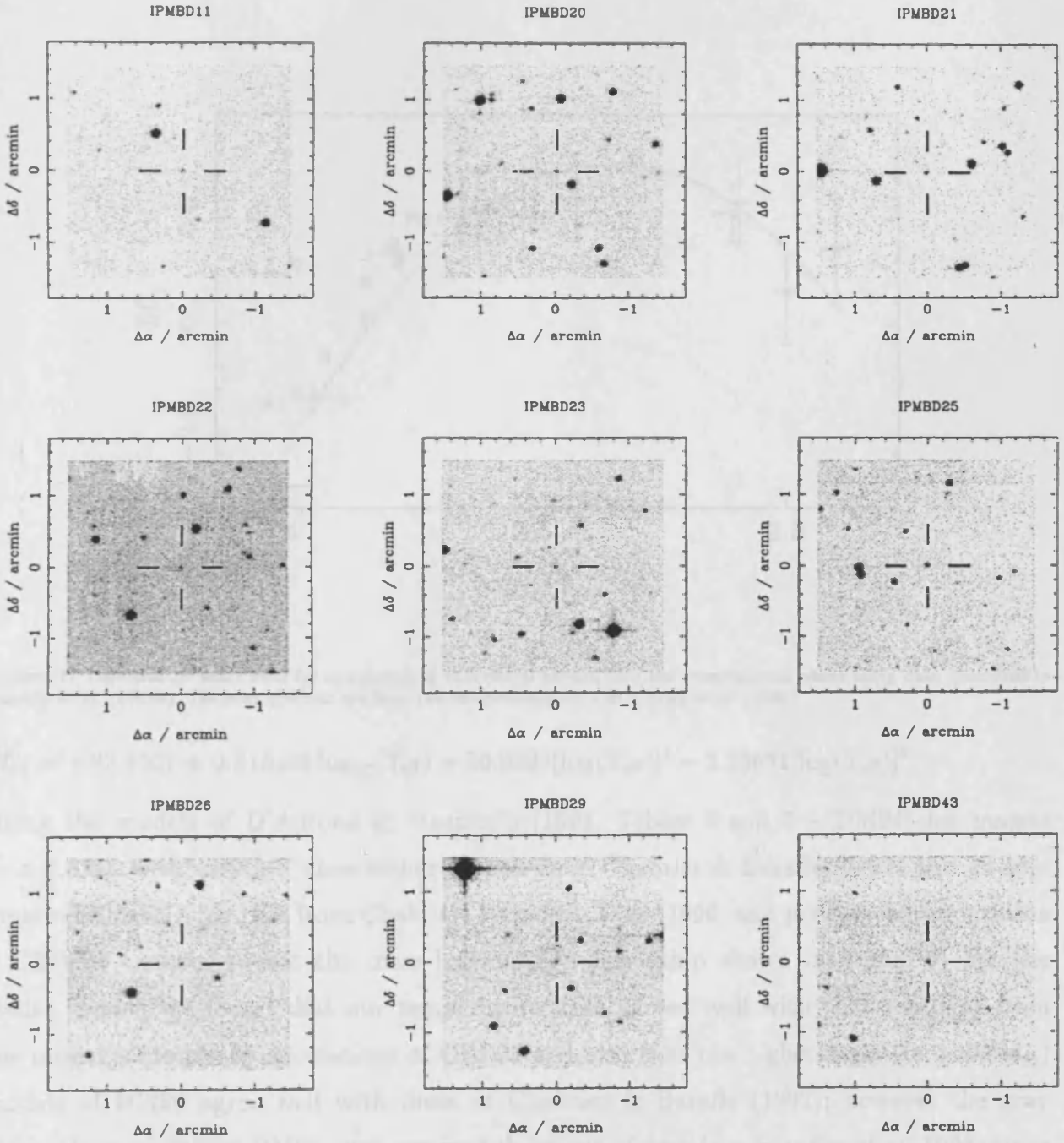

Figure 6. Finder charts for the 9 candidate BDs. North is to the top and east to the left. The charts were prepared from the deep 'stack' of 8 I plates, and reach I∼ 19.5.

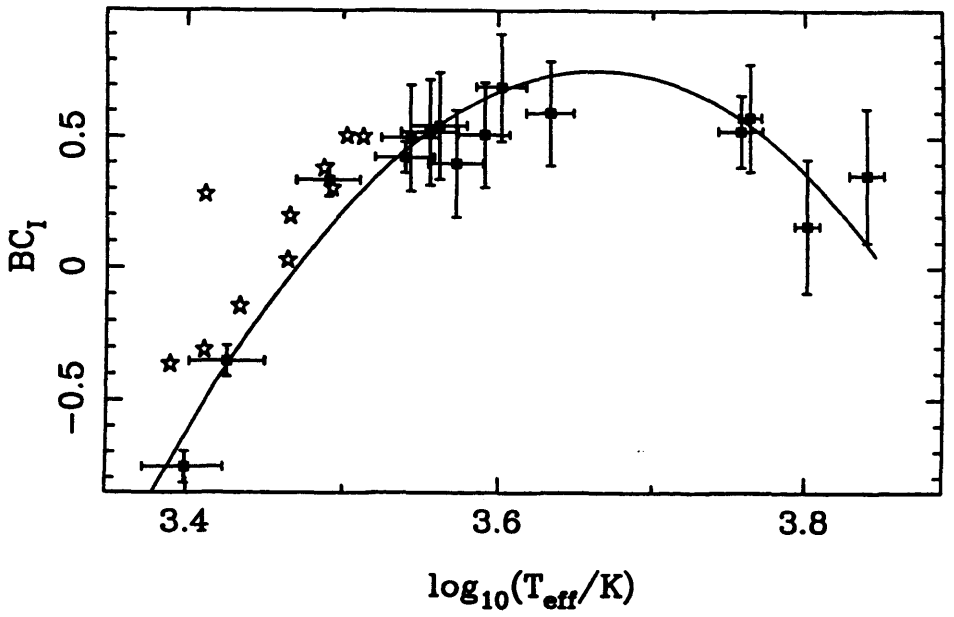

Figure 7. Temperature scale used for conversion of theoretical models into the observational plane using data described in Hambly et al. (1995b). The star symbols are from the temperature scale of Tinney et al. (1993).

$$BC_I = -93.8507 + 0.815193\log_{10}(T_{\rm eff}) + 20.6998[\log(T_{\rm eff})]^2 - 3.78681[\log(T_{\rm eff})]^3.$$

Using the models of D'Antona & Mazzitelli (1994, Tables 3 and 5 - DM94) for masses $m > 0.8M_\odot$ with very low mass stellar models from Chabrier & Baraffe (1997) and an M_I–mass relationship for BDs from Chabrier, Baraffe & Plez (1996, and private communication - CBP96) we constructed the mass–luminosity relationship shown in Figure 8. For the stellar models we found that our temperature scale agreed well with that resulting from the model atmosphere calculations of CBP96 and also that the higher mass ($m > 0.6M_\odot$) models of DM94 agree well with those of Chabrier & Baraffe (1997); however the gray atmosphere models of DM94 were assumed to be out of date (e.g. Stauffer et al. 1998) since a non–gray model atmosphere treatment of the boundary condition has been shown to be more accurate (e.g. CPB96). We assumed an age for the Pleiades of 100 Myr (e.g. Basri et al. 1996), a distance modulus of $(m-M)_0$=5.53 (e.g. Basri et al. 1996; Zapatero–Osorio et al. 1997c; Stauffer et al. 1998), an extinction A_I=0.07 mag (Zapatero–Osorio et al. 1997c) and $M_{bol,\odot} = 4.75$ (Allen 1973). Interpolating cubic polynomials (also shown) were used to transform from given values of m_I to mass, The derived mass function is shown in Figure 9.

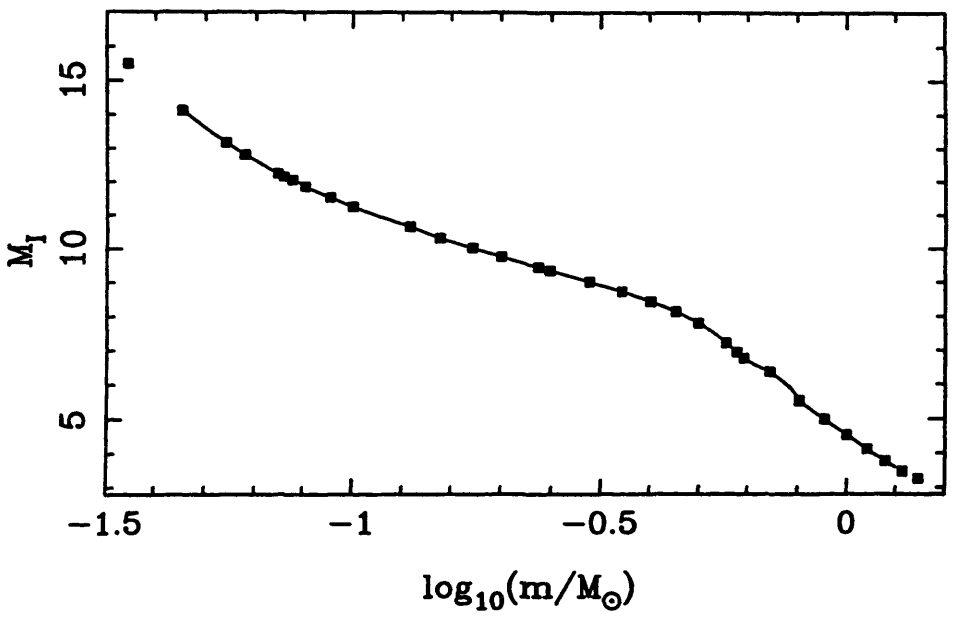

Figure 8. Mass–luminosty relation for the Pleiades (see text).

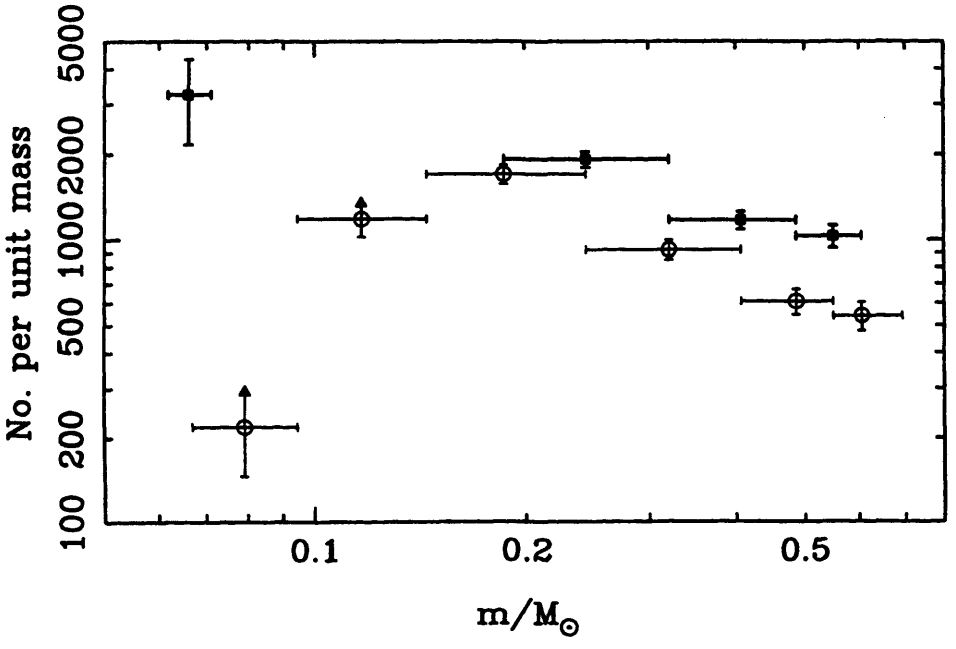

Figure 9. Initial mass function of the Pleiades. Open circles are the IMF from the survey of HHJ (see text).

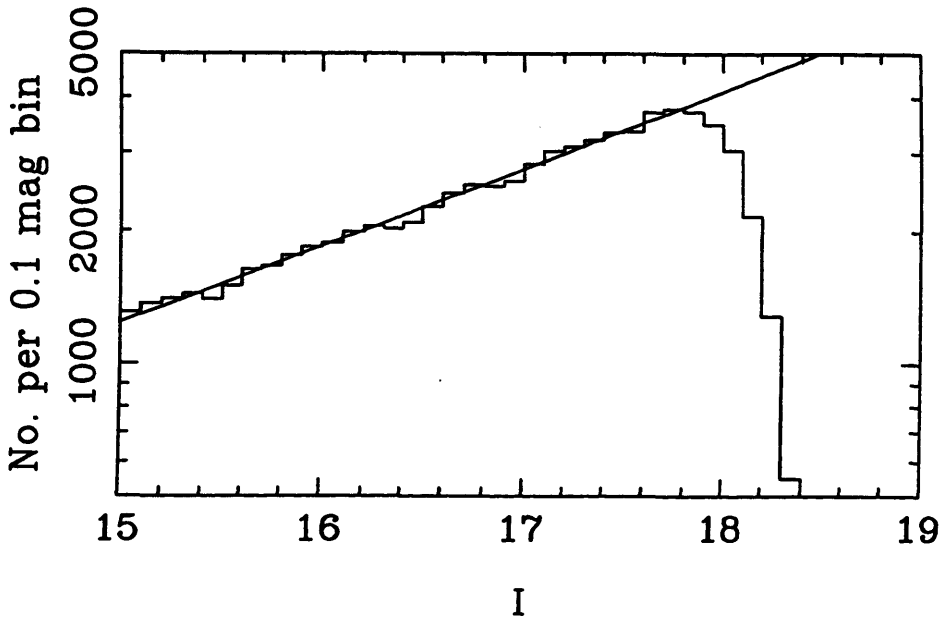

Figure 10. Number–magnitude histogram of stars detected on at least 6 single I plates when paired with the deep catalogue of objects from the stack of all 8 plates (100% complete to $I > 19$).

4 DISCUSSION

In order to correct the number of stars in the lowest mass bin in Figure 9 for completeness, two factors were employed. The first was derived from the proper motion selection. We chose objects having proper motions consistent with the cluster motion at the level of 1σ (i.e. 68% confidence); assuming independent normally distributed errors in the two dimensions of the PMVPD we therefore multiplied the number of objects by a factor $1/0.68^2$. In addition, the survey is not 100% complete down to the magnitude limit I = 18.3. Figure 10 shows a number–magnitude histogram for all stars when paired with a catalogue of objects from the deep I stack, which is 100% complete down to $I > 19$. The log–linear part of the data were fitted with a straight line and extrapolated to calculate a total photometric completeness of 65%. The total correction factor for the lowest mass bin was therefore $1/(0.68^2 \times 0.65)$.

Comparing with HHJ (open circles in Figure 9), the data agree very well since the estimated completeness of HHJ was $\sim$ 70% for the higher mass bins. Below $m \sim 0.1 M_\odot$ HHJ becomes increasingly incomplete, and no conclusion was drawn as to the shape of the IMF at this point. The present data allow us to say more about the form of the IMF across

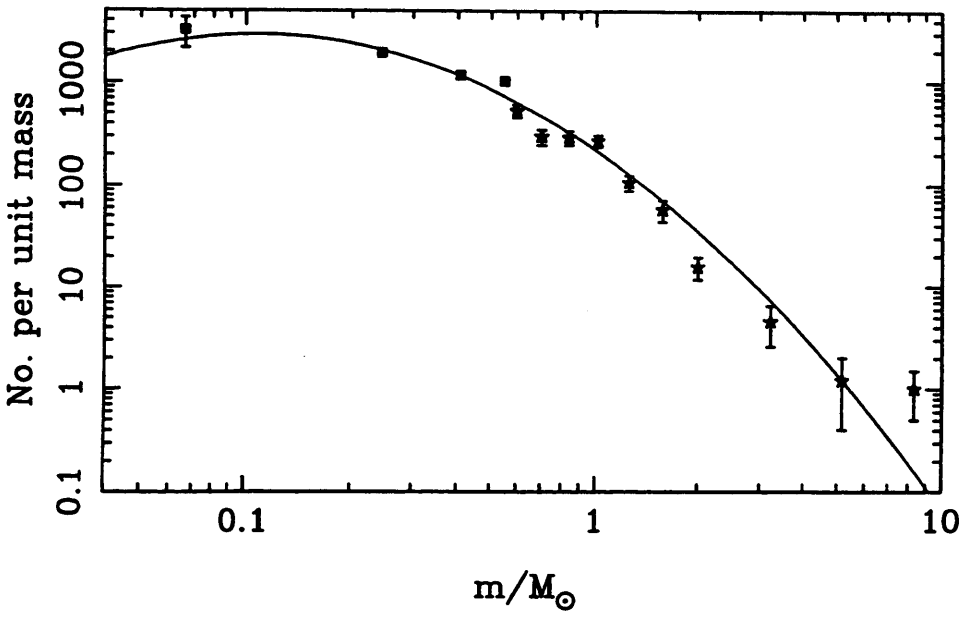

Figure 11. IMF for the Pleiades of the mass range $0.07 < m/M_\odot < 10$. The solid squares are the data from this survey; the star symbols are from higher mass data as described in the text. The solid line is a quadratic fit to the data (see text).

the stellar/substellar boundary. Clearly, the function is considerably flatter than at higher masses, and is consistent with a power law index of $\alpha \sim 0$ (see below).

In Adams & Fatuzzo (1996), arguments were presented for the IMF approximating a normal distribution in the $\mathrm{d}N/\mathrm{d}m - \log m$ plane. This is equivalent to a quadratic form in the $\log \mathrm{d}N/\mathrm{d}m - \log m$ plane (the so called 'log–normal' form, e.g. Miller & Scalo 1979). In Figure 11 we show our data in conjunction with higher mass points. The latter were derived using the Prosser & Stauffer compilation of Pleiades members (Prosser 1997), which lists objects from many sources and which we have therefore assumed to be largely complete. Mass–M_V relations as described in Pinfield (1998) were used to convert from V magnitudes to mass, again assuming $(m\text{–}M)_0$=5.53 and A_V=0.12 (e.g. Stauffer et al. 1998). The data were fitted, using weighted linear least–squares, with a quadratic polynomial of the form

$$\log_{10} \xi(\log m) = A_0 + A_1(\log m) + A_2(\log m)^2$$

(e.g. Miller & Scalo 1979). The data are clearly reasonably well represented, *in this mass range*, using this log–normal form. The coefficients of the fit are $A_0 = 2.3408$, $A_1 = -2.3134$ and $A_2 = -1.191$. For comparison with a power–law of the form $\xi = \mathrm{d}N/\mathrm{d}m = km^{-\alpha}$, the gradient of the quadratic at any point is given by $-\alpha = A_1 + 2A_2 \log m$. So, at $m = 0.1\mathrm{M}_\odot$,

$\alpha = +0.1$ and at $m = 1.0M_{\odot}$, $\alpha = +2.3$, which compares favourably with the Salpeter (1955) value. Interestingly, at high masses we find a gradient considerably steeper than Salpeter: at $m = 10M_{\odot}$, $\alpha = +4.7$

Needless to say, it is dangerous to extrapolate the symmetrical log–normal form below the lowest mass bin having data available here. There is growing evidence that there is a local minimum in the IMF at $m \sim 0.1M_{\odot}$, and that further into the BD régime the number of stars per unit mass begins to rise again (e.g. Martín, Zapatero–Osorio & Rebolo 1998, Jameson et al., in preparation).

A complicating factor in the derivation of the IMF is the vexing problem of unresolved binarity (URB). Estimates as to the degree of URB in the Pleiades vary. For example, Stauffer (1984) found 26% binarity amongst G– and K–type dwarfs, while Steele & Jameson (1995) found $\sim$ 50% amongst the M–type dwarfs. Moreover, there is a certain amount of evidence that PPL 15 itself is an URB (Basri & Martín 1998). Here, we have assumed that the binary fraction is low enough that the IMF can be derived, to first order, without correcting for URB (e.g. Martín et al. 1998).

Finally, in Figure 12 we show the spatial distribution of the BD candidates (solid circles), where open circles denote higher mass members from the Prosser & Stauffer compilation (for these, symbol size is proportional to brightness). Existing deep CCD surveys (e.g. Zapatero–Osorio et al. 1997c) have necessarily concentrated on the central few square degrees of the cluster to maximise the probability of finding members. Application of the Virial theorem to the cluster implies a tidal radius of $\sim$ 13pc (Pinfield 1998) or 5.5° at a distance of 130pc; in addition it is to be expected from energy equipartition that the lowest mass Pleiads will be scattered into the largest volume of space. Clearly, if the BD candidates presented here are indeed members then large areas need to be surveyed to fully account for still lower mass objects.

5 CONCLUSION

The main conclusions of this work are as follows:

- nine candidate BDs have been identified, seven of which are new discoveries while one of the two previously discovered is the lithium BD PPL 15;
- the IMF of the Pleiades appears to be flat across the stellar/substellar boundary;

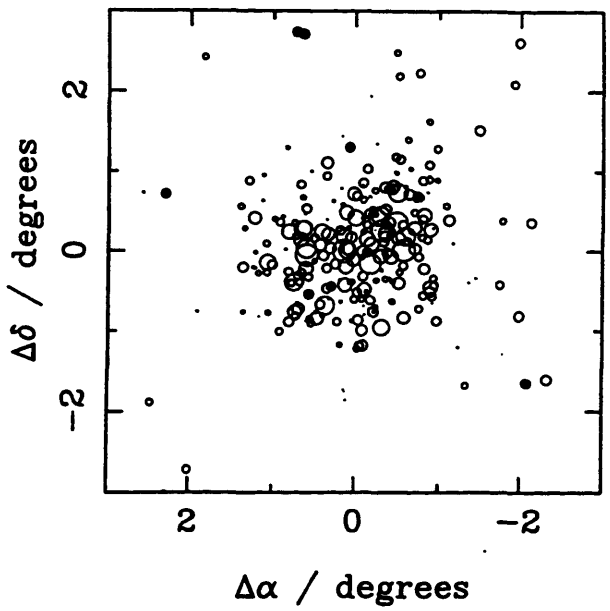

Figure 12. Spatial distribution of the BD candidates (stars) along with that of higher mass stars (open circles; symbol size proportional to magnitude).

- the IMF in the mass range $0.07 < m/\mathrm{M}_{\odot} < 10$ is reasonably well represented by a log–normal function;
- the candidates have been found at radii from the cluster centre of up to $\sim 3°$; future deep photoelectric surveys must cover a similar extent to well sample the Pleiades low mass BD membership.

ACKNOWLEDGEMENTS

We thank Sue Tritton and the United Kingdom Schmidt Telescope Unit for providing the plate material used here. Thanks are also due to Harvey MacGillivray and Eve Thomson for scanning the plates on SuperCOSMOS. It is a pleasure to thank Isabelle Baraffe, Gilles Chabrier, Charles Prosser and John Stauffer for providing unpublished data in electronic form. Financial support for STH and MRC is provided by the UK PPARC. The United Kingdom Infrared Telescope is operated by the Royal Observatory Edinburgh, and the Isaac Newton Telescope by the Royal Greenwich Observatory, on behalf of the UK PPARC.

REFERENCES

Adams F.C., Fatuzzo M., 1996, ApJ, 464, 256

Alcock C. et al., 1997, ApJ, 486, 697

Allen C.W., 1973, Astrophysical Quantities, The Athlone Press, London

Aubourg E. et al., 1993, Nature, 365, 623

Bahcall J.N, Flynn C., Gould A., 1992, ApJ, 389, 234

Basri G., Martín E.L., 1998, In: Rebolo, Martín & Zapatero–Osorio, in press

Basri G., Marcy G.W., Graham J.R., 1996, ApJ, 458, 600

Beard S.M., MacGillivray H.T., Thanisch P.F., 1990, MNRAS, 247, 311

Bienaymé O., Robin A., Crézé M., 1987, A&A, 180, 94

Chabrier G., Baraffe I., Plez B., 1996, ApJ, 459, L91

Chabrier G., Baraffe I., 1997, A&A, 327, 1039

Cossburn M.R., Hodgkin S.T., Jameson R.F., Pinfield D.J., 1997, MNRAS, 288, L23

D'Antona F., Mazzitelli I., 1994, ApJS, 90, 467

Festin L., 1998, A&A, in press

Greenstein J.L., 1989, Comments Astrophys., 13, 303

Hambly N.C., Hawkins M.R.S., Jameson R.F., 1991, MNRAS, 253, 1

Hambly N.C., Hawkins M.R.S., Jameson R.F., 1993, A&AS, 100, 607 (HHJ)

Hambly N.C., Steele I.A., Hawkins M.R.S., Jameson R.F., 1995a, A&AS, 109, 29

Hambly N.C., Steele I.A., Hawkins M.R.S., Jameson R.F., 1995b, MNRAS, 273, 505

Hambly N.C., Smartt S.J., Hodgkin S.T., 1997, ApJ, 489, L157

Hambly N.C., Miller L., MacGillivray H.T., Herd J.T., Cormack W.A., 1998, MNRAS, in press

Jameson R.F., Skillen W.J.I., 1989, MNRAS, 239, 247

Jones B.F., 1973, A&AS, 9, 313

Kafatos M.C., Harrington R.S., Maran S.P. (eds.), 1986, 'Astrophysics of Brown Dwarfs', Cambridge University Press

Knox R., Hambly N.C., Hawkins M.R.S., MacGillivray H.T., 1998, MNRAS, in press

Kormendy J., Knapp G.R. (eds.), 1987, IUA Symposium No. 117: Dark Matter in the Universe

Kuijken K., Gilmore G., 1989, MNRAS, 239, 571

Kuijken K., Gilmore G., 1991, MNRAS, ApJ, 267, L9

Kumar S., 1963, ApJ, 178, 1168

Liebert J., Probst R.G., 1987, ARA&A, 25, 473

Magazzù A., Martín E.L., Rebolo R., 1993, ApJ, 404, L17

Marcy G.W., Basri G., Graham J.R., 1994, ApJ, 428, L57

Martín E.L., Rebolo R., Magazzù A., 1994, ApJ, 436, 262

Martín E.L., Zapatero–Osorio M.–R., Rebolo R., 1998, In: Rebolo, Martín & Zapatero–Osorio, in press

Miller G.E., Scalo J.M., 1979, ApJS, 41, 513

Nakajima T., Oppenheimer B.R., Kulkarni S.R., Golimowski D.A., Mathews K., Durrance S.T., 1995, Nature, 378, 463

Oort J.H., 1960, Bull. Astr. Inst. Netherlands, 15, 45

Pinfield D.J., 1998, PhD Thesis, University of Leicester

Prosser C.F., 1997, private communication

Rebolo R., Martín E.L., Magazzù A., 1992, ApJ, 389, L83

Rebolo R., Zapatero–Osorio M.–R., Martín E.L., 1995, Nature, 377, 129

Rebolo R., Martín E.L., Basri G., Marcy G.W., Zapatero–Osorio M.–R., 1996, ApJ, 469, L53

Rebolo R., Martín E.L., Zapatero–Osorio M.–R. (eds.), 1998, 'Brown Dwarfs and Extrasolar Planets', ASP Conf. Ser., in press

Salpeter E.E., 1955, ApJ, 121, 161

Sanders W.L., 1971, A&A, 14, 226

Simons D.A., Becklin E.E., 1992, ApJ, 390, 431

Stauffer J.R., 1984, ApJ, 280, 189

Stauffer J.R., Hamilton D., Probst R.G., Rieke G.H., Mateo M., 1989, ApJ, 344, L21

Stauffer J.R., Hamilton D., Probst R.G., 1994, AJ, 108, 155

Stauffer J.R., Liebert J., Giampapa M., 1995, AJ, 109, 298

Stauffer J.R., Schild R., Barrado–y–Navascués D., Backman D.E., Angelova A., Kirkpatrick D., Hambly N.C., Vanzi L., 1998, ApJ, in press

Steele I.A., Jameson R.F., Hambly N.C., 1993, MNRAS, 263, 647

Steele I.A., Jameson R.F., 1995, MNRAS, 272, 680

Tarter J., 1975, PhD Thesis, University of California, Berkeley

Tinney C.G., Mould J.R., Reid I.N., 1993, AJ, 105, 1045

Tinney C.G. (ed.), 1995, 'The Bottom of the Main Sequence – and beyond', Proceedings of the ESO Astrophysics Symposium held in Garching, Germany, Springer–Verlag

Udalski A. et al., 1993, Acta Astron., 43, 289

Williams D.M., Boyle R.P., Morgan W.T., Rieke G.H., Stauffer J.R., Rieke M.J., 1996, ApJ, 464, 238

Zapatero–Osorio M.–R., Martín E.L., Rebolo R., 1997a, A&A, 317, 164

Zapatero–Osorio M.–R., Martín E.L., Rebolo R., 1997b, A&A, 323, 105

Zapatero–Osorio M.–R., Rebolo R., Martín E.L., Basri G., Magazzù A., Hodgkin S.T., Jameson R.F., Cossburn M.R., 1997c, ApJ, 491, L81

This paper has been produced using the Royal Astronomical Society/Blackwell Science LaTeX style file.

References

Adams, F. C. & Fatuzzo, M., 1996. *ApJ*, **464**, 256.

Allard, F. & Hauschildt, P., 1997. . in press.

Allard, F., Hauschildt, P. H., Baraffe, I. & Chabrier, G., 1996. *Astrophys. J. Letters.*, **465**, 123.

Allard, F., Hauschildt, P. H., Alexander, D. R. & Starrfield, S., 1997. *Ann. Rev. Astr. Astrophys.*, **35**, 137.

Allard, F., 1990. *PhD thesis*, Univ. Heidelburg.

Artjukhina, N. M., 1966. *Trudy Gos. Astron. Inst. Shternberga XXXIV*, .

Baraffe, I., Chabrier, G., Allard, F. & Hauschildt, P. H., 1998. *Astr. Astrophys.*, **in press.**

Basri, G., Marci, G. M. & Graham, J. R., 1996. *ApJ*, **458**, 600.

Becklin, E. E. & Zuckerman, B., 1988. *Nat*, **336**, 656.

Berriman, G., Reid, N. & Leggett, S. K., 1992. *Astrophys. J. Letters.*, **392**, 31.

Bessell, M. S., 1986. *PASP*, **98**, 1303.

Bessell, M. S., 1991. *Astron. J.*, **101**, 662.

Bouvier, J., Stauffer, J. R., Martin, E. L., y Navascues, D. B., Wallace, B. & Bejar, V. J. S., 1998. *Astr. Astrophys.*, **336**, 490.

Bryja, C., Jones, T. J., Humphreys, R. M., Lawrence, G., Pennington, R. L. & Zumach, W., 1992. *Astrophys. J. Letters.*, **388**, 23.

Bryja, C., Humphreys, R. M. & Jones, T. J., 1994. *Astron. J.*, **107**, 246.

Burrows, A., Hubbard, W. B., Saumon, D. & Lunine, J. I., 1993. *ApJ*, **406**, 158.

Chabrier, G. & Baraffe, I., 1997. *Astr. Astrophys.*, **327**, 1039.

Chabrier, G., Baraffe, I. & Plez, B., 1996. *Astrophys. J. Letters.*, **459**, 91.

Cossburn, M. R., Hodgkin, S. T., Jameson, R. F. & Pinfield, D. J., 1997. *MNRAS Lett.*, **288**, 23.

D'Antona, F. & Mazzitelli, I., 1985. *ApJ*, **296**, 502.

D'Antona, F. & Mazzitelli, I., 1994. *ApJS*, **90**, 467.

Delfosse, X., Tinney, C. G., Forveille, T., Epchtein, N., Bertin, E., Borsenberger, J., Copet, E., de Batz, B., Fouque, P., Kimeswenger, S., Bertre, T. L., Lacombe, F., Rouan, D. & Tiphene, D., 1997. *A&AS*, **327**, 25.

Festin, L., 1997. *Astr. Astrophys.*, **322**, 455.

Festin, L., 1998. *Astr. Astrophys.*, **333**, 497.

Hambly, N. C., Steele, I. A., Hawkins, M. R. S. & Jameson, R. F., 1995a. *A&AS*, **109**, 29.

Hambly, N. C., Steele, I. A., Hawkins, M. R. S. & Jameson, R. F., 1995b. *MNRAS*, **273**, 505.

Hambly, N. C., Hodgkin, S. T., Cossburn, M. R. & Jameson, R. F., 1998. *MNRAS*, , in press.

Hambly, N. C., Hawkins, M. R. S. & Jameson, R. F., 1991. *MNRAS*, **253**, 1.

Hambly, N. C., Hawkins, M. R. S. & Jameson, R. F., 1993. *A&AS*, **100**, 607.

Hawkins, M. R. S. & Bessell, M. S., 1988. *MNRAS*, **234**, 177.

Hawkins, M. R. S., Ducourant, C., Jones, H. R. A. & Rappaport, M., 1998. *MNRAS*, **294**, 505.

Hawkins, M. R. S., 1994. In: *Cool Stars Stellar Systems and the Sun*, 566, ed. Caillault, J. P.

Hodgkin, S. T., Jameson, R. F., Cossburn, M. R. & Pinfield, D. J., 1998. *in preparation*, .

Jameson, R. F. & Skillen, W. J. I., 1989. *MNRAS*, **239**, 247.

Jameson, R. F., Hodgkin, S. T., Pinfield, D. J. & Cossburn, M. R., 1998. *in preparation*, .

Jameson, R. F., Sherrington, M. R. & Giles, A. B., 1983. *MNRAS Lett.*, **205**, 39.

Jones, B. F. & Cudworth, K., 1983. *Astron. J.*, **88**, 215.

Jones, B. F. & Stauffer, J. R., 1991. *Astron. J.*, **102**, 1080.

Jones, H. R. A., Longmore, A. J., Jameson, R. F. & Mountain, C. M., 1994. *MNRAS*, **267**, 413.

Jones, H. R. A., Miller, L. & Glazebrook, K., 1994. *MNRAS Lett.*, **270**, 47.

King, I. R., 1962. *Astron. J.*, **67**, 471.

Kirkpatrick, J. D., Beichman, C. A. & Skrutskie, M. F., 1997. *ApJ*, **476**, 311.

Kirkpatrick, J. D., Kelly, D. M., Rieke, G. H., Liebert, J., Allard, F. & Wehrse, R., 1993. *ApJ*, **402**, 643.

Kirkpatrick, J. D., McGraw, J. T., Hess, T. R., Leibert, J. & Jr., D. W. M., 1994. *ApJS*, **94**, 749.

Kirkpatrick, J. D., Henry, T. J. & Simons, D. A., 1995. *Astron. J.*, **109**, 797.

Kirkpatrick, J. D., 1998. In: *Brown Dwarfs and Extra Solar Planets*, eds Rebolo, R., Martin, E. & Osorio, M. R. Z. ASP Conference Series.

Kumar, S. S., 1963. *ApJ*, **137**, 1211.

Landolt, A. U., 1992. *Astron. J.*, **104**, 340.

Leggett, S. K. & Hawkins, M. R. S., 1988. *MNRAS*, **234**, 1065.

Leggett, S. K., Allard, F., Berriman, G., Dahn, C. C. & Hauschildt, P. H., 1996. *ApJS*, **104**, 117.

Leggett, S. K., Harris, H. C. & Dahn, C. C., 1994. *Astron. J.*, **108**, 994.

Leggett, S. K., 1992. *ApJS*, **82**, 351.

Liebert, J. & Probst, R. G., 1987. *Ann. Rev. Astr. Astrophys.*, **25**, 473.

Magazzu, A., Rebolo, R., Zapatero-Osorio, M. R., Martin, E. L. & Hodgkin, S. T., 1998. *ApJ*, **497**, 47.

Marcy, G. W., Basri, G. & Graham, J. R., 1994. *Astrophys. J. Letters.*, **428**, 57.

Martin, E. L., Basri, G., Gallegos, J. E., Rebolo, R., Zapatero-Osorio, M. R. & Bejar, V. J. S., 1998. *Astrophys. J. Letters.*, **499**, 61.

Martin, E. L., Rebolo, R. & Zapatero-Osorio, M. R., 1996. *ApJ*, **469**, 706.

McCarthy, D. W., Probst, R. G. & Low, F. J., 1985. *Astrophys. J. Letters.*, **290**, 9.

Mera, D., Chabrier, G. & Baraffe, I., 1996. *Astrophys. J. Letters.*, **459**, 87.

Mermilliod, J. C., Weis, E. W., Duquennoy, A. & Mayor, M., 1990. *Astr. Astrophys.*, **235**, 114.

Nakajima, T., Oppenheimer, B. R., Kulkarni, S. R., Golimowski, D. A., Matthews, K. & Durrance, S. T., 1995. *Nat*, **378**, 441.

Nelson, L. A., Rappaport, S. A. & Chiang, E., 1993. *ApJ*, **413**, 364.

Nelson, L. A., Rappaport, S. A. & Joss, P. C., 1986. *ApJ*, **311**, 226.

Oort, J. H., 1960. *Bull. Astr. Inst. Netherlands.*, **15**, 45.

Pinfield, D. J., Hodgkin, S. T., Jameson, R. F., Cossburn, M. R. & von Hippel, T., 1997. *MNRAS*, **287**, 180.

Pinfield, D. J., Cossburn, M. R., Hodgkin, S. T. & Jameson, R. F., 1998. *in preparation*, .

Pinfield, D. J., Hodgkin, S. T. & Jameson, R. F., 1998. *MNRAS*, **299**, 955.

Pinfield, D. J., 1997. *PhD thesis*, Univ. Leicester, U.K.

Rebolo, R., Martin, E., Basri, G., Marcy, G. W. & Zapatero-Osorio, M. R., 1997. *Astrophys. J. Letters.*, **469**, 53.

Rebolo, R., Martin, E. & Magazzu, A., 1992. *Astrophys. J. Letters.*, **389**, 83.

Rebolo, R., Zapatero-Osorio, M. R. & Martin, E. L., 1995. *Nat*, **377**, 129.

Reid, N., 1987. *MNRAS*, **225**, 873.

Reid, N., 1992. *MNRAS*, **257**, 257.

Reid, N., 1993. *MNRAS*, **265**, 785.

Ruiz, M. T., Leggett, S. K. & Allard, F., 1997. *ApJ*, **491**, 107.

Salpeter, E. E., 1955. *ApJ*, **121**, 161.

Simons, D. A. & Becklin, E. E., 1992. *ApJ*, **390**, 431.

Skrutskie, M. F., Forrest, W. J. & Shure, M., 1989. *Astron. J.*, **98**, 1409.

Stauffer, J. R., Hamilton, D., Probst, R., Rieke, G. & Mateo, M., 1989. *Astrophys. J. Letters.*, **344**, 21.

Stauffer, J., Klemola, A., Prosser, C. & Probst, R., 1991. *Astron. J.*, **101**, 3.

Stauffer, J. R., Hamilton, D. & Probst, R., 1994. *Astron. J.*, **108**, 155.

Stauffer, J. R., Schultz, G. & Kirkpatrick, J. D., 1998. *ApJ*, **499**, 199.

Steele, I. A. & Jameson, R. F., 1995. *MNRAS*, **272**, 630.

Steele, I. A., Jameson, R. F., Hodgkin, S. T. & Hambly, N. C., 1995. *MNRAS*, **275**, 841.

Steele, I. A., Jameson, R. F. & Hambly, N. C., 1993. *MNRAS*, **263**, 647.

Stevenson, D. J., 1991. *Ann. Rev. Astr. Astrophys.*, **29**, 163.

Tarter, J. C., 1975. *PhD thesis*, Univ. California, Berkley.

Thackrah, A., Jones, H. R. A. & Hawkins, M. R. S., 1997. *MNRAS*, **284**, 507.

Tinney, C. G., Mould, J. R. & Reid, I. N., 1993. *Astron. J.*, **105**, 1045.

Tinney, C. G., 1998. *MNRAS Lett.*, **296**, 45.

Tsuji, T., Ohnaka, K. & Aoki, W., 1996. *Astr. Astrophys.*, **305**, 1.

Veeder, G. J., 1974. *aj*, **79**, 1056.

Williams, S. D., Stauffer, J. R., Prosser, C. F. & Herter, T., 1994. *PASP*, **106**, 817.

Williams, D. M., Boyle, R. P., Morgan, W. T., Rieke, G. H., Stauffer, J. R. & Rieke, M. J., 1996. *ApJ*, **464**, 238.

Williams, D. M., Rieke, G. H. & Stauffer, J. R., 1995. *ApJ*, **445**, 359.

Zapatero-Osorio, M. R., Rebolo, R., Martin, E., G.Basri, Magazzu, A., Hodgkin, S., Jameson, R. & Cossburn, M., 1997. *Astrophys. J. Letters.*, **491**, 81.

Zapatero-Osorio, M. R., Martin, E. L. & Rebolo, R., 1997. *Astr. Astrophys.*, **323**, 105.

Zapatero-Osorio, M. R., Rebolo, R. & Martin, E. L., 1997. *A&AS*, **317**, 164.

Zuckerman, B. & Becklin, E. E., 1988. *Nat*, **330**, 138.

Zuckerman, B. & Becklin, E. E., 1992. *ApJ*, **386**, 260.